A Computational Investigation of Gastric Electrical Stimulation

Aishwariya Kannan
B.Tech (Biotechnology), Anna University

Supervisor: Dr.Martin.L.Buist

A Thesis Submitted in Partial Fulfillment of the Requirements for the Degree of
Master of Engineering in Bioengineering

Division of Bioengineering
National University of Singapore.
August, 2011.

ABSTRACT

The intrinsic electrical activity (slow waves) and mechanical activity of the gastric musculature is a coordinated sequence of events influenced by interstitial cells of Cajal, smooth muscle cells and the enteric nervous system. These complex control mechanisms have been developed by the gastric musculature to perform the basic physiological functions of synchronized contraction and relaxation which is known as gastric motility. Disturbances at any level of the control mechanisms can result in number of GI motility disorders such as gastroparesis. Following the success of cardiac pacemakers, it was thought that injecting an electrical stimulus into the stomach's wall (gastric electrical stimulation) may restore its motility. Gastric electrical stimulation (GES) is an alterative strategy attempting to alleviate gastroparetic and other gastric dysmotility symptoms by improving overall gastric motility.

In this research project we have developed an electrophysiological model for gastric electrical stimulation based on realistic description of the interstitial cells of Cajal and smooth muscle cells. The physiological significance of single and multi channel GES along with their energy efficiency has been examined. Electrical parameter selection for different types of stimulus protocols that are currently employed in experimental GES have also been examined to achieve efficient and effective slow wave entrainment. This model allows the demonstration of normal gastric electrical activity as well as gastric dysrhythmia based on the underlying mechanisms and also provides a framework for predicting the energy requirements of the applied pacing parameters. We have integrated a large quantity of information from experimental GES ranging from various stimulus protocols to the number of channels used for delivering stimulus and have packed it succinctly into the developed GES model. This model allows us to manipulate the stimulus parameters for different types of gastric dysrhythmia and pave the way for the development of an effective and energy efficient gastric pacemaker.

ACKNOWLEDGEMENTS

First of all let me thank the lord almighty for successful completion of the research project.

I offer my sincerest gratitude to my supervisor, Dr.Martin Buist, who has supported me throughout my project with his patience and knowledge whilst allowing me the room to work in my own way. I attribute the level of my Masters degree to his encouragement and effort and without him this thesis, too, would not have been completed or written. His words of encouragement and the enthusiasm he had for research has been motivational for me and kept me going even during the tough times of my research pursuit.

The members of the computational bioengineering group have been a source of great friendship as well as good advice. I would like to extend my sincere thanks to Dr.Alberto Corrias for sharing vast amount of knowledge and helping me understand the single cell models which laid the foundation for my research project. The support offered by Viveka, Yong Cheng, William and Nicholas has made my research experience in the lab enriching.

A special thanks to my roommates Soumiya and Shiyamala for their support and encouragement. I am grateful to National University of Singapore and the division of bioengineering for giving me an opportunity to pursue this research.

Dedicated to my parents

Contents

Abstract iii

Acknowledgements iv

List of Figures xii

List of Tables xv

1 Introduction

1.1 Gastrointestinal tract in humans …… 2

1.2 Stomach …….. 3

1.2.1 Anatomy of the stomach …… 3

1.2.2 Motility in the stomach …….. 5

1.3 Motility disorders in the stomach ……... 8

1.4 Underlying mechanisms …….. 9

1.4.1 Gastroparesis …….. 9

1.4.2 Functional dyspepsia ……... 10

1.4.3 Dumping syndrome ……. 11

1.5 Treatment options …… 11

1.5.1 Dietary modifications ……. 11

1.5.2 Prokinetic agents …….. 11

1.5.3 Gastrectomy and enteral nutrition …… 12

1.5.4 Gastric electrical stimulation (GES) …… 12

1.6 GES: effects and mechanism …… 13

1.6.1 Long-pulse stimulus …… 14

1.6.2 Short-pulse stimulus …… 14

1.6.3 Trains of short pulse …… 15

1.6.4 Dual pulse stimulus …….. 15

1.6.5 Synchronized stimulus …… 16

1.6.6 Enterra Therapy ……... 16

1.6.7 Implantable device ……... 17

1.6.8 Single channel GES vs multi channel GES …… 17

1.7 Morbid obesity and GES ……... 18

1.7.1 Retrograde gastric pacing …… 19

1.8 Thesis overview …… 19

2 GES review **20**

2.1 Review of experimental work on GES …… 20

2.1.1 Long-pulse stimulus …… 21

2.1.2 Short-pulse stimulus …… 22

2.1.3 Pulse train stimulus …….. 22

2.1.4 Dual pulse stimulus …….. 22

2 .1.5 Synchronized stimulus …… 23

2.1.6 GES for obesity treatment …… 23

2.2 Review of GES models …… 23

2.2.1 Relaxation oscillator model ……. 23

2.2.2 Conoidal dipole model ……. 26

2.2.3 Model of nonlinear coupling mechanism of gastric slow wave propagation ... 27

2.2.4 Three dimensional object oriented model …… 29

2.2.5 Rule based computer model ……. 30

2.2.6 Tissue framework for GES …….. 32

3 GES model development

3.1 Single cell model of ICC …… 35

3.1.1 Pacemaker unit of ICC …… 36

3.1.2 Calcium extrusion ……... 39

3.1.3 Model validation ……. 39

3.2 Single cell model of SMC …… 40

3.2.1 Calcium homeostasis …….. 42

3.2.2 Model validation ……. 43

3.3 Extended bidomain framework …… 44

3.3.1 Conventional bidomain framework …… 44

3.3.2 Extended bidomain framework ……... 45

3.3.3 Frequency gradient ……... 47

3.4 Development of GES model …… 49

3.4.1 Extending the extended bidomain framework: Inclusion of a bath …… 49

3.4.2 Inclusion of Intracellular IP_3 dynamics ……... 50

3.4.3 Decreasing the time constant for inactivation of IP_3 receptors 53

3.4.3.1 Removing I_{VDDR_PU} 54

4 Single channel GES **56**

4.1 Background 56

4.2 Modeling single channel GES 58

4.3 Simulation results 62

4.3.1 Generating dysrhythmia 62

4.3.2 Long pulse stimulus 63

4.3.3 Short pulse stimulus 65

4.3.4 Pulse train stimulus 66

4.3.5 Dual pulse stimulus 68

4.3.6 Synchronized stimulus 69

4.3.7 Enterra Therapy 70

4.4 Discussion 71

5 Multi channel GES **79**

5.1 Background 79

5.2 Modeling multi channel GES 81

5.3 Simulation results 83

5.3.1 Generating dysrhythmia 84

5.3.2 Long pulse stimulus 85

5.3.3 Short pulse stimulus 86

5.3.4 Pulse train stimulus …….. 86

5.3.5 Dual pulse stimulus …….. 87

5.3.6 Synchronized stimulus ……. 88

5.3.7 Enterra Therapy ……..... 89

5.4 Discussion …… 89

6 GES for obesity treatment **92**

6.1 Background ……... 92

6.2 Modeling retrograde gastric pacing …….. 92

6.3 Simulation results …….. 93

6.3.1 Long pulse stimulus …….. 93

6.3.2 Short pulse stimulus ……. 94

6.4 Discussion …….. 95

7 Conclusions **97**

7.1 Limitations and future work ……. 98

7.2 Publication and seminar ……... 99

8 Bibliograpghy **101**

List of Figures

1.1 Anatomy of the stomach …… 5

1.2 Electrical activity along different regions of the stomach …….. 7

1.3 Electrogastrogram during pre prandial and post prandial state ……... 8

1.4 Diagram of long pulse stimulus …… 14

1.5 Diagram of short pulse stimulus …….. 14

1.6 Diagram of pulse train stimulus ……... 15

1.7 Diagram of dual pulse stimulus ……... 15

1.8 Diagram of synchronized stimulus …….. 16

1.9 Implantable device: Enterra ……. 17

1.10 Single and multi channel GES ……... 19

1.11 Schematic of the developed GES modeling framework …… 20

2.1 Arrangement of oscillators in gastric ECA model developed by Sarna et al ……... 25

2.2 Results obtained by Sarna et al ……... 25

2.3 Temporal characteristics of the threshold stimulus adapted by Familoni et al …… 31

2.4 Outline for cellular automata algorithm adopted by Du et al …….. 33

3.1 Schematic view of the Corrias & Buist ICC model ……. 37

3.2 Slow wave profile generated by Corrias and Buist ICC model ……... 40

3.3 Schematic view of the Corrias and Buist SMC model …… 42

3.4 Smooth muscle depolarization profile generated by Corrias Buist SMC model ……. 43

3.5 Schematic of Buist Poh extended bidomain framework …….. 47

3.6 Slow wave profile of ICC and SMC generated by Buist and Poh extended bidomain framework …….. 48

3.7 Spatiotemporal plot of V_m^{ICC} from Buist and Poh extended bidomain framework ….. 48

3.8 Schematic of the extended bidomain framework after inclusion of the bath …….. 50

3.9 Schematic of IP_3 dynamics as suggested by Imtiaz et al …….. 51

3.10 Relationship between slow wave frequency and the parameter β …… 53

4.1 Origin and propagation of slow wave activity in the stomach ……... 57

4.2 Cable model of the stomach …… 59

4.3 Slow waves generated by the GES model at bradygastric frequency …… 62

4.4 Spatiotemporal plot of V_m^{ICC} at bradygastric frequency …….. 63

4.5 Normalization of bradygastric slow waves with long pulse stimulus ……. 64

4.6 Spatiotemporal plot of V_m^{ICC} stimulated with long pulse stimulus ……... 65

4.7 Normalization of bradygastric slow waves with pulse train stimulus …… 67

4.8 Spatiotemporal plot of V_m^{ICC} stimulated with pulse train stimulus …….. 67

4.9 Normalization of bradygastric slow waves with dual pulse stimulus ……... 68

4.10 Spatiotemporal plot of V_m^{ICC} stimulated with dual pulse stimulus …… 69

4.11 Effect of synchronized stimulus on slow waves ……... 70

4.12 Spatiotemporal plot of V_m^{ICC} stimulated with Enterra therapy parameters …… 71

4.13 Intersection of antegrade and retrograde propagation of slow waves …….. 73

4.14 Effect of first stimulus instant …….. 74

4.15 Effect of high frequency of the injected stimulus ……. 75

4.16 Limitation of single channel GES ……. 77

5.1 Placement of electrodes in multi channel GES ……..……... 81

5.2 Greater curvature of the stomach with defective ICC-ICC coupling ...…… 82

5.3 Normalization of bradygastric slow waves with multi channel GES ……. 84

5.4 Gastric dysrhythmia due to defective ICC-ICC coupling …… 85

5.5 Spatiotemporal plot of V_m^{ICC} stimulated with long pulse stimulus ……... 86

5.6 Spatiotemporal plot of V_m^{ICC} stimulated with pulse train stimulus …….. 87

5.7 Spatiotemporal plot of V_m^{ICC} stimulated with dual pulse stimulus …….. 88

5.8 Spatiotemporal plot of V_m^{ICC} stimulated with synchronized stimulus ……. 89

6.1 Placement of electrode at the distal stomach …….. 93

6.2 Spatiotemporal plot of V_m^{ICC} stimulated with long pulse stimulus ……. 94

6.3 Spatiotemporal plot of V_m^{ICC} stimulated with pulse train stimulus …….. 95

List of Tables

1.1 Organs of the gastrointestinal tract …….. 3

1.2 Motility disorders in the stomach and their symptoms …… 9

3.1 Details of ICC ionic current and the corresponding ion channels ……... 38

3.2 Details of SMC current and the corresponding ion channels …….. 41

Chapter 1

Introduction

The functional role of gastrointestinal tract (GI) is to digest and absorb nutrients. These processes are facilitated by the coordinated movement of the food from mouth to the anus. This movement is referred to as motility. Impairment of gastric motility is the cause of a number of GI motility disorders. These GI motility disorders are associated with various complications including vomiting, nausea, stomach obstruction, abdominal pain, malnutrition, food hardening into bezoars and early satiety [1]. People suffering from GI motility disorders experience a significant loss in quality of life to the extent of some being housebound. They can strike anyone, at any time in their lives. GI motility disorders affect 35 million people in USA alone. Next to the common cold, gastrointestinal motility disorders cause the highest percentage of absenteeism from the workplace. The economic burden for digestive disorders is $123 billion per year [2]. Gastroparesis is a motility disorder of the stomach affects more than 1.5 million Americans, with almost 1 million patients in an advanced stage of gastroparesis. 20% of type 1 diabetic patients also develop gastroparesis [3]. The number of hospitalizations for gastroparesis increased by close to 158% from 1995 to 2004 [4]. These stats are in austere contrast with the inadequate cognizance of the physiological mechanisms underlying GI motility disorders leading to limitations in the available treatment options.

Following the cardiac stimulation field, it was initially thought that injecting an electrical stimulus into the wall of the stomach (gastric electrical stimulation) may be able to restore its motility. However, this idea turned out to be more complicated than expected and has remained an enigma for decades [5]. This is because gastric electrical activity is more complex than that of the heart. As a consequence computational modeling of gastric electrical stimulation and the development of a gastric pacemaker also lies far behind its

cardiac counterpart. Gastric electrical stimulation (GES) has also been suggested as a potential therapy for the treatment of morbid obesity [6].

Computational electrophysiology represents a unique way to understand the mechanism behind gastric electrical stimulation. Computational models can compile the results from a large number of experiments and prove to be a valuable tool for understanding and optimizing GES. The electrophysiological model for GES developed in this research project aims at providing a realistic mathematical description of GES and to employ a computational approach to determine the most efficient type of stimulus along with its parameters for GES pacing for the treatment of gastric motility disorders and obesity. It can also be used for simulating retrograde entrainment of slow wave. The model presented here is directed at providing a realistic description of the mechanism behind GES, to aid in the development of a gastric pacemaker to be used in the treatment of drug refractory gastroparesis, associated motility disorders and morbid obesity.

1.1 Gastrointestinal tract in humans

The gastrointestinal tract (GI tract), also called the digestive tract, alimentary canal or gut, is the system of organs that produces energy and nutrients from food, and expels the remaining waste [7]. In humans, the gastrointestinal tract is a long tube with muscular walls comprising four different layers: the inner mucosa, submucosa, muscularis externa, and the serosa. It is the contraction of the various types of muscles in the tract that propel the food. In a normal human adult male, the GI tract is approximately 6.5 meters (20 feet) long. The GI tract may also be divided into foregut, midgut and hindgut based on their embryological origin [8].

Alternatively, the GI tract can be divided into the upper and lower tract (Table 1.1). The upper GI tract consists of the mouth, pharynx, esophagus, and stomach. The lower GI tract is made up of the intestines and the anus [8].

Table 1.1: Organs of the gastrointestinal tract

Gastrointestinal Tract	Organs	
Upper GI Tract	Mouth, Pharynx, Esophagus, Stomach	
Lower GI tract	Small Intestine	Duodenum
		Jejunum
		Ileum
	Large Intestine	Cecum
		Colon
		Rectum
	Anus	

1.2 Stomach

The stomach is a hollow muscular organ located below the esophagus in the GI tract. It has the ability to expand or contract depending on the amount of food contained within it. It serves as a storage reservoir where the initial mechanical and chemical breakdown of ingested food occurs. When the stomach contracts, the interior walls fold to form rugae; the rugae disappear when the walls relax. The surface along the lateral side of the stomach is called the greater curvature where as the surface on the medial side is referred to as lesser curvature [9].

1.2.1 Anatomy of the stomach

The stomach is commonly divided into three parts namely the fundus, corpus and antrum (Figure 1.1). The fundus is dome-shaped and is located below the diaphragm. The corpus is the largest part and is referred to as the body of the stomach. It can be further subdivided into orad corpus, mid-corpus and caudad corpus. Finally the antrum is connected to the small intestine through the pyloric sphincter [9].

The stomach wall can be divided into four layers: the mucosa, submucosa, muscularis externa and serosa (Figure 1.1). The mucosa is the innermost layer and its surface is coated with an epithelial layer composed entirely of goblet cells. The smoothness of this surface is interrupted by the presence of large number of gastric pits. The second layer is the highly vascular submucosa that helps to absorb nutrients. The muscularis externa possesses smooth muscle layers and is responsible for gastric motility. In the muscularis externa the smooth muscle cells are present in layers with different orientations. The circular layer, whose fibers are oriented circumferentially, plays an important role in formation of peristaltic waves to push the ingested food. The longitudinal layer, with fibers oriented in the longitudinal direction, hold responsibility for changes in the stomach's length. The oblique layer is scarcely distributed in the gastric wall and may have a small role in gastric motility [9]. Interstitial cells of Cajal (ICC) are believed to be the pacemaker cells of the gastric musculature. ICC variants have been found in several locations along the stomach's musculature [10]. In between circular and longitudinal muscle layer ICC-MY are present lying in the plane of myentric plexus. ICC-MY (myentric plexus) posses a greater share in the generation and propagation of slow waves. ICC–IM (intra muscular), placed between the circular muscle layers, plays an important role in the propagation of slow waves [11]. ICC–SEP, lying between the septa of smooth muscle bundles, is believed to conduct stimuli to surrounding muscle layers [12]. The outermost layer, the serosa, is a vascularised connective tissue covering the entire stomach [9].

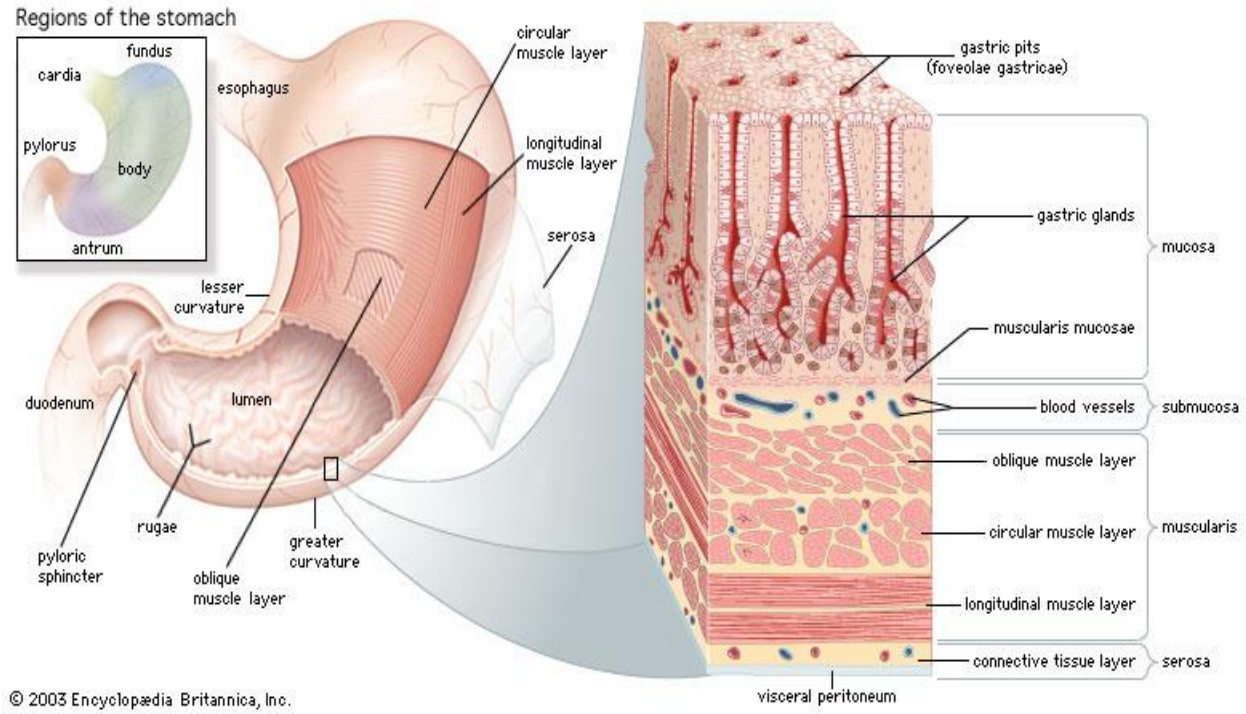

Figure 1.1: A Schematic diagram of anatomy of the stomach and the microstructure of a section of stomach wall (adapted from Britannica encyclopedia (2003)).

1.2.2 Motility in the stomach

Electrical excitability of cells and tissues is a basic function of life. It is the ability of cells to respond to stimuli. The excitability of cells depends on many factors such as the ion distribution and transport mechanisms (ion channels) associated with their plasma membrane structure. The stomach possesses complex motor patterns to aid in the digestion of food which includes mixing and grinding followed by the emptying of ingested food from the stomach into the small intestine when the food particle size has been reduced. The stomach exhibits rhythmic, 3 per minute, coordinated contractions which grind the food into small particles. Intrinsic mechanical activity of the gastric musculature primarily arises from smooth muscle cells (SMC) which possesses the property of contractile behavior to permit the synchronized contraction and relaxation activity on receiving sufficient electrical stimuli [10]. Gastric myoelectrical activity in humans consists of a sequence of electrical potential variations, called slow waves, that are generated at a frequency of about three per minute in proximal gastric corpus along the

greater curvature and these propagate along the gastric wall toward the pylorus. Interstitial cells of cajal (ICC) are currently believed to be the pacemaker cells responsible for the omnipresent electrical activity of the stomach [13]. In the gastric musculature ICCs are electrically coupled to the neighboring ICCs and to SMCs through electrical connections referred to as gap junctions. ICCs are self exciting and are believed to be the origin of slow waves which propagate within the ICC network via gap junctions [14]. The ICC network is extensively ramified, spanning the entire greater curvature sending activation signals in both the circumferential and longitudinal directions.

The existence of gap junctions between SMCs has been an issue of controversy and no specific functional role for such a connection has been proposed [15]. Electrical activity of the SMCs depends on the electrical stimuli supplied by the ICC. When the depolarization reaches a pre determined threshold, the smooth muscle cell membrane depolarizes. This depolarization is followed by contraction [10].

Further to this level of control, the enteric nervous system (ENS), hormonal and paracrine factors (to a small extent) also influence the contractile activity of SMCs. The enteric nervous system regulates the amplitude of depolarization and force of contraction corresponding to the depolarization to a considerable extent. Finally the SMCs compile the input from all the above mentioned sources and produce a corresponding mechanical response. So the intrinsic electrical and mechanical activity of the gastric musculature is generated from the interplay among smooth muscle cells, interstitial cells of Cajal and the enteric nervous system [10]. Figure 1.2 shows the progression of slow wave along different regions of a guinea pig's stomach [16].

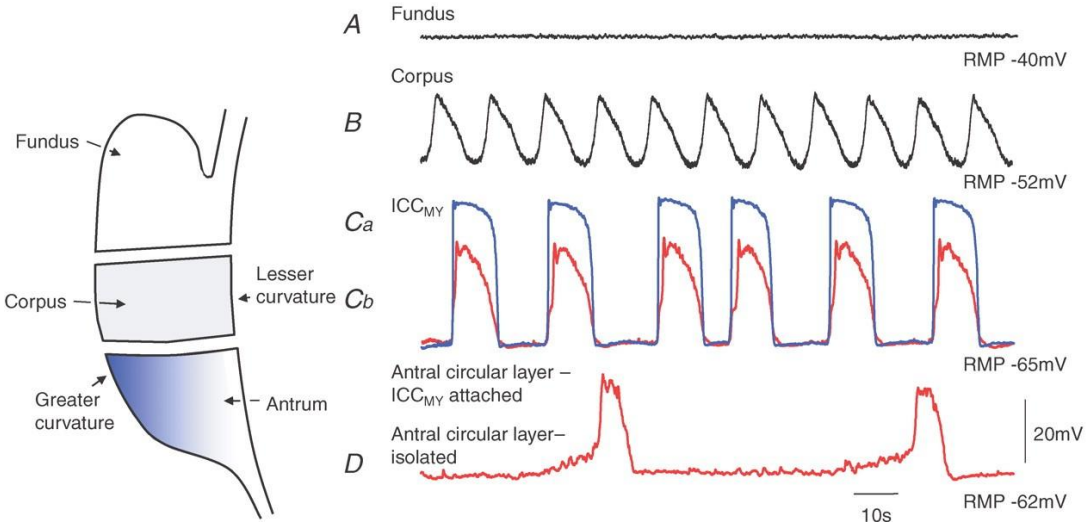

Figure 1.2: Electrical activity recorded from the guinea pig stomach. The trace A shows a electrical activity in fundus. Trace *B* shows slow waves recorded from corpus. The following set of superimposed traces show simultaneous recordings from an ICC-MY (blue trace) and a nearby smooth muscle cell in the circular layer (red trace). Trace *D* shows slow waves recorded in the antrum [16].

In the absence of food gastric myoelectrical activity and hence the synchronized contractions still exist. However, the percentage of 3cpm slow waves will be reduced during pre prandial or fasting state. The maximum membrane potential (amplitude) attained by the slow waves will also be reduced in comparison to the post prandial slow waves [Figure 1.3] [17]. In addition to this the regulation for amplitude of depolarization contributed by the enteric nervous system also decreases. So the smooth muscle cell complies the resulting weak input from ICC and enteric nervous system to produce contractions that are not as strong as in post prandial state, but still exists. Hunger or the feeling to consume food is aroused due the rhythmic contraction of the stomach walls. Gastric contractions are omnipresent but it is felt when the stomach is empty. It should also be noted that the duration of fasting also influences the strength of slow waves and hence the gastric contractions, longer duration of fasting (more than 24 hours) may decrease the contractile activity. This may be the reason for a person not feeling hungry after very long periods of fasting [18].

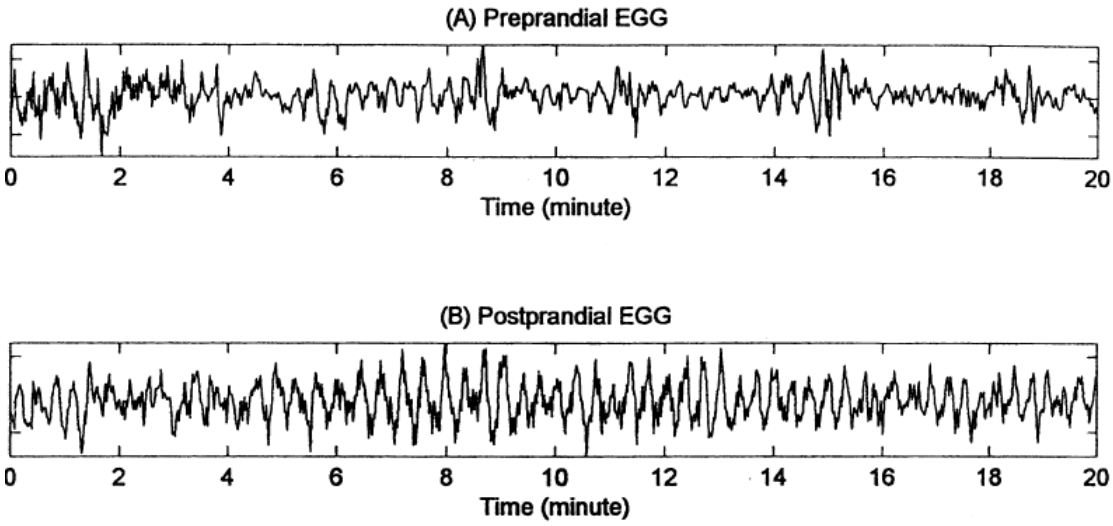

Figure 1.3: Electrogastrogram recorded during A) pre prandial state and B) post prandial state [17].

1.3 Motility disorders of the stomach

A complex level of interacting control mechanisms regulates the stomach's intrinsic electrical and mechanical activity thereby providing an ample opportunity for things to go wrong. Impairment in the stomach's myoelectrical activity are the cause of several known motility disorders (Table 2) like delayed gastric emptying (gastroparesis), rapid gastric emptying (dumping syndrome), and functional dyspepsia, and are associated with clinical symptoms like early satiety, nausea, vomiting and delayed gastric emptying [19]. The causes may include disturbances in the functioning of ICCs, smooth muscle cells, vagus nerve, enteric neurons, or humoral factors. Genetic factors may also contribute since gastric dysmotilities occur predominantly in females. A loss of ICCs is associated with a disruption of the generation and propagation of electrical slow waves, resulting in gastric dysrhythmias and abnormal gastric emptying. Motility disorders are chronic in nature and may lead to a situation of the patient being a societal burden due to decreased productivity.

Table 1.2: Motility disorders in the stomach and their symptoms

Motility Disorder	Symptoms
Gastroparesis	Nausea, vomiting, Poor emptying of the stomach, bloating, abdominal pain
Cyclic Vomiting Syndrome	Recurrent episodes of severe nausea and vomiting
Dumping syndrome	Rapid gastric emptying(jejunum fills too quickly with undigested food from the stomach)
Functional dyspepsia	Pain or discomfort that is felt in the center of the abdomen above the belly button, early satiety (feeling full soon after starting to eat), bloating, or nausea.

1.4 Underlying mechanisms

1.4.1 Gastroparesis

Gastroparesis means stomach paralysis (gastro = stomach and paresis = paralysis). The term refers to a variety of disorders characterized by clinical symptoms like nausea, vomiting, poor emptying of the stomach, bloating and abdominal pain. Many different mechanisms have been identified to be the underlying cause for gastroparesis.

Any disorder that affects even a single constituent of the complex control mechanisms responsible for generation of slow wave can result in gastroparesis. However, the two most established causes for gastroparesis are diabetes and surgery. Postsurgical gastroparesis can result from surgery with or without a vagotomy (surgical procedure for resection of the vagus nerve). The vagus nerve controls the movement of food through the stomach. Gastroparesis occurs when the vagus nerve is damaged and the muscles of the stomach are partially or totally paralyzed. People with diabetes have high blood glucose thereby leading to chemical changes in nerves and damaging the blood vessels that carry oxygen and nutrients to the nerves. As this condition prevails over a period of time high blood glucose can damage the vagus nerve [20].

Apart from demyelination of the vagus nerve, loss of parasympathetic and sympathetic fibers, and severe injury or degeneration of the interstitial cells of Cajal may also be responsible for the pathology of gastroparesis. On the other hand, no underlying etiology can be found in about 40% of gastroparetic patients, a condition called idiopathic gastroparesis [21]. Viral infection has been suspected in some patients with idiopathic gastroparesis, but the association has been based on a history of acute viral-like illness, not by identifying the virus [22]. Hypomotility of the stomach, a condition specific for diabetic gastroparetic patients results in bezoars of indigestible solids and may also attract bacterial growth. Antral hypomotility, pylorospasms, bradygastria (decrease in slow wave frequency) and tachygastria (increase in slow wave frequency) have been described in patients with diabetic and idiopathic gastroparesis [20]. Both tachygastria and bradygastria may result from ICC loss. A patchy disruption of ICC networks may lead to tachygastria or loss of generation of the slow waves, resulting in bradygastria [23].

1.4.2 Functional dyspepsia

Functional dyspepsia is a medical condition characterized by recurrent pain in the upper abdomen, upper abdominal fullness followed by early satiety. Impaired fundic accommodation, visceral hypersensitivity, delayed gastric emptying and *Helicobacter pylori* infection have been postulated to be the underlying cause giving rise to various clinical symptoms of functional dyspepsia. Approximately 30% of patients with functional dyspepsia exhibit gastric hypersensitivity to distension in the fundus and antrum [24]. Even though delayed gastric emptying is present in 23% to 32% of patients with functional dyspepsia it still remains as an object of controversy whether delayed gastric emptying is the underlying cause of dyspeptic symptoms [25]. There exists a poor correlation between *H. pylori* and functional dyspepsia. However it is not known how *H. pylori* can cause symptoms in the absence of a peptic ulcer and gastritis. The presence of *H. pylori* does not appear to correlate with the gastric motor or sensory disturbance associated with functional dyspepsia [26].

1.4.3 Dumping syndrome:

Dumping syndrome is characterized by totally unregulated or chaotic and rapid movement of food and gastric juices from the stomach to the small intestine. This accelerated emptying of food is usually associated with postsurgical changes in the stomach. Dumping syndrome may occur at least mildly in one-quarter to one-half of people who have had gastric bypass surgery. It develops most commonly within weeks after surgery, once the patient returns to the normal diet. The severity of this disorder is directly proportional to the extent of stomach removed or bypass. When the opening junction between pylorus and the duodenum has been severely injured or removed during an operation, dumping syndrome may develop. It at times becomes a chronic disorder. Gastrointestinal hormones also are believed to play a role in this rapid dumping process [20].

1.5 Treatment options

1.5.1 Dietary modifications

Dietary recommendations mainly revolve around adjusting meal content and frequency. Dietary treatments include advising the patient to take 5 to 6 small meals each day instead of 3 large meals. Small proportioned meals are suggested ensuring that the meals are spread throughout the day [27]. The best choices for gastroparetic patients include liquid diet comprising higher quantities of nutrients, such as soups, stews, milk, liquid supplements, fruit juices or smoothies. Solid foods are often better tolerated earlier in the day and the patient is suggested to eat and drink all foods and beverages while sitting up. Fatty foods tend to aggravate the release of hormones to slow down the emptying of the stomach. Therefore, low fat foods are preferred and in severe cases fatty foods are completely avoided [28]. But it is generally observed that these dietary changes are not highly effective in alleviating the chronic symptoms of gastric motility disorders [5].

1.5.2 Prokinetic agents

Prokinetic agents used in the attempt to treat motility disorders have a dismal record of doing harm with little or sometimes no benefit. Most of the gastroparetic patients are refractory to treatment with prokinetic drugs due to the occurrence of severe adverse

effects. For example metoclopramide induces anxiety, tremors, dystonia, Parkinson's like symptoms, and depression. Erythromycin disrupts the bacterial flora in the stomach, promotes antimicrobial resistance. Cisapride has been severely restricted due to risk for prolongation of the cardiac QT interval. Tegaserod has recently been withdrawn from the United States market due to cardiovascular side effects. Domperidone is a prokinetic agent that shows some promise. Domperidone improves gastrointestinal transit with the side effect being it minimally crosses the blood-brain barrier and may be responsible for few central nervous system disorders [29]. However, In addition, tachyphylaxis may occur sooner or later with some drugs, such as domperidone and erythromycin, and refractoriness to prokinetic agents is observed in a significant number of patients [5].

1.5.3 Gastrectomy and enteral nutrition

If dietary and pharmacological treatments fail surgery is considered as a treatment for gastroparesis. Surgery is used to create a larger opening between the stomach and the intestine in order to aid the process of emptying the stomach's contents. Alternatively, the entire stomach may be removed [30]. A jejunostomy tube is a specially designed tube through nutrition can be supplemented to a gastroparetic patient. It is inserted through the skin, directed to the jejunum (a part of the intestines which lies a little way after the stomach).If gastric resection is risky or refused or does not resolve the nutritional problems, the patients must undergo enteral nutrition with a jejunostomy tube [31], provided that there are no motor disturbances of the intestine, such as pseudo obstruction. In the latter case, the patient must undergo permanent parenteral nutrition. Gastrectomy may give rise to potential complications after the surgery.

1.5.4 Gastric electrical stimulation (GES)

From the above sections it becomes clear that in spite of the fact that stomach motility disorders have been tremendous burden to the patient in terms of both the symptoms and an overall decreased quality of life, no reliable treatment option is available there by darkening the future for severe gastroparetic patients. Due to the limited efficacy of all the

above mentioned conventional therapeutic options for gastroparesis treatment, there was a strong need to develop a comparatively efficient alternative treatment option.

No alternative to surgery and chronic parenteral nutrition seems to have been available until 1963, when the concept gastric electrical stimulation was thought as a new approach to cure refractory gastroparesis. Gastric electrical stimulation (GES) is a strategy that aims to modulate GI electrophysiology to ameliorate motility and symptoms in gastroparesis as well as other motility disorders [32]. Electrical stimulation by means of a pacemaker has made a recognized therapeutic contribution in the field of cardiology. However, gastric electrical stimulation remains as an object of controversy and conflicting results have been reported [33]. The principle behind GES is similar and borrowed from cardiac stimulation. But our understanding and the advancement in the development of gastric pacemakers lies far behind its cardiac counterpart.

Gastric electrical stimulation is an approach that aims to restore recurring myoelectrical activity. It has been shown to be effective in normalizing gastric dysrhythmia, accelerating gastric emptying and improving nausea and vomiting [34]. During the past decade, a considerable amount progress has been made on the effects, mechanisms and clinical applications of gastric electrical stimulation (GES). This research project focuses on gastric electrical stimulation of stomach. Even if the solution is focused on curing the gastric dysrhythmia in the stomach the concepts behind GES are general and can be extended to other organs of the GI tract such as the small intestine.

1.6 Gastric electrical stimulation: effects and mechanism

Gastric electrical stimulation is usually carried out by injecting series of rectangular pulses with a constant current into the outer most layer, (serosa) that wraps the entire stomach. Methodologies of electrical stimulation depend on a number of factors including patterns of stimuli, placement of electrodes and delivery time of stimuli. Frequency, pulse width and amplitude are the three most important stimulation parameters involved in electrical stimulation. Various methods of electrical stimulation are derived from the variations of

these three parameters [34]. In this section, various methods published in the literature are summarized and critically discussed.

1.6.1 Long-pulse stimulation

Long–pulse stimulus is characterized by of repetitive electrical pulses with a pulse width in the order of milliseconds (10–600 ms), and a stimulation frequency near the physiological frequency of the gastric slow wave (0.05 Hz) (Figure 1.4). Long pulse stimulus is able to entrain slow waves at the stimulated frequency and hence improves gastric motility [35]. However, currently implantable devices available in not capable of generating electrical pulses with a width longer than 2 ms [34].

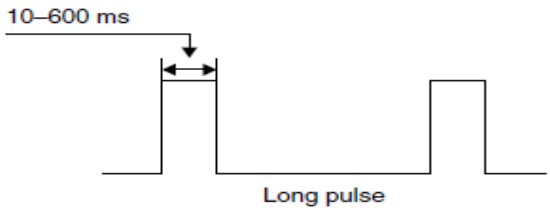

Figure 1.4: Long pulse stimulus adapted from [34].

1.6.2 Short-pulse stimulation

In contrast to long-pulse stimulation, the pulse width in this method is comparatively shorter and is in the order of a few hundred microseconds. The stimulation frequency is usually a 3 - 4 times higher than the physiological frequency of the gastric slow wave (Figure 1.5). GES with short pulses is known to improve symptoms of nausea and vomiting in patients with gastroparesis [36]. However it does not affect the intrinsic slow wave activity. Commercially available gastric pacemakers are able to generate short pulses [34].

Figure 1.5: Short pulse stimulus adapted from [34]

1.6.3 Trains of short-pulses

In this method, the stimulus is composed of repetitive trains of short pulses with a control signal. It posses continuous short pulses with a high frequency (in the order of 5–100 Hz) and a control signal to turn the pulses on and off. The control signal determines the frequency of the pulse train (Figure 1.6). Trains of short pulses were designed to mimic long – pulse stimulus and obtain its effects on gastric myoelectric activity through short pulses. Commercially available stimulators are capable of generating trains of short pulse stimuli [34].

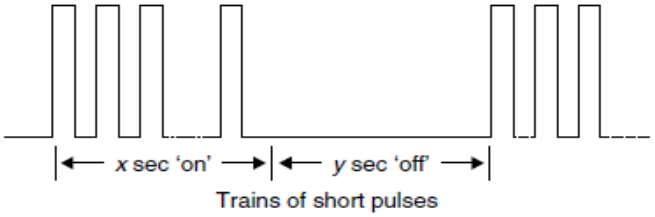

Figure 1.6: Trains of short pulses [34]

1.6.4 Dual pulse stimulus

Dual pulse GES is a combination of short pulses and long pulses. Usually a dual pulse stimulus is composed of a short pulse (in the order of a few hundred microseconds) followed by a long pulse (in the order of a few hundred milliseconds) (Figure 1.7). Dual pulse GES was designed to obtain the combined effects of long as well as short pulse stimulus, i.e., both normalizing gastric dysrhythmia and improving symptoms suggestive of nausea and vomiting. As a result, the proposed method of dual pulse GES is more efficient and attractive than the conventional single duration method of electrical stimulation [34].

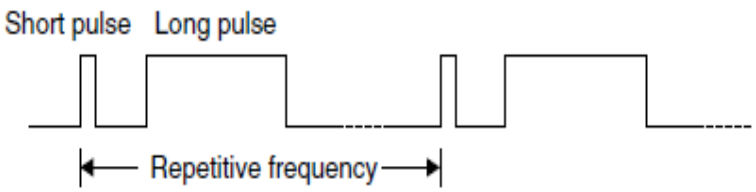

Figure 1.7: Dual pulse stimulus adapted from [34]

1.6.5 Synchronized stimulus

Each gastric slow wave represents the depolarization of gastric smooth muscles, hence it was expected that the electrical stimulation injected on detecting the occurrence of the already existing slow waves (Figure 1.8) was to enhance the depolarization process and apparently improve the existing gastric contractions. It requires the implantation of two pairs of electrodes, one for the detecting intrinsic slow waves and the other for stimulation [34]. Synchronized gastric electrical stimulation was able to normalize gastric emptying in diabetic mice with gastroparesis [37].

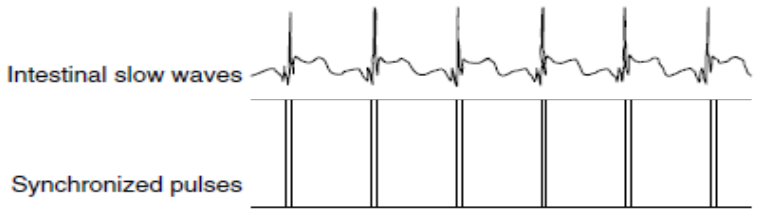

Figure1.8: Synchronized stimulus adapted from [31]

1.6.6 Enterra therapy

The Enterra system (frequency: 14Hz, 0.1seconds on and 5 seconds off, duration: 0.3ms, amplitude: 60µA), a low energy high frequency gastric electric stimulation, was approved by the FDA under the humanitarian use device designation in 2000 for treatment of patients with refractory nausea and vomiting due to gastroparesis. The symptoms of nausea and vomiting improve considerably with application of Enterra therapy, as do quality of life and nutritional status in gastroparetic human volunteers. The mechanism of action of Enterra therapy is still not known; the data suggest that afferent neural mechanisms and perhaps modulation of gastric biomechanical activity may play a role [38].

1.6.7 Implantable device

Any of the above mentioned stimuli can be delivered to the outer most layer of the stomach wall with an implantable, pacemaker-like device which is similar in size and function to a cardiac pacemaker with electrodes at one end. However, currently the device is used to deliver only Enterra Therapy parameters. The device implantation is carried out under general anesthesia. The stimulation electrodes are sutured to the outer lining of the stomach wall and connected to the device, which is implanted just under the skin on the abdomen. The connector of each lead is attached to a device, placed in the abdominal wall under the patient's skin [39].

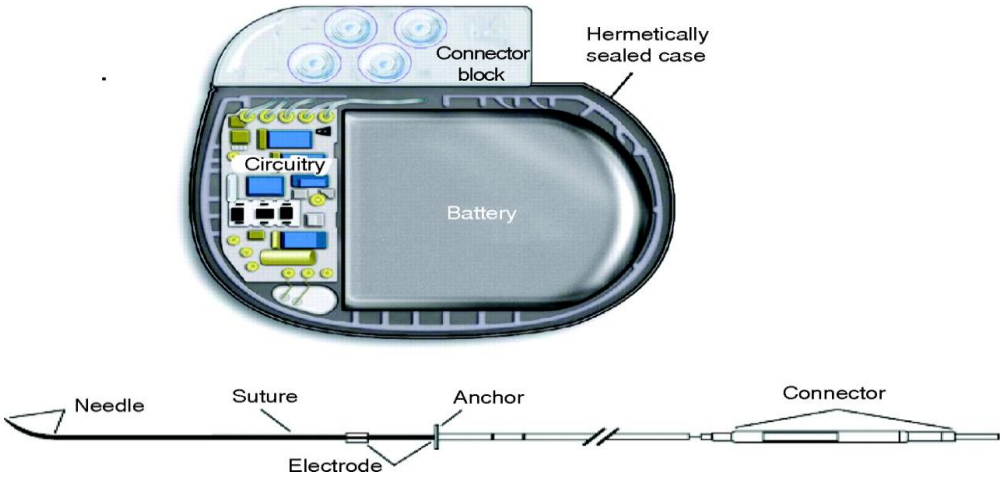

Figure 1.9: Implantable device Enterra adapted from [40].

1.6.8 Single channel vs multi channel GES

Single channel GES, as the name implies, is the technique of injecting electrical impulses through a single set of electrodes usually placed in the proximal corpus to deliver one channel of stimuli (Figure 1.10a). In a healthy stomach a slow wave originates in the proximal corpus and propagates circumferentially and distally towards the pylorus. The principle behind single channel GES is that an electrical stimulus applied through the proximal stomach would propagate distally and normalize abnormalities in the stomach. The proximal to distal propagation of slow waves is referred to antegrade propagation whereas the reverse propagation of slow waves (distal to proximal) is called retrograde propagation.

The distal stomach plays a crucial role in the emptying of food particles from the stomach to the duodenum. It was thought that stimulating the distal stomach may be more effective in alleviating the symptoms of gastroparesis. However, a single electrode stimulating the distal stomach has a higher probability of triggering retrograde pacing of gastric slow waves. This would result in a further delay of emptying rather than acceleration. Multi-channel GES (Figure 1.10b) delivers electrical pulses to multiple locations along the greater curvature of the stomach. It can be used to mimic the natural propagation and characteristics of the slow wave. Two- to four-channel GES has been proposed in a number of studies [41], [42], [43], and [44].

a) b)

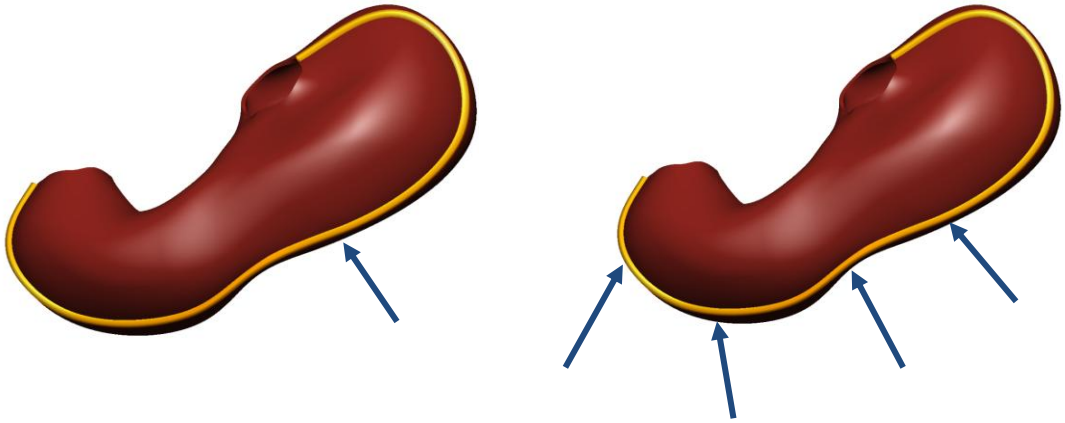

a) Single channel GES b) Multi channel GES

Figure 1.10: Blue arrow indicate the position of the electrodes

1.7 Morbid obesity and GES

Obesity is a growing worldwide epidemic. In the United States, nearly one-third of adults are obese (body mass index, BMI >30%). Morbid obesity or clinically severe obesity affects more than 15 million Americans and causes an estimated 300 000 deaths per year [6]. Obesity creates major health problems because of its co-morbidities, such as type 2 diabetes and cardiovascular diseases. Treatment of obesity and its primary comorbidities costs the US healthcare system more than $100 billion each year. GES has proposed as an innovative method to reduce weight in morbidly obese individuals [45]. While various

methods of GES have been under investigation for the treatment of obesity, clinical studies have been confined to the use of GES with trains of short pulses. GES has been proposed to increase the feeling of satiety with subsequent reduced food intake and weight loss [35].

1.7.1 Retrograde gastric pacing (RGP)

The principle of RGP in treatment of obesity is to impair the intrinsic electrical activity resulting in satiety and a reduction of food intake. RGP is delivered at a tachygastrial frequency in the distal stomach to set up an artificial ectopic pacemaker. This artificial ectopic pacemaker may result in retrograde propagation of electrical waves. Consequently, gastric dysrhythmia is induced and the regular propagation of gastric electrical waves is impaired. This hypothesis was tested in a number of animal studies [46]. RGP was shown to impair normal gastric slow waves, induce tachygastria, delay gastric emptying, and reduce food intake due to early satiety in dogs, and resulted in weight loss in obese rats [47] [48].

1.8 Thesis overview

This thesis focuses on the development of a realistic computational model for gastric electrical stimulation and is directed to performing an investigation of its potential as a medium for exploring the efficiency of different types of GES as well as to examine the physiological significance of various stimulus protocols. A general overview of the gastric musculature, physiology, motility disorders and the need for gastric electrical stimulation is discussed in Chapter 1. Experimental work carried out in GES will be covered in the first section of Chapter 2. Following this, in the second section of Chapter 2 a critical literature review of previous modeling work in this area is presented. In Chapter 3, detailed descriptions of previously developed single cell models of ICC and SMC and extended bidomain framework for gastric musculature will by explained. Following this, light will be thrown on the development of the GES model from the extended bidomain framework. Chapter 4 highlights the results obtained with single channel GES. Different stimuli protocols that are currently practiced in experimental GES are modeled and their

efficiency as single channel GES is demonstrated. In Chapter 5, detailed descriptions of various stimuli protocols when delivered as multi channel GES are presented. In Chapter 6 capability of the GES model to trigger retrograde propagation of slow waves for obesity treatment has been discussed. Chapter 7 presents the concluding remarks and outlines the potential future work. Figure 1.11 presents schematic of the GES modeling framework developed in this research project.

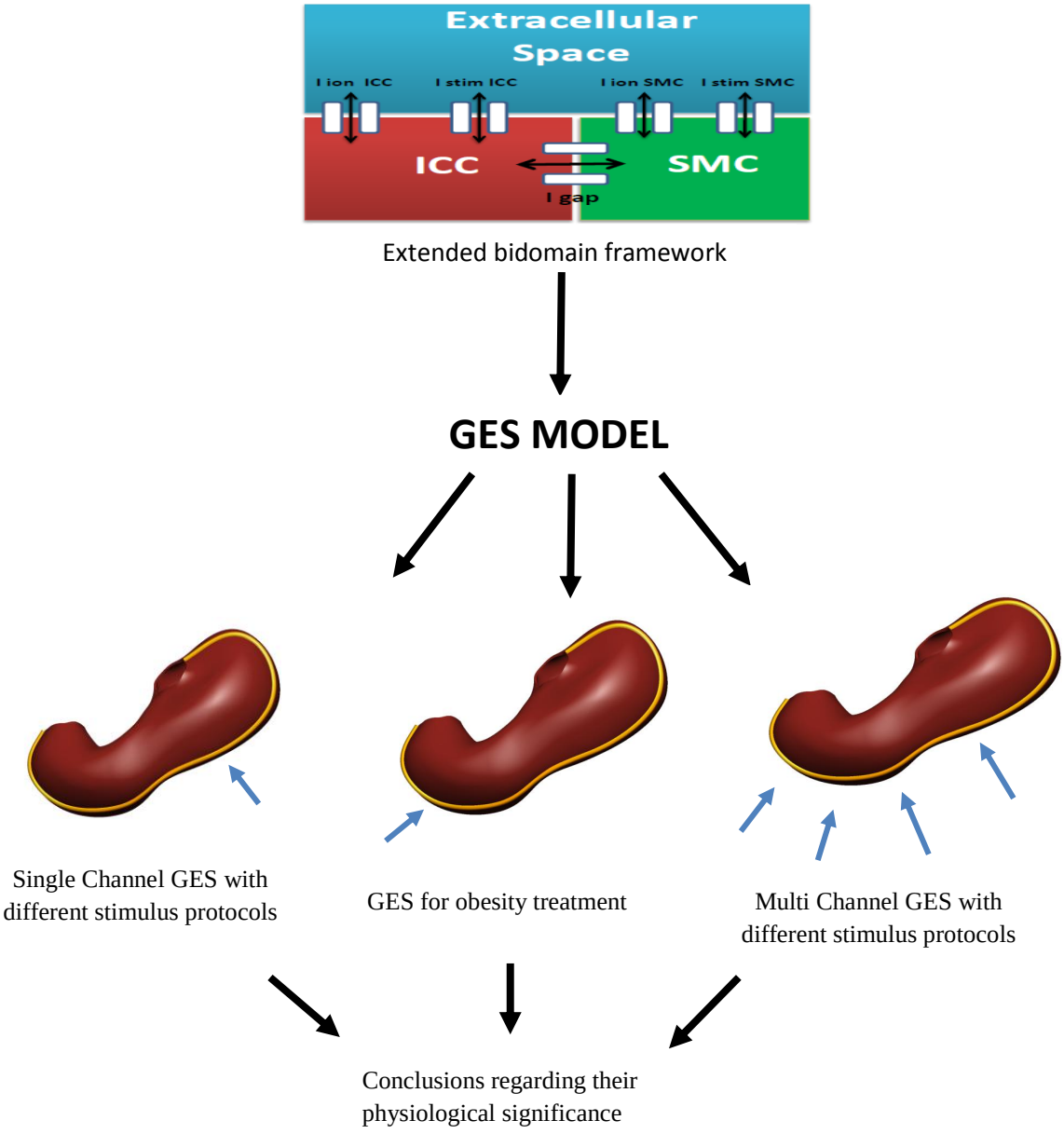

Figure 1.11: Schematic of the GES modeling framework developed in this research project. Blue arrows indicate position of electrodes.

Chapter 2

GES Review

The therapeutic potential of GES has gained importance in the last few decades. A number of experimental studies have been carried out to explore the feasibility of different types of stimuli, as mentioned in the previous chapter, and their efficiency in treating gastroparesis and obesity. In Section 2.1 the experimental work on GES will be discussed. Following this in Section 2.2 computational models in the area of GES that have been developed in the past few decades are described in detail. For each model an assessment of its strengths and weaknesses is provided.

2.1 Review of experimental work on GES

GES for the treatment of gastroparesis

Experimental studies for gastroparesis are usually carried out in dogs, diabetic mice and sometimes in human volunteers. The patient is operated on, under anesthesia and electrodes are affixed on to the serosal layer of the stomach by means of non absorbable sutures. The electrode wires are brought out through the anterior abdominal wall percutaneously and placed under a sterile dressing. Sometimes, in the case of human gastroparetic volunteers instead of bringing out the wires they are fixed to the implantable Enterra device which is placed beneath the abdominal wall. The electrodes are arranged in an arching line along the greater curvature (for treating gastroparesis) and along the lesser curvature (for treating obesity) from the corpus to the pylorus. Generally, electrodes are placed in pairs with a distance of 1 – 0.5 cm between them, the former electrode for injecting the stimulus and the latter for recording the resulting myoelectrical activity. The most proximal electrode pair is at least 14 – 20 cm from the pylorus with an inter electrode pair distance of 2 - 4cm. For single channel GES, the stimulus is applied through the most proximal electrode set alone. In the case of two channel GES; the stimulus is

applied via the first and the third pairs of electrode. For multi channel GES (usually 4 channels) the stimulus is applied through 4 electrode pairs, covering entire length of the corpus and antrum.

2.1.1 Long pulse stimulus

Chen et al (2005) has shown that multi channel GES in dogs with stimulus parameters of amplitude 6 mA, width 550ms and at a frequency 10% higher than the intrinsic frequency was more efficient in terms of entrainment and consumed less energy in comparison to single channel GES with the same stimulus parameters [42]. McCallum et al (1998) have reported that in humans GES with stimulus parameters of amplitude 4 mA, width 300ms and at a frequency 10% higher than the intrinsic frequency was effective for entrainment of the gastric slow wave. Further they have reported that gastric pacing with this stimulus substantially reduced the gastric emptying time and alleviated other symptoms of gastroparesis (nausea, vomiting, bloating and abdominal pain) at the end of the outpatient treatment [49]. Lin et al (2010) also confirmed the efficiency of the stimulus reported by McCallum et al and with a reduction in the width of the stimulus to 3 ms or stimulus amplitude to 2 ms entrainment of slow waves ceased [50]. Xing et al (2003) based on the experimental studies conducted on dogs have concluded that maximal driven frequency for GES with long pulse stimulus was 6 cpm (compared to intrinsic frequency of 5 cpm in dogs). Duration of the stimulus was varied between 0-650 ms with a range of amplitude from 1 - 6 mA [51]. Conclusions reported by Xing and Chen (2006) suggest that long pulse GES in dogs induces gastric relaxation irrespective of the location of the electrode pair along the grater curvature along with a reduction in gastric volume and accommodation [35]. Song et al (2005) has shown that two channel GES in dogs with stimulus parameters 1 mA and 0.6 mA for first and second electrode respectively, a pulse width of 200 ms and with a frequency 1.1 times the intrinsic frequency entrained gastric slow waves as well as improved delayed gastric emptying induced by vasopressin in comparison to single channel GES with the same frequency (stimulus and width 5 mA and amplitude 550 ms) [41].

2.1.2 Short pulse stimulus

Abell et al (2002) has reported that short-pulse stimulation is effective against nausea and vomiting with no or little effect on gastric dysrhythmia, slow waves, or gastric emptying. The authors have employed a stimulus with amplitude 5mA, at a frequency of 12 cycles per minute, injecting 2 discrete pulses of duration 330μS with an inter pulse interval of 70ms [52]. Song et al (2006) have concluded that short-pulse GES with a pulse width of 0.3 ms and frequency of 14 Hz is most effective in preventing vasopressin induced emetic responses in dogs [53].

2.1.3 Pulse train stimulus

Mason et al (2005) has reported that delivering a pulse train stimulus (width : 330 μs, amplitude 5 mA, frequency 14 Hz, cycle on for 0.1 sec and off for 5.0 sec) by means of an implantable device to humans volunteers ameliorated gastroparetic symptoms and improved gastric emptying rates [54]. Yang et al (2009) showed that application of pulse train stimulus through two channel GES with stimulus parameters of pulse frequency 30 Hz, amplitude 5 mA, duration of 8 ms train on time of 3 sec and off time of 8 sec accelerated gastric emptying in healthy dogs. They have also reported that pulse train stimulus below a duration of 4 ms could not produce the desired effect [55]. Lei and Chen (2009) based on experimental results on dogs has suggested that effect of GES varies with stimulus injection site and stimulation conditions. Stimulus (40 Hz, 5 mA, 0.3 ms, 0.1s on, 5 s off) injected into lesser curvature increased gastric volume. On the other hand, changing the stimulation site to greater curvature decreased the gastric volume [56]. McCallum et al (2010), based on his experimental results in human volunteers, concluded that in patients with diabetic gastroparesis 6 weeks of GES therapy with Enterra significantly reduced vomiting and gastroparetic symptoms. Patients had improvements with chronic stimulation after 12 months of GES, compared with baseline [38].

2.1.4 Dual pulse stimulus

Song et al (2007) introduced dual pulse stimulus where a combination of short pulse and long pulse is delivered. They have reported that 2 channel dual pulse GES is able to

accelerate gastric emptying, improve dysrhythmia and emetic responses induced by vasopressin in dogs. The stimulus parameters employed were 1 mA for a duration of 0.3 ms (short pulse) followed be 200 ms (long pulse) separated by 1 sec gap at a frequency of 6 cpm [57].

2.1.5 Synchronized stimulus

Song et al (2007) have reported that synchronized gastric stimulation (SGES) with pulse width 4 ms and amplitude 2 mA was capable of increasing the gastric emptying time in diabetic gastroparetic mice without producing any significant effect on gastric slow waves [37]. Chen et al (2008) have shown that SGES normalized impaired gastric accommodation induced by vagotomy. Application of SGES enhanced rhythmicity and amplitude of gastric slow waves in the antrum [58].

2.1.6 GES for obesity treatment

Yao et al (2005) has observed that retrograde pacing of the stomach with long pulse stimulus (5 mA for 500 ms) at tachygastrial frequency of 9 cpm resulted in a significant reduction of food and water intake with a delay in gastric emptying in human volunteers [59]. Zhang et al (2009) employed two different pulse trains stimulus (A: 6 mA, 0.3 ms, 40 Hz, 2 s on, 3 s off, B: same as A except duration increased to 3 ms) and observed that GES with wider pulses (B) was more potent in reducing the body weight and reducing body weight [60].

2.2 Review of GES models

2.2.1 Relaxation oscillator model: Sarna et al (1972) [61]

Sarna et al used an array of bidirectionally coupled relaxation oscillators as the origin of gastric slow wave activity (Figure 2.1). The term “control potential” used by the authors in the paper can be assumed to be synonymous with the term “depolarization of ICC” that is in usage currently. The authors called any control potential before the predicted time of occurrence of a normal control potential as a premature control potential (PCP). A

Premature control potential in an oscillator was produced by applying electrical pulses of amplitude 60V at the input of the oscillator. The earliest that a PCP could be produced was 75% of the period control wave cycle. Application of an input pulse at 50% of period of wave cycle could be carried out but with no effect on the control waves. The term propagation was used to imply to the phenomenon in which the occurrence of a control potential (normal or premature) causes the control potentials to be initiated in the neighboring oscillators. The propagation of PCP in the proximal and distal directions depended on the time of their occurrence and based on the refractoriness and threshold properties of the neighboring oscillators (Figure 2.2). The refractoriness of an oscillator depended to a great extent on its coupling to the neighboring oscillators. Coupling an oscillator to increasing number of oscillators not only increased it threshold values but also lengthened its absolute refractory period. The results of the model were tested in dogs.

This publication should be credited for having given a start for mathematical modeling of GES. The premature control potential used by the authors here is synonymous with gastric electric stimulation, making the oscillators respond to an external stimulus to produce control wave activity, keeping in mind the refractoriness and threshold property of the oscillators.

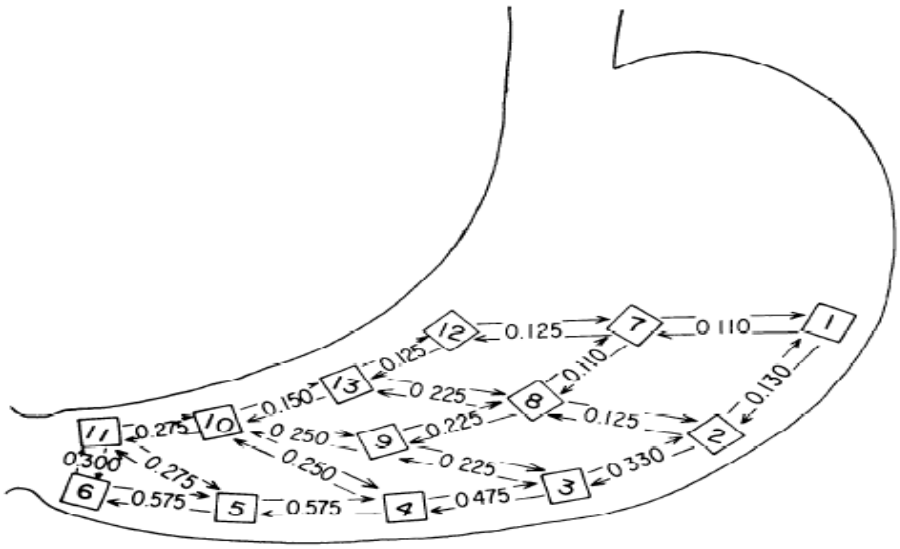

Figure 2.1: Arrangement of oscillators in gastric ECA model developed by Sarna et al (1972).

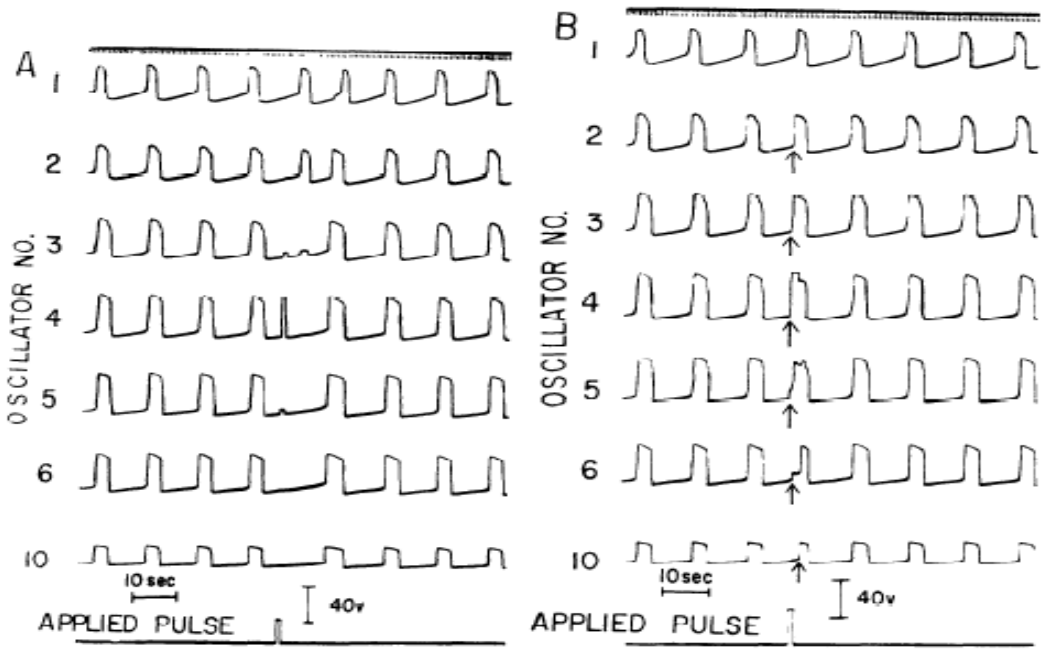

Figure 2.2: Results obtained by Sarna et al (1972). A) input pulse applied to 4th oscillator after 9 seconds of beginning of control wave cycle. B) input pulse applied to 4th oscillator after 7 seconds of beginning of control wave cycle.

Unfortunately, due to lack of understanding concerning the electrophysiological role of the ICC at that time, the relaxation oscillator approach was quiet elementary. Also the model did not take into account the multiple cell types involved gastric myoelectric activity. The concept of refractoriness has not been explained in terms of ion permeability changes. A comparison of the lengths of proximal and distal propagations in the model to the dog's stomach was limited due to smaller number of oscillators present in the model compared to the stomach. Overall this model paved the way with an idea for modeling gastric electric stimulation of the stomach.

2.2.2 Conoidal Dipole Model: Mintchev et al (1997) [62]

Mintchev et al developed a model based on the assumption that local non propagated contractions can be produced circumferentially using four rings of stimulating electrodes. The temporal and propagation organization of gastric electric activity were used to derive the geometry of stimulating electrodes and the time shifts for phase locking of the electrical stimuli applied to the circumferential electrode set. The authors were of the opinion that the conical dipole approach stimulates the cholinergic nerves directly hence producing artificially propagated circumferential contractions. The charge distribution on each side of a given polarized cells in the ring is considered to be approximately equal and the number of polarized cell in the ring remains the same but the density of the cells increases in the distal direction with a decrement of S where S is the area S of a δ wide ring of depolarized cells represented as dipoles pointing towards the center was given by Equation 2.1.

$$S = 2 * \pi * \delta * r(t) \tag{2.1}$$

Here, $r(t)$ is the radii of dipoles that circles that built up the ring of dipoles. The relationship between vector of dipole density D and vector of equivalent dipole moment P is given by Equation 2.2.

$$D = P/S \tag{2.2}$$

A net of circumferential stimulating electrodes was built up on the truncated conoid representing the stomach. All active electrodes and all reference electrodes in a given circumferential setup were separately short-circuited. Four separate circumferential setups each having 6, 5, 4, and 3 electrodes respectively were used. The inter electrode distance in each set of circumferential electrode was also calculated.

The model takes into account the phase shift that is to be present between the stimuli injected through set of circumferential electrode. Each subsequent set of stimulating electrodes was located at a position corresponding to the maximal allowed duration of the stimulation train, in this case 4 seconds. The model predicts the position and geometry of the stimulating electrodes along with the actual pace locking of the stimulus. The major assumptions and results of the model were tested on two unconscious dogs. Propagation of electric activity along the length of the stomach is not considered as the scope of the model is restricted with producing local non propagated contractions. The mathematical model does not consider the electrophysiology of ICC and SMC in gastric electric activity. Ultimately, the model lacks a sound electrophysiological foundation on which any GES model should be built upon.

2.2.3 Model of nonlinear coupling mechanisms of gastric slow wave propagation: Wang et al (2000) [63]

Wang et al have constructed a mathematical model implemented with a SIMULINK circuit to simulate normal and dysrythmic gastric slow waves. The effect of GES is applied to the model by means of the SIMULINK circuit. Even though the authors have stated two mechanisms that may be responsible for generation of gastric dysrhythmia i.e., impairment in the pacemaker cells or abnormal coupling in between the pacemaker cells the mathematical model has been developed on the hypothesis that non linear coupling between the pacemaker cells generates gastric dysrhythmia. Nonlinear Van der Pol's equation has been used to model gastric electric activity of the pacemaker cells as follows:

$$\frac{dx_1}{dt} = x_2 \quad (2.3)$$

$$\frac{dx_2}{dt} = -\beta(1 - x_1^2)x_2 - \omega^2 x_1 \quad (2.4)$$

Where, $x_1$is the extracellular potential, $x_2$is the membrane current, ω ($\omega = \frac{2\pi}{T}$) is the frequency parameter and β is a parameter determining the waveform. The authors have highlighted the importance of the following four characteristics of the coupling mechanism i.e., electrical capacity coupling (gap junctions), electric filed coupling, non linear characteristics and resistance. A value of 20s and 2.2 has been adopted by the authors for T and β respectively in order to simulate gastric slow waves close to the real wave form at a frequency of 3 cpm. Gastric dysrhythmia has been simulated by altering the parameters associated with the coupling mechanisms. The simulated gastric dysrhythmia was normalized when an external stimulus of appropriate amplitude was delivered at intrinsic frequency as well as 5% above the intrinsic frequency. The authors have reported an increase in amplitude to normalize gastric dysrhythmia when the stimulus is delivered at frequency higher than the intrinsic one. The model should be appreciated for simulating gastric dysrhythmia based on an underlying mechanism and thereby attempting to normalize it using GES. However it should be noted that in most cases damaged or severely injured pacemaker cells are responsible for gastric dysrhythmia. The model is a pure electrical model and hence does not highlight the importance of the electrophysiological background of the pacemaker cells. Moreover the model is constructed using Van der Pol's equation which may not generate the accurate gastric slow wave profile. The coupling mechanisms that the authors have adopted have not been clearly explained. Inspite of including the coupling mechanism the propagation of the stimulated gastric electric activity has not been established. So, the major limitation of the model is that more stress is laid on the electrical concepts hence completely ignoring the biological background of the gastric dysrhythmia. As a result no conclusive results can be drawn from an electrical model to solve the biological problem of gastric dysrhythmia.

2.2.4 Three dimensional object oriented model: Rashev et al (2002) [64]

A 3-D object oriented electromechanical model of the stomach was constructed for the purpose of microprocessor controlled functional stimulation. Anatomical modeling of the stomach was carried out using generalized cylindrical surfaces. The stomach was modeled using generalized cylindrical objects, fitting them axially to produce a continuous and monotonous surface. Distal antrum was represented by toroid, proximal antrum, proximal and distal corpus and fundus by a conoid. Utilizing a predefined set of initial and boundary conditions gastric electric stimulation was modeled with different values of stimulating voltage by numerically solving Laplace's equation for electric potential in a 2-D, linear, homogenous and isotropic medium.

$$\frac{\partial^2 \mathrm{U(x,y)}}{\partial \mathrm{x}^2} + \frac{\partial^2 \mathrm{U(x,y)}}{\partial \mathrm{y}^2} = 0 \qquad (2.5)$$

The coordinate variables x and y were defined in the intervals x [0; l] and y [0; h] where l and h are horizontal and vertical dimensions of a patch respectively. The field strength was calculated from the gradient of the potential distribution

$$\mathrm{E_{ext}} = -\nabla \mathrm{U(x,y)} \qquad (2.6)$$

The Laplace's equation was solved with a MATLAB stimulator implemented with standard finite difference expansion methods for solving linear partial difference equations. Stimulating electrodes are viewed as linear voltage sources of equal and opposite magnitude (V+ and V-) located on the grid surfaces of the stomach. Considering the electrophysiology of smooth muscle contraction it was assumed that voltage fluctuations can be artificially induced by a) electrical stimulation of cholinergic nerves to release acetylcholine b) direct stimulation of SMC via an externally generated electric field that dominates the spontaneous intrinsic gastric electric activity. The problem of electromechanical coupling was addressed by describing an elementary stress distribution followed by calculation of elementary deflection after quantification of stimulating electric filed. Video clippings from canine experiments were used to obtain contraction shapes to aid in electromechanical coupling process. The model should be commended for

theoretically explaining the production, synchronization and propagation of invoked circumferential contractions with an advantage of electromechanical coupling. Also this model is the first attempt to develop a 3-D model of the stomach for GES. The model has used parametric modeling approach with an edge for producing patient specific configuration of patient specific electrodes and voltage sequences. On the other hand the model aims at directly producing artificial contractions by direct stimulation of SMC thereby completely ignoring the electrophysiological role of ICC in gastric myoelectric activity. As the main focus is to develop a 3-D model of the stomach with electromechanical coupling less stress is laid upon pure electrical activities in the stomach. The authors are of the view that GES is different from gastric pacemaking, while the latter assumes the underlying cause for gastric motility disorders when the former aims at directly producing artificial contractions (neglecting the role of ICC).

The field problem of high frequency GES was modeled using 2-D Laplace's equation (as it was assumed that electric field was homogenous in a direction perpendicular to the gastric plane) which may not accurately replicate the physiological gastric electric activity. Succinctly the model can be considered as a very good and the first attempt for 3-D electromechanical coupling for GES ignoring the role of the gastric pacemaker cells.

2.2.5 Rule based computer model of GEA: Familoni et al (2005) [65]

Familoni et al have developed a Matlab-based analytic model of gastric electrical stimulation considering the interaction between tissue electrical refractoriness and the onset of tissue activation. The model was used to analyze the results of GES in dogs as well as in predicting what configuration of stimulation may be required to regularize a given abnormality. Intrinsic gastric electrical activity (slow waves) is considered to be a recurring cycle of cellular depolarization and repolarization and has been referred to as electrical control activity by the authors. Fluctuations in the concentrations of sodium, calcium and potassium ions around the cell are assumed to be the reason for potential oscillations. Hodgkin Huxley approach has been adopted to model the potential oscillations (fluctuations) in ionic concentrations around the cell. The resulting electric control activity [$e_i(t)$] was periodic with a period (T_0) of 20 seconds in humans. The stimuli threshold value was

modeled as an exponentially decreasing function of time in the relative refractory period as mentioned below (Figure 2.3). The stimulation code was writtern in MATLAB with the major assumptions contained in a rule–based algorithm.

$$A(t) = \text{infinity at } t < T_{ar} \quad (2.7)$$

$$A(t) = A_0 \, e^{(\alpha/(t-T_{ar}))} \text{ at } T_{ar} <= t <= T_{ar} + T_{rr} \quad (2.8)$$

$$A(t) = A_0 \text{ at } t > T_{ar} + T_{rr} \quad (2.9)$$

Here, T_{ar} is the absolute refractory period, T_{rr} is the relative refractory period and α is a constant chosen by the authors.

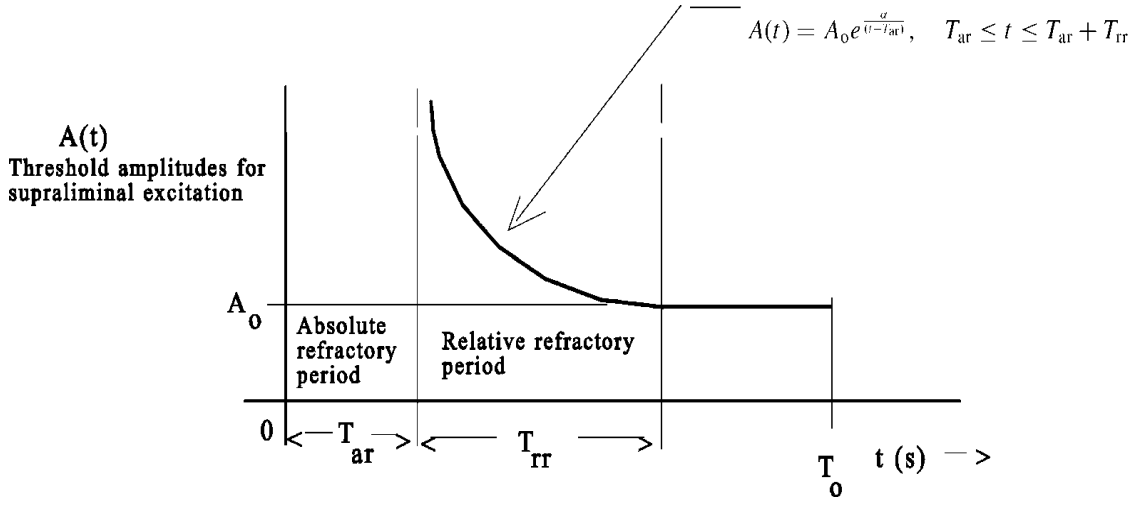

Fig 2.3: Temporal characteristics of the threshold stimulus adapted by Familoni et al (2005).

Entrainment of native electrical activity by the pacing signal results in a dominant frequency. For the purpose of quantifying the stability of the model when stimulated at a frequency higher than the intrinsic one, a wobble factor was defined. It was calculated as the ratio of sum of changes in the dominant fundamental frequency to the duration. This factor mirrors the efficiency of the stimulated response. The strength of model is that it comes with an advantage of user ascribing the values for T_0,T_{rr},T_{ar}. The authors have preferred the usage of a general term “cell” rather than specifying gastric pacemaker cells

or the ICC's. The paper does not throw light on electrophysiology of the "cell" considered on which the model of GES is based. The fluctuations of only three ions, namely sodium, potassium and calcium have been taken into account which may not be sufficient to describe the complete electrophysiology of the "cell" considered. The model ignores the fact that chloride channel have also been functionally characterized in gastric pacemaker cells, taking part in generation of gastric electric activity. Further the authors have not made an attempt to incorporate the electrophysiological role of SMC and hence its electrical activity. The problem of entrainment across oscillating regions that would be responsible for the propagation of the response to simulation has not been examined. Local entrainment will result in a contractile response but will not result in transportation of chyme. The question of whether electrical entrainment translates into motility is not handled by this model. So, these discrepancies would prevent the user from depending on this model for reliable conclusions for optimizing the parameters for gastric electric stimulation.

2.2.6 Tissue framework for GES: Du et al (2009) [66]

The model is based on the concept of multi-scale modeling providing an integrated description of electrophysiological events from the cellular level to tissue level (by using cell models). The mathematical model was developed by taking into account the electrophysiology of ICC and SMC there by treating them as two interconnected tissue domains. Each layer was represented as a 2-D continuum tissue, into which mathematical descriptions of the ICC (Corrias and Buist, 2008) and SMC (Corrias and Buist, 2007) were implanted. A cellular automata algorithm was used to simulate the entrainment of single cell behavior in the ICC layer (Figure 2.4). The automata algorithm also checked whether entrainment occurred in advance of a pacemaker potential arising due to the intrinsic frequency in the resting ICC continuum cell. The counter of the resting ICC was then assigned "delay time" before the next pacemaker event occurred. The time delay (n) was calculated using the following equation:

$$n = (d/V_{circ}) * sqrt(1 - (1 - V_{circ}^2/V_{long}^2) * \cos^2(\theta)) \quad (2.10)$$

Here *d* and θ are the distance and angle between the resting and depolarizing ICC, respectively, and V_{circ} and V_{long} are the conduction velocities in the circular and longitudinal directions respectively. A monodomain approach was adopted to model the conduction of electric activity in smooth muscle cells.

$$\nabla \cdot (\sigma_i^{SMC} \nabla V_m^{SMC}) = A_m^{SMC} (C_m^{SMC} \frac{\partial V_m^{SMC}}{\partial t} + I_{ion}^{SMC}) \quad (2.11)$$

Where, σ_i^{SMC} is the conductivity in the intracellular space, I_{ion}^{SMC} is the SMC ionic current, A_m^{SMC} is the surface area of the membrane per unit volume, C_m^{SMC} is the membrane capacitance, V_m^{SMC} is the potential difference across the cell membrane i.e. the difference between the intracellular and extracellular potential.

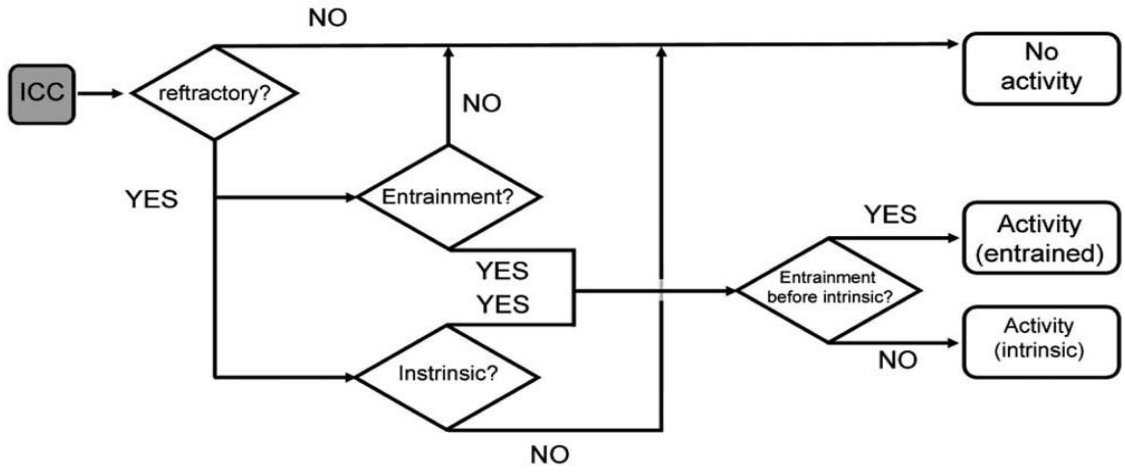

Figure 2.4: Outline for cellular automata algorithm of ICC-ICC entrainment. An ICC continuum cell in a non refractory state (Gray Square) is capable of either generating a new pacemaker potential due its own intrinsic frequency, or being entrained by one of the eight neighboring continuum cells.

On increasing the time between the intrinsic slow wave activity and the injection of stimuli the stable zone of entrainment (ZOE) progressively decreased. ZOE can be defined as the area of the tissue through which the injected stimulus travels. The maximum ZOE achieved was 78% of the tissue area. Experimental validation of the model results were conducted in porcine models. The authors have reported 100% correspondence between the developed model and their validation study carried out in dogs. The model should be credited for throwing light on the electrophysiological role of ICC in gastric electric activity. This can be considered as the first mathematical model for GES with an electrophysiological background. On the other hand the mechanism of ICC entrainment along the length of the tissue considered is not clearly established. Rather than modeling cell–to–cell entrainment mechanism, a cellular automata algorithm was chosen to simulate entrainment of single cell behavior in ICC. Further geometry of the tissue considered is substantially small (approximately 82 cm^2) in comparison to the realistic stomach tissue size there by not replicating real GES of the stomach. So the question regarding the stability of the model and the accuracy of the results that would be produced on increasing the geometry of the tissue size to match the realistic scenario remains unanswered. As pointed out by the authors themselves, the model lacks a realistic mechanism of ICC entrainment.

In conclusion, to date there is no mathematical model for gastric electric stimulation of the stomach available based solely on underlying electrophysiological principles. We therefore present in this research project an electrophysiological model for GES taking into account the results published by the experimental work on GES as well as giving room to the physiology of the multiple active cell types in the gastric musculature, which will overcome the major limitations highlighted in the previously published models.

Chapter 3

GES Model Development

The objective of this research project is to construct a biologically realistic tissue level model, thus offering a platform to optimize stimulation protocols by predicting whether effective entrainment is likely to be achieved in experiments. In Section 3.1 and Section 3.2 a mathematical description of the of the main intracellular processes and membrane ion channels that are currently believed to mediate the electrical cellular response of gastric pacemaker cells (ICC), and the electrical response of SMC stimulated by ICC is presented. The extended bidomain framework (Buist and Poh, 2010) is a tissue level electrophysiology model that extends the classical bidomain framework to allow multiple cell types to be incorporated. Here we have adapted this framework to model the interaction between ICC and SMC. Through this it is possible to simulate GES, ascertaining the effects of pacing parameters on gastric slow wave entrainment. In Section 3.3 detailed mathematical description of the extended bidomain model will be discussed. In Section 3.4 light will be thrown the development of tissue level GES model from extended bidomain framework.

3.1 Single cell model of ICC

The Corrias & Buist (2008) [67] ICC model can be considered as the first electrophysiological model of gastric ICC that highlights the importance of mitochondria in the generation and propagation gastric electric activity. It also provides an elaborate description of all ion transport mechanisms (ion channels) associated with the plasma membrane structure that have been identified. This ICC model derives its strong foundation from the classical Hodgkin Huxley methodology of modeling which considers cell membrane as an electrical circuit having a capacitance connected in parallel with variable conductances, where each conductance represents a specific transport mechanism for movement of charged ions. The time dependence of the membrane potential is governed by the following equation.

$$\frac{dV_m}{dt} = -\frac{I_{ion}}{C_m} \tag{3.1}$$

Here, V_m (in mV) represents the transmembrane potential, C_m is the cell capacitance, and I_{ion} (in pA) represents the sum of the ionic currents crossing the cell membrane.

3.1.1 Pacemaker Unit of ICC

ICC cells are of mesenchymal origin and were first described by Santiago Ramon y Cajal in 1893. But their role of pacemaker cell in the GI tract was established much later [13]. Currently ICCs are believed to the origin of the omnipresent electrical activity in the GI musculature. Even after establishment of ICCs as pacemaker cells, the intracellular ion transport mechanisms that gives raise to the pacemaker activity still remains controversial. Based on the review of several experimental papers it was established that calcium dynamics, as handled by mitochondria and endoplasmic reticulum (ER) are the key event in process of slow wave initiation. Taking into account the interplay between mitochondria and endoplasmic reticulum the following pacemaking theory was applied to the Corrias & Buist ICC model. The region in the cell enclosed by mitochondria, endoplasmic reticulum and plasma membrane is referred to as subspace (SS). Ca^{2+} is released from the IP_3 receptor operated stores of ER into the SS. As a consequence to the increasing concentration of Ca^{2+} ion in the subspace, Ca^{2+} uniporter of mitochondria opens thereby facilitating the movement of Ca^{2+} ions due to the existing electrochemical gradient. The gradient is steep to an extent that an excess of Ca^{2+} ion is evacuated from the SS in comparison to the Ca^{2+} ions that entered the SS. As a response to this event a non selective cation conducting channel (NSCC) opens to allow the inflow of cationic ions hence depolarizing the plasma membrane. These small depolarizations are referred to as unitary potentials, which in turn activate the entire voltage–gated ion channels in the plasma membrane thereby triggering slow wave activity.

All the important ion transport mechanisms (Figure 3.1) that were experimentally accepted to be responsible for the observed slow wave profile were included in the I_{ion} term of Equation 3.1, as follows

$$I_{ion} = I_{CaL} + I_{VDDR} + I_{Na} + I_{ERG} + I_{KV11} + I_{BK} + I_{ClCa} + I_{NSCC} + I_{bK} + 2 * F * V_{cyto} * J_{Ca-EXT} \quad (3.2)$$

Details of the currents are given in Table 3.1.

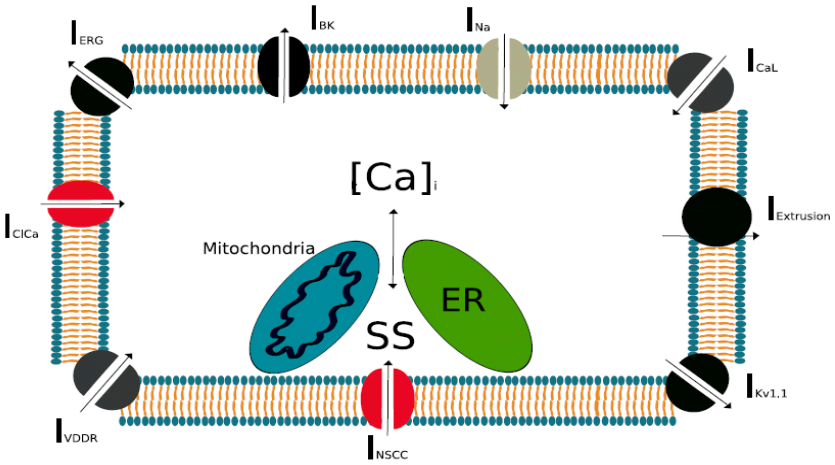

Figure 3.1: Schematic view of the Corrias & Buist ICC model (2008).

The calculation of the Nernst potential for each of the ion channels was based on the ionic concentrations. All the ion channels have been modeled based on the classical based on a classical Hodgkin- Huxley approach. A generalized explanation for the classic HH approach for modeling ion channels as adapted by the authors is provided below.

For an ion channel x having activation and inactivation gates, current I_x may be given by

$$I_x = G_x * d_x * f_x * (V_m - E_x) \quad (3.3)$$

For an ion channel x having activation gates, current I_x may be given by

$$I_x = G_x * d_x * (V_m - E_x) \quad (3.4)$$

Where, G_x is the maximal conductance for the ion channel x, d_x represents the activation gating variable, f_x represents the activation gating variable, E_x is the Nernst potential of the ion crossing through the channel x.

Details of the currents are as follows:

Table 3.1: Details of ICC ionic current and the corresponding ion channel

Ionic Current	**Corresponding ion channel**
I_{CaL}	Current from L-type calcium channels.
I_{VDDR}	Current from voltage dependant dihydropyridine resistant calcium channels.
I_{Na}	Current from sodium channels.
I_{Kv11}	Current from voltage dependant potassium channels.
I_{BK}	Current from calcium activated potassium channels
I_{ClCa}	Current from calcium activated chloride channels.
I_{NSCC}	Current from channels permeable to both sodium and potassium ions (non selective cationic conductance)
I_{bK}	Current from potassium channels (background potassium conductance)
J_{Ca-EXT}	Calcium efflux; a phenomenological description of calcium extrusion mechanism was adopted to provide long term homeostasis (Section 3.1.2).

3.1.2 Calcium extrusion

Ca^{2+} pump and Na/Ca^{2+} exchanger are known to play an important role in Ca^{2+} efflux kinetics from the cytoplasm. Due to lack of experimental data regarding their extrusion kinetics in ICC, a phenomenological model of Ca^{2+} extrusion (Equation 3.5) was modeled. The parameters were chosen such that long term homeostasis was achieved.

$$I_{Ca-EXT} = I_{Ca-EXT-MAX} * \left(\frac{1.0}{1+\frac{K_{Ca-EXT}}{[Ca]_i}}\right) \quad (3.5)$$

Where, I_{Ca-EXT} is the Ca^{2+} efflux in mM/s, $I_{Ca-EXT-MAX}$ is the maximal flux (0.0885 mM/s), K_{Ca-EXT} is the half concentration (298 nM).

3.1.3 Model validation

The model has been validated by comparing the simulated profile of the slow waves with experimental recordings. For example magnitude of the mitochondrial membrane potential was reduced to simulate the condition of presence of mitochondrial uncouplers, the model showed termination of slow waves corresponding to the experimental results. Similarly the model exhibited a reversible cessation of slow waves when the presence of 2-APB was simulated there by agreeing with the experimental results. Hence, the model has shown good agreement in terms of frequency, amplitude, and shape in both control and pharmacologically altered conditions.

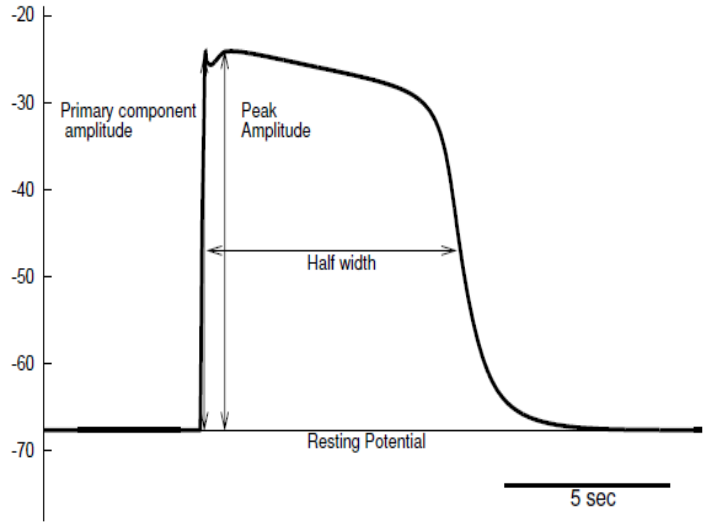

Figure 3.2: Slow wave profile generated by Corrias and Buist ICC model (2008).

3.2 Single cell model of SMC

A complex level of control holds responsibility for the generation and propagation of slow waves and hence gastric motility. The primary level of control comes from the interstitial cells of Cajal. The enteric nervous system and the humoral factors constitute the secondary level of control. The SMC compile and integrate the stimuli from both the levels of control to produce synchronized contraction generating motility. The electrical activity of the smooth muscle cells in response to the pacemaking activity of the ICC has been referred by the authors as "smooth muscle depolarization".

The Corrias and Buist SMC model [68] provides a mathematical description of single cell gastric SM electrophysiology, constructed from the predominant aspects of the underlying physiology and fitted to experimental data. The classical Hodgkin–Huxley approach was adopted, the cell membrane being described by an equivalent circuit consisting of a capacitance connected in parallel with variable conductances representing the different pathways for ion movement. The time dependence on the membrane potential was described by Equation 3.6

$$\frac{dVm}{dt} = -\frac{I_{ion}+I_{stim}}{C_m} \quad (3.6)$$

Where Vm (in mV) is the membrane potential, C_m (in pF) is the cell capacitance, I_{stim} (in pA) is a stimulus current supplied by the ICC network, and I_{ion} (in pA) represents the sum of the ionic currents crossing the cell membrane. All the major membrane ionic currents of the smooth muscle cell (Figure 3.3) were included in the I_{ion} term of Equation 3.8

$$I_{ion} = I_{CaL} + I_{LVA} + I_{Na} + I_{BK} + I_{K-DR} + I_{K-A-type} + I_{bK} \quad (3.8)$$

Descriptions of these ionic currents are explained in Table 3.2

Table 3.2: Details of SMC ionic current and the corresponding ion channels

Ionic currents	**Corresponding ion channel**
I_{CaL}	Current from L-type calcium channels.
I_{LVA}	Current from low voltage activated calcium channels.
I_{Na}	Current from sodium channels.
I_{BK}	Current from calcium activated potassium channels (large conductance).
I_{K-DR}	Current from delayed rectifier potassium channels.
$I_{K-A-type}$	Current from A-type potassium channels.
I_{bK}	Current from potassium channels (background potassium conductance).

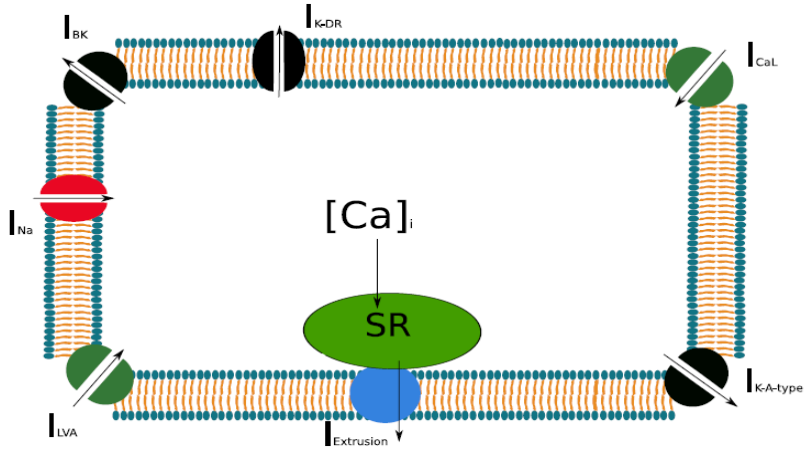

Fig 3.3: Schematic view of the Corrias and Buist SMC model (2007).

3.2.1 Calcium homeostasis

Sarcoplasmic reticulum and Na/Ca^{2+} exchanger are believed take part in Ca^{2+} extrusion kinetics. Plasma membrane calcium pumps and mitochondrial Ca^{2+} uptake also share the responsibility of calcium homeostasis. Due to lack of experimental data regarding their extrusion kinetics, a phenomenological model of Ca^{2+} uptake and extrusion was included (Equation 3.9). The parameters were chosen such that long term homeostasis was achieved.

$$I_{Ca-EXT} = 0.317 * [Ca^{2+}]_i^{1.34} \quad (3.9)$$

Where, I_{Ca-EXT} is the total rate of Ca^{2+} uptake by the SR, mitochondria and extrusion via plasma membrane calcium ATPase (PMCA) and NaCa exchanger (sodium calcium exchanger).

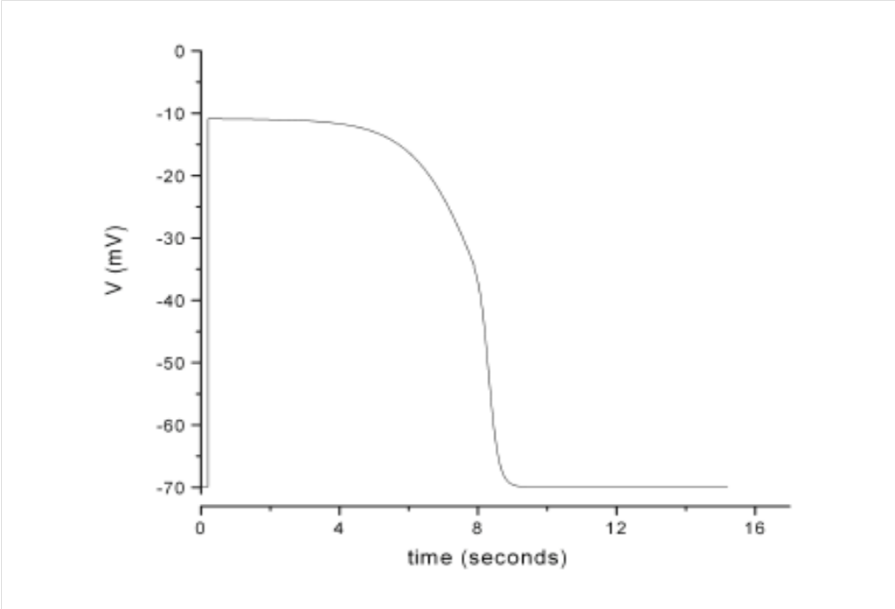

Figure 3.4: Smooth muscle depolarization profile generated by Corrias Buist SMC model (2007)

3.2.2 Model validation:

The model has been validated by comparing the simulated profile of the slow waves with experimental recordings. For example the presence of potassium channel blocker 4-aminopyridine was simulated by setting the conductances of the respective ion channels to zero. The results obtained were in complete agreement with the experimental results with a raise in the resting membrane potential and plateau potential. The injection of a potassium channel blocker into the cell was simulated by reducing the background potassium conductance to zero. A rise in the plateau phase was observed corresponding with the experimental results. A small discrepancy was observed regarding the repolarization of the membrane as observed experimentally. This issue was addressed by indicating that ICC was not coupled to SMC as in gastric musculature but mimicked by injecting a stimulus from ICC. Overall, the model showed good agreement in terms of frequency, amplitude, and shape in both control and pharmacologically altered conditions.

3.3 Extended bidomain framework

The bidomain model is a mathematical model of the electrical properties of cardiac muscle that takes into account the anisotropy of both the intracellular and extracellular spaces. It is a generalization of one-dimensional cable theory.

Cardiac modeling posses an edge over gastric modeling as the modeling work in the cardiac field can be carried out by considering a single cell type. On the other hand the GI musculature is quiet complicated with the walls of the GI tract housing two considerably different cell types i.e. the ICC and SMC. The GI modelers have to consider the fact that the volume averaged properties of the bidomain framework should contain the parameters of ICC, SMC and the gap junctions that connect these two cell types.

Keeping in mind the problem face by the gastric modeling field, the extended bidomain framework was constructed using the conventional bidomain set up as it foundation to handle the multiple active cell types present in the gastric musculature. The principle behind extended bidomain framework is quiet general with it key advantage of being exportable to model other tissues with more than a single type of cell.

3.3.1 Conventional bidomain framework

The bidomain equations have been conventionally applied in the field of cardiac modeling for a long time. In a bidomain set up of a cardiac tissue (or any tissue considered), it is represented by intracellular and extracellular regions, each filling the space occupied by the actual tissue, the two domains being separated by a membrane at each point. The parameters of this continuum framework are derived by average of the actual structure over the tissue volume. The bidomain framework can be further extended by the addition of spatially varying parameters, for example the variation of ion channel densities with space can be included into the conventional framework.

The conventional bidomain framework can be written as

$$\nabla \cdot (\sigma_i \nabla \emptyset_i) = A_m (C_m \frac{\partial V_m}{\partial t} + I_{ion}) \quad (3.10)$$

$$\nabla \cdot (\sigma_e \nabla \emptyset_e) = A_m (C_m \frac{\partial V_m}{\partial t} + I_{ion}) \quad (3.11)$$

Where, σ_i is the conductivity in the intracellular space, σ_e is the conductivity in the extracellular space, I_{ion} is the ionic current, $\emptyset_i$ is the intracellular potential, $\emptyset_e$ is the extracellular potential, A_m is the surface area of the membrane per unit volume, C_m is the membrane capacitance, V_m is the potential difference across the cell membrane i.e. difference between intracellular and extracellular potential.

3.3.2 Extended bidomain framework [69]

In the conventional bidomain equations, the surface to volume ration A_m depends only on the properties of single cell type. This concept has to be extended when applied to GI musculature. So, the extended bidomain framework modifies the parameter A_m by incorporating into it the properties of ICC, SMC and the gap junctions. The reason being attributed to the fact that total area available for ion transfer is a sum of membrane area available for ion transfer between ICC and extracellular space, membrane area available for ion transfer between SMC and extracellular space and finally the membrane area of gap junctions through which ions are exchanged between ICC and SMC. So surface to volume ratio in the extended bidomain framework was expressed as:

$$A_m = A_m^{ICC} + A_m^{SMC} + A_m^{gap} \quad (3.12)$$

The superscripts represent the parameters relating to the respective cell types. Interaction of ICC with extracellular space is given by Equation 3.13.

$$\nabla \cdot \left(\sigma_i^{ICC} \nabla \emptyset_i^{ICC}\right) = A_m^{ICC} (C_m^{ICC} \frac{\partial V_m^{ICC}}{\partial t} + I_{ion}^{ICC}) \quad (3.13)$$

Similarly, the interaction between the SMC and the extracellular space will be governed by Equation 3.14

$$\nabla \cdot \left(\sigma_i^{SMC} \nabla \emptyset_i^{SMC}\right) = A_m^{SMC}\left(C_m^{SMC} \frac{\partial V_m^{SMC}}{\partial t} + I_{ion}^{SMC}\right) \quad (3.14)$$

In the shared extracellular space, ionic currents will cross a total membrane area of A_m^{ICC} and A_m^{SMC} hence giving Equation 3.15

$$\nabla \cdot (\sigma_e \nabla \emptyset_e) = -A_m^{SMC}\left(C_m^{SMC} \frac{\partial V_m^{SMC}}{\partial t} + I_{ion}^{SMC}\right) - A_m^{ICC}\left(C_m^{ICC} \frac{\partial V_m^{ICC}}{\partial t} + I_{ion}^{ICC}\right) \quad (3.15)$$

With a membrane conductance per unit area (g_{gap}), the current between ICCs and SMCs will be governed by a difference in their intracellular potentials as follows:

$$I_{gap} = g_{gap}(\emptyset_i^{ICC} - \emptyset_i^{SMC}) \quad (3.16)$$

Provision to inject external stimuli was also included. Current can be introduced into ICC, SMC or into the extracellular space through I_{stim}^{ICC} and I_{stim}^{SMC} terms respectively. The stimulus injected into ICC and SMC will be similar to injecting a stimulus across the cell membrane and hence will behave like ionic currents (Figure 3.5). On the other hand stimulus injected into the extracellular space (I_{stim}^{EXT}) will act like an impressed current without directly crossing the cell membrane. Including these stimulation mechanisms and the charge transfer across the gap junctions the governing equations can be written as in Equation 3.17, 3.18 and 3.19.

$$\nabla \cdot \left(\sigma_i^{ICC} \nabla \emptyset_i^{ICC}\right) = A_m^{ICC}\left(C_m^{ICC} \frac{\partial V_m^{ICC}}{\partial t} + I_{ion}^{ICC} - I_{stim}^{ICC}\right) + A_m^{gap} I_{gap} \quad (3.17)$$

$$\nabla \cdot \left(\sigma_i^{SMC} \nabla \emptyset_i^{SMC}\right) = A_m^{SMC}\left(C_m^{ICC} \frac{\partial V_m^{SMC}}{\partial t} + I_{ion}^{SMC} - I_{stim}^{SMC}\right) - A_m^{gap} I_{gap} \quad (3.18)$$

$$\nabla \cdot (\sigma_e \nabla \emptyset_e) + \nabla \cdot \left(\sigma_i^{ICC} \nabla \emptyset_i^{ICC}\right) + \nabla \cdot \left(\sigma_i^{SMC} \nabla \emptyset_i^{SMC}\right) + I_{stim}^{EXT} = 0 \quad (3.19)$$

The ionic currents models were taken from single cell models discussed above (Sections 3.1 & 3.2). The equations were discretized using forward-time, central space finite difference scheme and assembled into a single matrix system. The above system of equations was solved using stabilized biconjugate gradient method. A time step of 0.1 ms was used. As a constraint to system, the average extracellular potential was set to zero.
The resulting slow wave profile is shown in Figure 3.6.

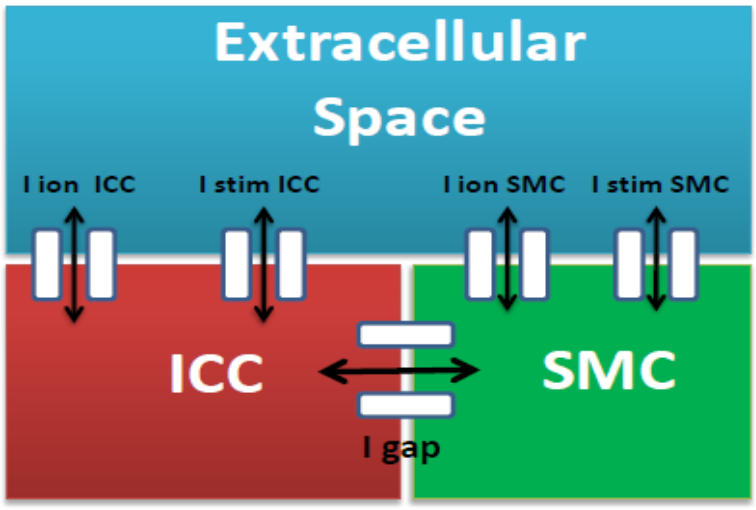

Figure 3.5: Schematic of Buist Poh extended bidomain framework (2010).

3.3.3 Frequency gradient

The myoelectric activity of the stomach results in coordinated contraction and relaxation and this contractile behavior proceeds in a distal direction starting from the corpus towards the antrum. This indicates the importance of a frequency gradient for the pacemaker cells when propagation of slow waves from one point of the stomach to another is considered. In the absence of a frequency gradient all pacing cells would activate as well as depolarize at the same time indicating that the entire stomach contracts and relaxes simultaneously. The frequency is higher in the corpus and lower in the antrum [1]. However, when the entire stomach is taken into consideration, higher frequency corporal slow waves entrain antral slow waves thereby giving rise to a dominant frequency throughout the stomach [10]. The intrinsic ICC frequency was therefore regulated by setting a decreasing gradient of the

intracellular IP_3 concentration. The gradient was from 635 nM at the proximal corpus to 615 nM at the pylorus. This concept was adapted from the previously published paper by Buist et al (2010) [70].

A decreasing gradient of the intracellular IP3 concentration was set by the following equation:

$$\text{Conc of IP3 at nth space point} = 0.000635 - \text{nth space point} * \left(\frac{0.00002}{\text{number of space points}}\right) \quad (3.20)$$

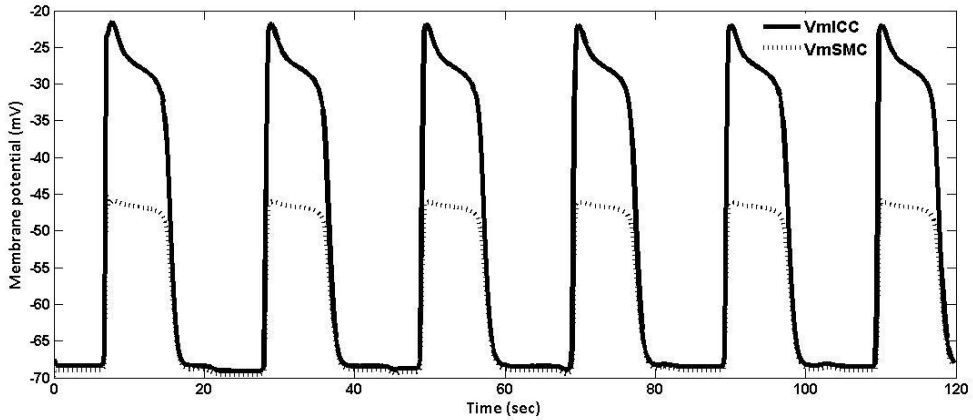

Figure 3.6: The resulting slow wave profile of ICC and SMC generated by Buist and Poh extended bidomain framework (2010).

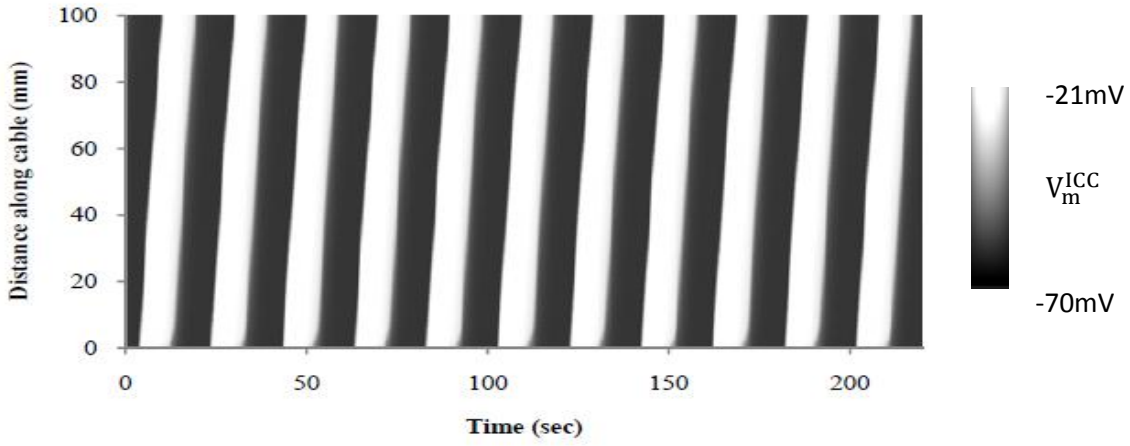

Figure 3.7: Spatiotemporal plot of ICC's electrical activity adapted from Buist and Poh extended bidomain framework (2010).

3.4 Development of GES model

3.4.1 Extending the extended bidomain framework: Inclusion of a bath

Similar to all electronic equipments, implantable devices also require a complete pathway i.e., a closed circuit for current to flow. The circuit is usually composed of stimulator, active electrode, patient and return electrode. The electric current flow from the stimulator to the active electrode, passes through the patient and finally to the return electrode thus completing the circuit. Bipolar and monopolar electrodes have been used to deliver stimulus in most of the experimental work carried out in GES. A bipolar pacing system possesses a lead with two electrodes i.e., both anode and cathode. So in a bipolar lead system both the active electrode and the return electrode are embedded in the same lead wire. In gastric pacing the current flows from the stimulator to the electrode located at the end of the lead wire, stimulates the stomach and finally returns through the electrode above the lead wire tip thus completing the circuit. A monopolar system possesses only one electrode usually the cathode. In this type of pacing system current flows from the stimulator to the active electrode, stimulates the stomach and returns through the body fluid or tissue. The monopolar pacing system resembles a set up of placing the organ to be stimulated in a bath that acts line the anode. In order to develop a GES model as a close approximation to the realistic GES it is necessary to simulate the presence of a return electrode. We have simulated the condition of monopolar pacing system where the current returns to the stimulator through the body tissue or fluid by addition of a domain called bath. The boundary conditions of the bath are set in such a way that it simulates the condition of the bath being grounded (Figure 3.8), hence facilitating the injection of an external stimulus through any syncytia of the extended bidomain framework in comparison with the realistic GES. The bath can be considered as an extension of the extracellular space which is grounded.

The bath is represented by Equation 3.21

$$\nabla \cdot (\sigma_{bath} \nabla \emptyset_{bath}) + I_{stim}^{bath} = 0 \qquad (3.21)$$

Where σ_{bath} represents the conductivity of the bath, $\emptyset_{bath}$ is the bath potential, I_{stim}^{bath} is the stimulus that can be injected into the bath. As the bath was considered as an extension of the extracellular space, conductivity of the bath (σ_{bath}) was given a value equal to the conductivity of extracellular space (σ_{EXT}). A value of 0.4 mS.mm^{-1} was assigned to σ_{bath} and σ_{EXT}. Equations 3.17, 3.18, 3.19 and 3.21 were assembled into a single matrix system. The resulting system of equations was solved using stabilized biconjugate gradient method.

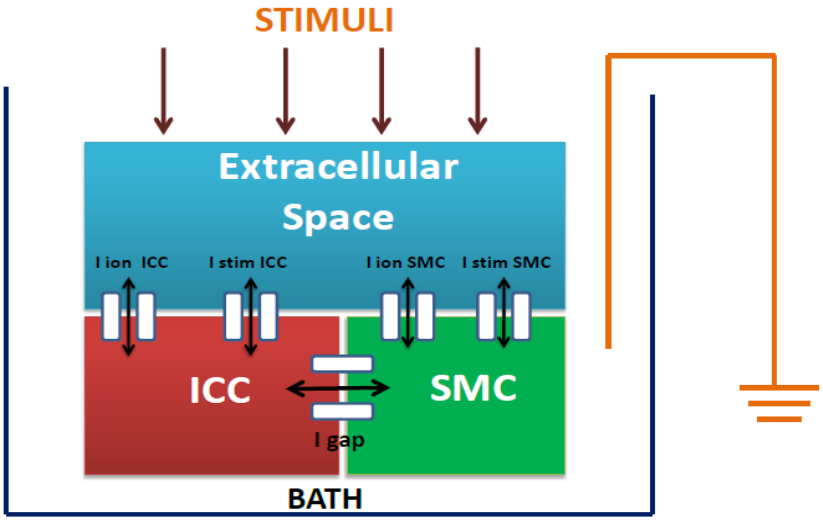

Fig 3.8: Schematic of the extended bidomain framework after inclusion of the bath

3.4.2 Inclusion of intracellular IP_3 dynamics

In GES when a stimulus of appropriate strength is injected, it is expected to trigger the pacemaker cells and invoke an active slow wave response at stimulated frequency. The invoked slow wave should also be entrained along the length of corpus and antrum to ensure that the delivered stimulus reproduces the normal slow wave activity rather than producing local depolarization only at the point where stimuli is injected. In order for the injected stimulus to be passed from one pacemaker cell to the adjacent one the mathematical model should posses a sufficient level of voltage dependant communication between the pacemaker cells. The entrainment mechanism suggested by the Corrias and Buist ICC model (2008) was not adequate enough to propagate the delivered stimulus through the entire region of corpus and antrum. To enhance the voltage dependant

entrainment of slow waves in the extended bidomain framework, intracellular IP_3 dynamics, as suggested by Imtiaz et al (2002) [71] were introduced.

Voltage dependent regulation of IP_3 synthesis had been postulated as one of the key mechanisms in slow wave generation. Membrane potential has a positive feedback on IP_3 synthesis [72]. Based on this concept Imtiaz et al (2002) put forward a mathematical description of voltage dependant IP_3 regulation based on the experimental observations from muscle preparation of the guinea pig stomach (Figure 3.9). Rather than having a constant value for the intracellular IP_3 concentration a membrane potential dependant IP_3 synthesis was introduced. The IP_3 value would be subject to changes at every time step depending the value of the membrane potential recorded at the previous time step. To achieve this feedback mechanism between the membrane potential and IP_3 synthesis a voltage dependant IP_3 synthesis was incorporated into the Corrias and Buist ICC model.

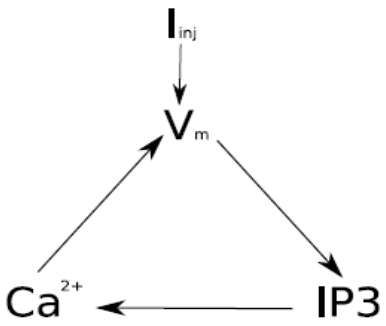

Figure 3.9: Schematic of IP_3 dynamics as suggested by Imtiaz et al (2002)

The intrinsic frequency gradient that was set by introducing an IP_3 gradient along the length of the cable in extended bidomain model was modified. A voltage-dependent, IP_3-related mechanism based on the equations previously published by Imtiaz et al (2002) was incorporated. The effect of this modification was to invoke an active slow wave in response to an appropriate current from another depolarizing ICC. The governing equation is given by Equation 3.22 and Equation 3.23

$$P(V) = P_{MV}(1 - \frac{V^r}{K_V^r + V^r}) \quad (3.22)$$

$$\frac{dP}{dt} = \beta - \varepsilon P - V_{M4}(\frac{P^u}{K_4^u + P^u}) + P(V) \quad (3.23)$$

Where, β is the modulator of sensitivity of IP_3 toV_m, ε is the rate constant for linear IP_3 degradation, u is the hill coefficient, V_{M4} is the maximal rate of voltage dependent IP_3 synthesis K_4 is the half saturation constant for the nonlinear IP_3 degradation, P_{MV} is the maximal rate of voltage dependent IP_3 synthesis, K_V is the half saturation constant for voltage dependent IP_3 synthesis, r is the hill coefficient. P(V) describes the dependence of IP_3 on voltage. All the parameters values were redimensionalized to be consistent with the units of Buist and Poh extended bidomain framework (2010).

IP_3 can be modulated by external stimuli, denoted by the term β (Figure 3.10). The intrinsic frequency of the slow waves is set by β with a higher value of β giving a higher intrinsic frequency. A value of $2.9 * 10^{-8} \frac{mM}{mS}$ was assigned to β to set the intrinsic frequency to 3cpm (i.e., the frequency of gastric slow waves in humans). Linear gradient of intrinsic frequency was maintained by varying (decreasing gradient) the parameter β over the cable length. Both linear and nonlinear mechanisms degrade IP_3, as described by the second and third terms of the equation (3.27). The fourth term describes the dependence of IP_3 on voltage. Equation (3.28) was solved by the forward Euler method and incorporated into the Corrias and Buist ICC model (2008). Hence the extended bidomain framework was modified to entrain the gastric electrical activity in a voltage dependant manner.

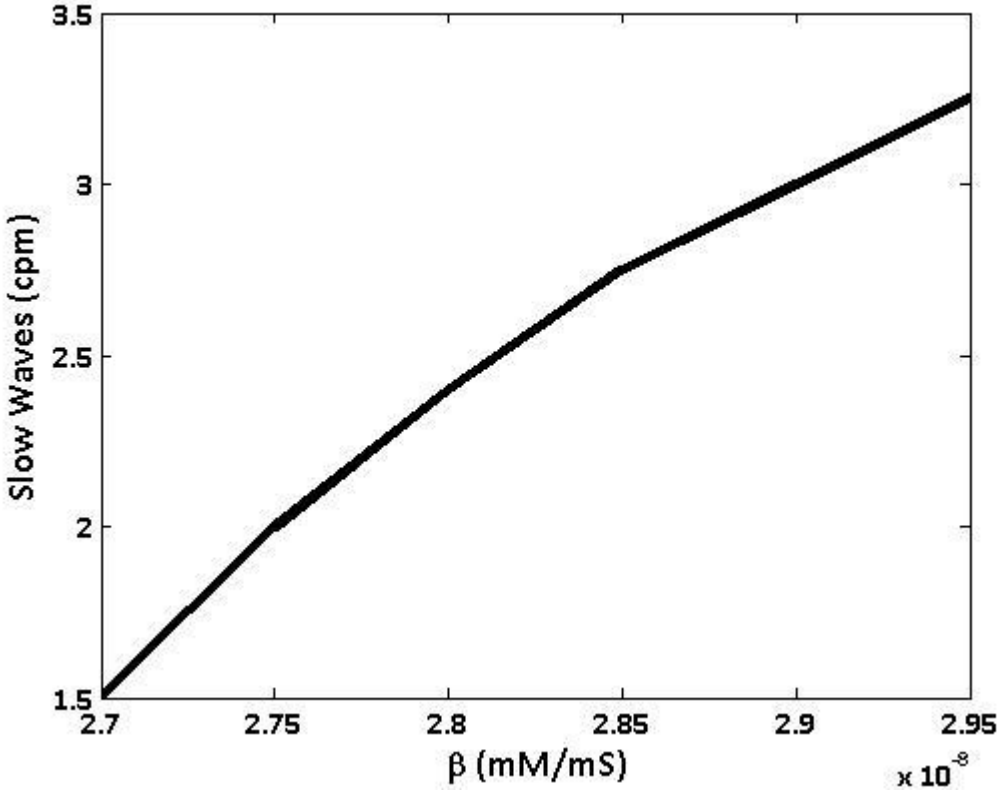

Figure 3.10: Relationship between slow wave frequency in cycles per minute and the parameter β

3.4.3 Decreasing the time constant for inactivation of IP_3 receptors

The mechanism of slow wave propagation (including stimulus propagation) has been an object of discussion. The question of how each ICC could be entrained to produce coordinated slow wave propagation was raised. In stomach tissue, being an electrically coupled system with each ICC being self exciting, a coordinated mechanism capable of entraining the injected stimulus and invoking slow wave activity is necessary. The Corrias and Buist ICC (2008) was adjusted to enhance the existing entrainment mechanism. The Corrias and Buist ICC (2008) uses on ODE (Equation 3.24) to represent IP_3 receptor inactivation

$$\frac{dh}{dt} = \frac{d_{INH} - (Ca_{PU} + d_{INH}) * h}{\tau_h} \tag{3.24}$$

Where h represents the fraction of IP_3 channels not inactivated by Ca^{2+}. The value of h varies between 0 and 1. d_{INH} (0.014mM) is the calcium concentration needed for inhibition, Ca_{PU} is the calcium concentration in the pacemaker unit and τ_h (4 seconds) is the time constant for calcium dependant inactivation of IP_3 receptors. The values of the parameters have been obtained from Fall and Keizer (2001) [73]. Changing τ_h does not alter the steady state but may change the stability of the steady states of the IP_3 receptors [74].

As an attempt to enhance the existing mechanism of entrainment along the cable length the value of $\tau_h$was decreased to 0.002 seconds. It should be noted that altering τ_h will alter the balance between endoplasmic reticulum calcium release rate and endoplasmic reticulum calcium filling rate to a small extent. This change in the value of τ_h is expected to make the pacemaker cells more responsive to the external stimulus thereby triggering the depolarization of the neighboring ICCs. This change would activate the pacemaker cells one by one like in a chain reaction when the stimulus is injected into a single ICC.

3.4.3.1 Removing I_{VDDR_PU}

The original Corrias and Buist ICC model demonstrates insufficient voltage dependant coupling between the ICCs with an external stimulus stimulating a single ICC not able to propagate along the cable and provide stable entrainment of slow waves. In order to enhance voltage dependant entrainment of the ICCs Corrias and Buist ICC model was modified by introducing dihydropyridine-resistant Ca^{2+} channels into the pacemaker unit [70]. This is in line with experimental evidence that suggests Ca^{2+} entry through voltage dependent, dihydropyridine-resistant pathways into the cell is involved in the coordination of slow wave discharge in the stomach [75]. This concept was simulated by channeling 4% of dihydropyridine-resistant Ca^{2+} entry into the submembrane space [70]. To prevent the accumulation Ca^{2+} ions entering the submembrane space through this current, I_{VDDR_PU}, a phenomenological model of Ca^{2+} extrusion was also included. Apart from non selective cationic channels on the plasma membrane of the submembrane space the addition of dihydropyridine-resistant Ca^{2+} (I_{VDDR_PU}) was expected to convert voltage signal from an

ICC into a Ca^{2+} signal for pacemaker unit of the neighboring ICC. Hodgkin Huxley approach was adopted to model I_{VDDR_PU} with a maximum conductance of $G_{VDDR} * d_{PU}$ where d_{PU} is fraction of dihydropyridine-resistant Ca^{2+} channels directed into the submembrane space. The updated Corrias and Buist ICC model was incorporated into the extended bidomain framework and hence the GES model as well.

The decrease in the value of τ_h (Section 3.4.3) decreased the endoplasmic reticulum calcium release rate through the IP_3 receptor channels directly, followed by a reduction in calcium ions circulating in the submembrane space. In addition to this reduction in the calcium concentration, extrusion by the phenomenological model would further decrease calcium concentration in the subspace preventing the active generation of slow waves in the absence of any external stimulus. However when an external stimulus is delivered balance between calcium concentration in the submembrane space and extrusion mechanism is maintained by increase in the calcium cycling rate due to increased stimulus frequency and voltage dependant calcium release due to inclusion of intracellular IP_3 dynamics (Section 3.4.2). In order to restore the stability of the GES model in the presence as well as in the absence of an external stimulus and to maintain long term homeostasis I_{VDDR_PU} and the associated phenomenological calcium extrusion mechanism were removed from the Corrias and Buist model. Deletion of I_{VDDR_PU} did not substantially weaken the voltage coupling (and entrainment mechanism) as a new form of voltage coupling had been introduced by the inclusion of intracellular IP_3 dynamics (Section 3.4.2).

Chapter 4

Single Channel GES

Introduction

After the development of the GES model framework with the incorporation of ICC and SMC single cell models as in a real stomach, the study of the propagation of gastric electrical activity in response to a stimulus delivered along the greater curvature of stomach constitutes the next logical step towards the complete the understanding of the effects and mechanisms of GES on the stomach. Having presented the development of GES model from the extended bidomain frame work in Chapter 3, in this chapter we will throw light on single channel gastric electrical stimulation.

4.1 Background

As mentioned in Section 1.2.1, two types of ICC variants are distributed along the stomach's musculature i.e., ICC-MY (ICC myentric plexus) and ICC-IM (ICC intra muscular). While the former is involved in generation and propagation of slow waves the latter takes part only in the propagation of slow waves. Many investigators have highlighted the diversity in slow wave profile in different regions of the stomach. For example the stomach fundus is referred to as electrically silent inspite of the fact that it displays a dense population of ICC, mostly ICC-IM [1]. The stomach fundus is the most depolarized region in comparison with the other parts of the stomach and its resting membrane potential is always above the mechanical threshold [76] [77]. Slow waves are believed to arise in the corpus region along the greater curvature of the stomach (Figure 4.1) and propagate aborally towards the pylorus [78]. Gastric electric activity terminates at the pylorus, which is an electrical barrier for slow wave propagation, preventing the slow waves from propagating into the small intestine. An electrically quiescent muscle is

present between the pyloric sphincter and the duodenum preventing further propagation of slow waves [79]. The small intestine exhibits its own intrinsic pacemaker activity from the duodenum to the distal ileum [80].

It was conceived that injecting a stimulus through an electrode at the proximal corpus, which is believed to be the origin of slow waves, would dictate the stomach's electrical activity and hence help in normalizing gastric dysrhythmia. It was expected that the degree of entrainment of the gastric myoelectrical activity in response to the externally injected stimulus should be associated with the improvement of gastroparetic symptoms like delayed gastric emptying, nausea and abdominal pain.

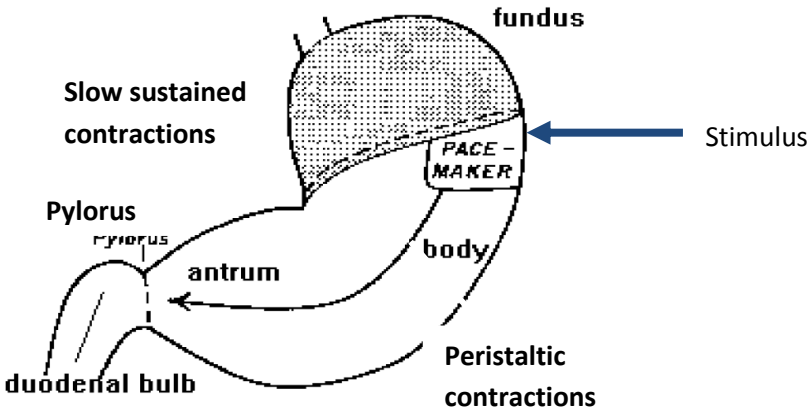

.

Figure 4.1: Origin and propagation of slow wave activity in the stomach. Blue arrow indicate the position for placement of electrode in single channel GES.

In single channel gastric electrical stimulation the stimulus is injected only into proximal part of the corpus i.e., in the area of the physiologic gastric pacemaker. Many experimental investigators have reported the efficacy of single channel in normalizing gastric dysrhythmia as well as in alleviating the chronic symptoms of gastroparesis like reducing gastric emptying time, nausea, vomiting, bloating and abdominal pain [41] [49]. All stimulus types as mentioned in Chapter 1 can be delivered as single channel GES. The concept of GES was initially commenced with single channel GES following which dual and multi channel GES was introduced. The stimulus usually consists of a series of rectangular pulses with a constant current. The pertinent stimulus parameters involved in

GES are pulse width, amplitude and pacing frequency. To date researchers employed a variety of pacing frequencies ranging from 3 cpm (cycles per minute) to 12 cpm in humans.

In this chapter we aim to investigate the effects and physiological significance of single channel GES using different stimuli parameters. We have simulated GES in a cable model representing the stretch along the greater curvature from the proximal corpus to the pylorus. Cable models have been used to simulate the electrophysiology of many tissues like neural [81] tissue, skeletal [82] and cardiac [83] muscle tissues. In comparison to the phenomenological GES models developed previously, a biophysical GES model based on the realistic computational descriptions of the electrophysiology of gastric ICC and SMC (Chapter 3) enables us to make predictions regarding different stimulation protocols.

4.2 Modeling single channel GES

Electrical parameter selection plays a fundamental role in achieving efficient and effective slow wave entrainment by GES. Slow wave activity in response to an external stimulus has been simulated in a cable model (GES model, Chapter 3) that runs from proximal corpus to the antrum. The distance between the proximal point of fundus and distal point of pylorus along the greater curvature of the stomach is around 337 mm [84]. In Figure 4.2 the yellow line depicts the cable along the stomach's greater curvature. A cable length of 180mm was chosen for the GES model as the fundus was excluded due to the fact that it is electrically silent. All the experimental investigators have also suggested the placement of electrodes at proximal corpus for single channel GES. All the stimuli types that are currently in practice have been simulated.

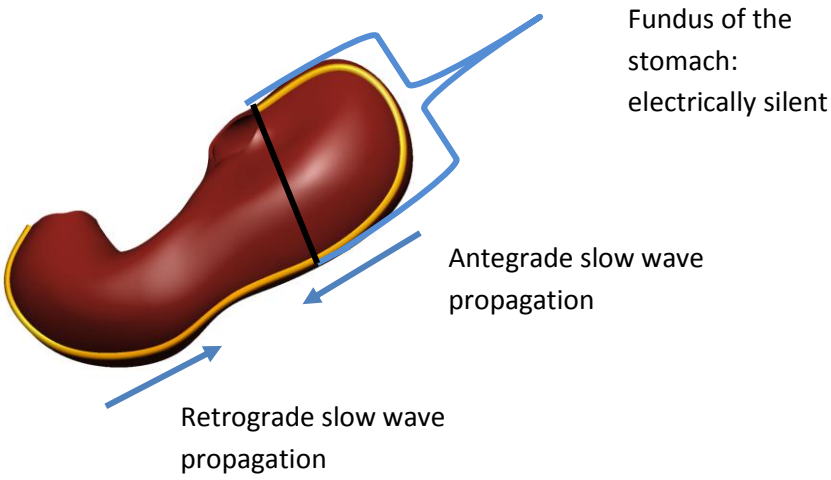

Figure 4.2: The yellow line depicts the cable along the stomach's greater curvature. A cable length of 180mm was chosen for the GES model as the fundus was excluded due to the fact that it is electrically silent (no slow wave activity).

A stimulus is delivered to the GES model through I_{stim}^{EXT} of Equation 3.19, hence simulating the condition of having an electrode sutured into the serosal layer of the stomach as adapted from the experimental work on GES. Alternatively the stimulus can also be injected through the I_{stim}^{ICC} term of Equation 3.17 which would simulate the situation of directly stimulating the pacemaker cells, hence requiring lesser energy than the former technique. In both the methods ultimately the pacemaker cells are triggered, resulting in depolarization of the pacemaker cells. Following this event SMCs are triggered by means of the gap junction coupling. But in real case scenario the electrodes are inserted into the serosal layer of the stomach which is a vascularised connective tissue. The serosal layer possesses neither the ICCs nor the SMCs [9]. The electrodes cannot be expected to directly pierce the pacemaker cells when they are sutured to the stomach walls. Hence, we have chosen to inject the stimulus through I_{stim}^{EXT} to model GES which would be more close to the experimental GES. However the results obtained on using I_{stim}^{ICC} to deliver the stimulus are also explained in this chapter.

For single channel GES we have chosen to inject the stimulus at a distance of 2mm from the proximal corpus. The first stimulus was delivered at the proximal corpus after 6.5 seconds of simulated time. Subsequent stimuli were delivered thereafter as dictated by the stimulus frequency that was set. The first stimulus time was decided based on the appearance of rising phase of slow waves at its intrinsic frequency. The GES models responded to the injection of subsequent stimuli and generated slow waves at the stimulated frequency.

On the basis of published experimental data (Chapter 2) starting values for the above mentioned stimulus parameters i.e., pacing frequency, pulse width and amplitude were determined. The stimulus frequency was chosen such that it was higher than the intrinsic slow wave frequency, with a starting value of 1.1 times the intrinsic frequency (for low frequency stimuli types) and up to 1.25 times intrinsic frequency (for high frequency stimuli types). Pulse width was decided depending upon the type of stimuli employed. In most of the experimental work on GES, stimulus intensity of the order of mA was employed. However the cable model for GES required stimulus in the order of $\frac{\mu A}{mm^3}$. The current amplitude of the stimuli was started with a low value and was gradually increased until stable entrainment was achieved. The stimuli parameters for all types of stimulus were optimized on the basis of results obtained from GES model. Stability of entrained slow wave activity was ensured by observing ten minutes of stimulated slow wave activity. The parameters were optimized such that least amount of energy was consumed without compromising on the stability of slow wave entrainment. Emphasis was laid on different techniques employed in the experimental GES and also the data obtained from the published experimental work was used as a starting value for the simulations with the aim of arriving at optimized stimulus parameters and in developing a GES model that would be a close approximation of realistic gastric electrical stimulation.

A parameter called percent entrainment was introduced to assess the efficiency of the pacing parameters [50]. Percent entrainment was defined as the ratio of the difference between the recorded slow wave frequency on application of stimulus and the intrinsic

frequency of the system to the difference between the pacing frequency and the intrinsic frequency. Entrainment can be considered to be 100% if the recorded frequency was exactly the same as the pacing frequency i.e., slow waves are entrained at the stimulated frequency.

$$\%\text{entrainment} = \frac{\text{recorded frequency} - \text{intrinsic frequency}}{\text{stimulus frequency} - \text{intrinsic frequency}} \quad (4.1)$$

The stimulation energy (E) for each run was calculated using the following formula [85] where frequency is in Hertz, pulse width is in milliseconds and amplitude in μA.

For long pulse stimulus:

$$\frac{\text{E}}{\text{min}} = \text{pulse width} * \frac{\text{number of pulses}}{\text{min}} * \text{amplitude}^2 \quad (4.2)$$

For Pulse strain stimulus:

$$\frac{\text{E}}{\text{min}} = \text{on time(sec)} * \text{pulse frequency} * \text{pulse width} * \frac{\text{trains}}{\text{min}} * \text{amplitude}^2 \quad (4.3)$$

The energy requirements here are represented in units of ms*μA^2. This can also be interpreted in terms of Joules.

1KWh = 3.6*10^6 Joules (4.4)

Watts = Volts*Amps (4.5)

On considering this example
Stimulus amplitude used for single and multi channel GES = 5.0 μA (Section 4.3)
Peak volt for enterra (gatric pacemaker) device = 10.5V [86]
The energy requirements corresponding to 24750 ms* μA^2 using Equations (4.4) and (4.5) would be $4.375 * 10^{-9}$ Wh or $1.575 * 10^{-5}$5 Joules.

4.3 Simulation results

4.3.1 Generating dysrhythmia

A variety of mechanisms are involved in the generation of gastric dysrhythmia. For example, the pacemaker cells may be severely injured or damaged hence generating abnormal electrical activity like an increase (tachygastria) or decrease (bradygastria) in the frequency of slow wave activity. On the other hand slow wave impairment may also be attributed to abnormal coupling among cells. The key advantage of the GES model developed here is that it can be used to simulate normal gastric slow wave activity, conditions such as bradygastria and tachygastria and the impairment that arises due to abnormal coupling between the pacemaker cells as well. We have simulated bradygastria at a frequency of 2.4cpm (normal frequency: 3cpm in humans) with the GES model (Figure 4.2 and 4.3) and have shown that application of GES at a frequency higher than 3cpm restored the slow wave activity at the stimulated frequency. Figure 4.3 displays the bradygastric slow wave activity recorded at a distance of 20mm from the proximal corpus. Bradygastric conditions have been simulated by reducing the value of β (the modulator of sensitivity of IP_3 to membrane potential). The efficiency of various stimuli types in normalizing bradygastric slow waves has been demonstrated in this chapter.

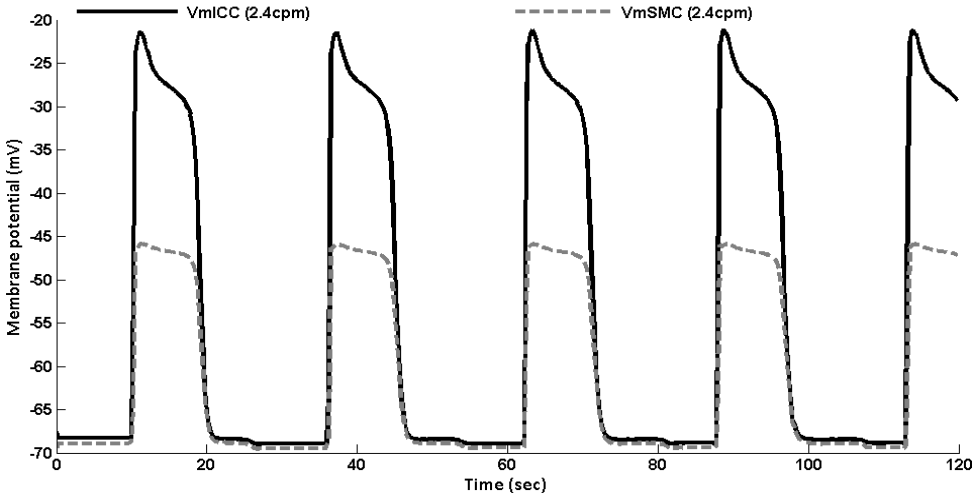

Figure 4.3: Slow waves generated by the GES model at bradygastric frequency of 2.4cpm recorded at a distance of 20mm from the proximal corpus.

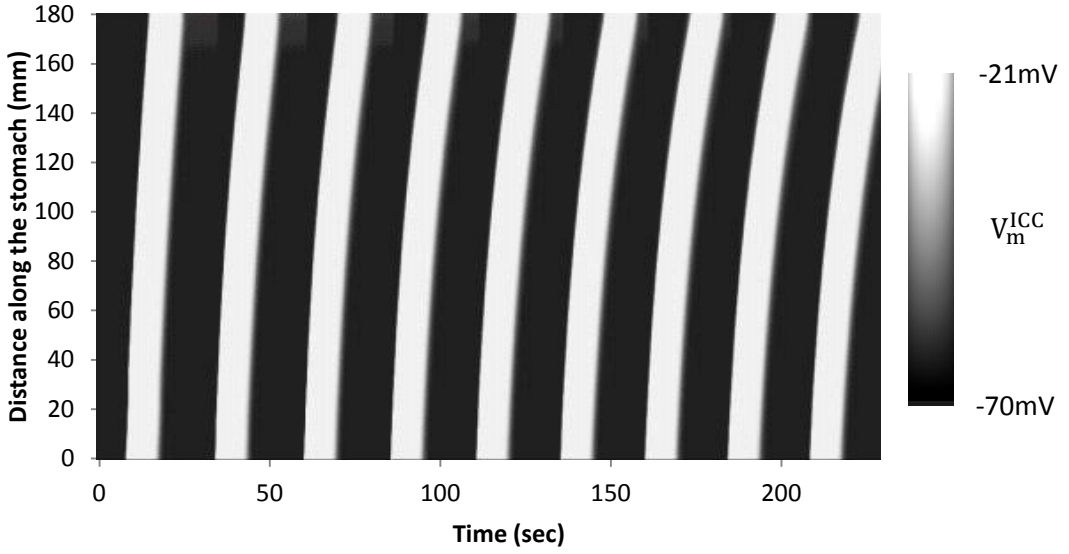

Figure 4.4: Spatiotemporal plot of V_m^{ICC} at bradygastric frequency (4 minutes of slow wave activity) demonstrating propagation of slow waves along the greater curvature.

4.3.2 Long pulse stimulus

As mentioned in Section 1.6.1, the duration of the stimulus was taken to be in the order of milliseconds. For duration of 300ms stimulus amplitude of 5.0 $\frac{\mu A}{mm^3}$ was required for triggering the pacemaker activity. Results have indicated that reciprocal variation in pulse duration and amplitude can be used to entrain gastric electric activity. Entrainment of slow waves at stimulated frequency can be achieved with low current amplitude given an appropriate increase in pulse width. However, it was taken into consideration that either current amplitude or pulse width was not reduced to extremely low values. The frequency of the stimulus was chosen to be slightly above the intrinsic frequency. The most optimal frequency for stimulation was found to be 1.1 times the intrinsic gastric slow wave frequency. In humans as mentioned earlier (Section 1.2.2) the frequency of gastric slow waves is 3 per minute. Therefore, a stimulated frequency of 3.3 cpm was used (Figure 4.5 and 4.6). Figure 4.5 displays the stimulated slow wave activity recorded at a distance of 20mm from the proximal corpus. The energy required for entrainment was 24750 ms $*$

μA^2. When the stimulus was injected into ICC, pulse amplitude of 0.04 $\frac{\mu A}{mm^3}$ was sufficient to stimulate pacemaker activity. However, there existed a maximum driven frequency that was about 126% (3.8 cpm) of intrinsic slow waves, beyond which stable entrainment of slow waves was not achieved. 100% entrainment was obtained for all frequency below the maximal driven frequency.

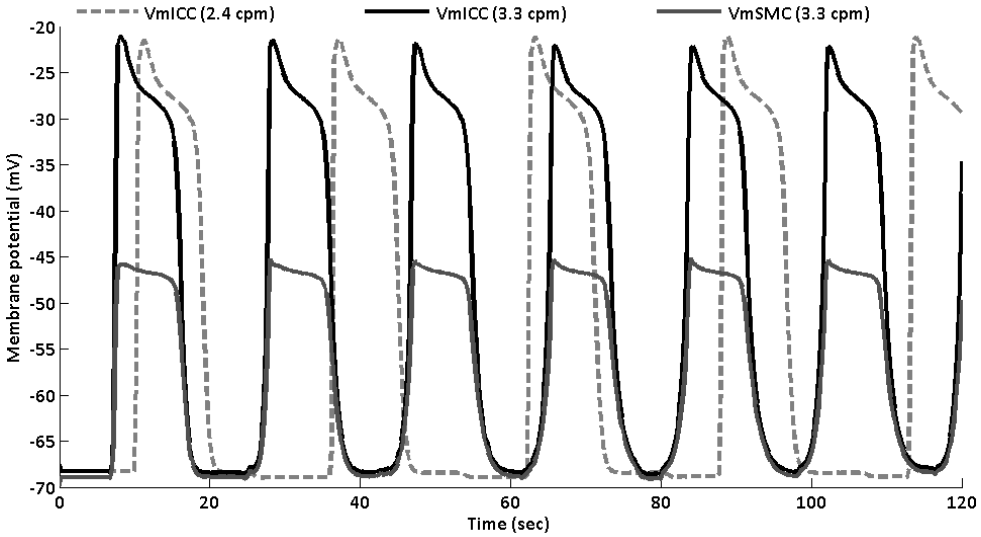

Figure 4.5: Normalization of bradygastric slow waves with long pulse stimulus (parameters: pulse width 300ms, amplitude: 5.0$\frac{\mu A}{mm^3}$, frequency 3.3 cpm).

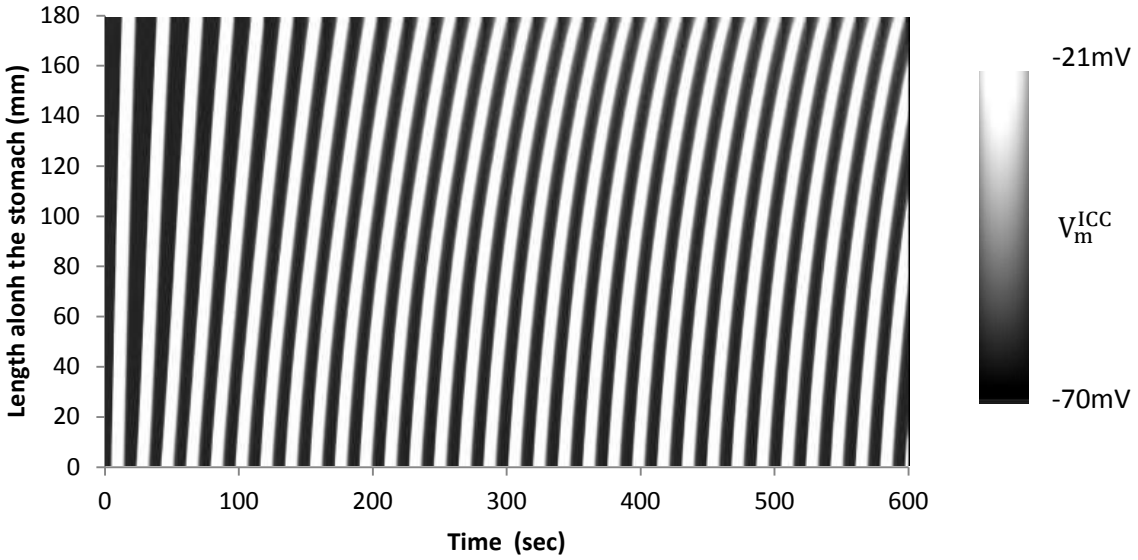

Figure 4.6: Spatiotemporal plot of V_m^{ICC} stimulated with long pulse stimulus (parameters: pulse width 300ms, amplitude: $5.0\frac{\mu A}{mm^3}$, frequency 3.3 cpm) for 10 minutes demonstrating the stability stimulated slow wave activity.

4.3.3 Short pulse stimulus

In the case of short pulse stimulus the duration is in the order of microseconds. As concluded by the experimental investigators on GES, the GES model, when injected with short pulse GES, did not produce any effect on gastric slow wave activity i.e., it was not able to entrain the slow waves at the stimulated frequency. However if the stimulus amplitude was very high, $75\frac{\mu A}{mm^3}$ (in comparison to $5.0\frac{\mu A}{mm^3}$), active entrainment of slow waves was achieved. However, even if slow waves were entrained, 100% entrainment was not achieved as the short pulse stimulus is delivered at very high frequency. Short pulse stimulus may not be very important from the slow wave aspect of GES as it does not affect the slow wave activity of the stomach when the stimulus amplitude and pulse width were given in the physiologic range.

4.3.4 Pulse train stimulus

Train of pulses when injected into the GES model entrained gastric slow waves only when the width of the pulses in the train was greater than 4ms. Reciprocal variation in current amplitude and pulse width was observed above pulse width duration of 4ms. The experimental studies on GES that have employed pulse strain stimulus have claimed that slow waves can be stimulated to a frequency that is 180% of the intrinsic frequency. The results obtained from GES model have shown that the most optimum frequency for GES with pulse train stimulus is 110% of the intrinsic frequency with a maximum driven frequency of around 126% (3.8cpm) of the intrinsic frequency. However, when the frequency of the supplied stimulus was increased beyond this upper limit stable entrainment of slow waves was not achieved. 100% entrainment was obtained for all frequency below the maximal driven frequency. GES with pulse train stimulus of parameters: amplitude: 5.5ms, amplitude: 5.5$\frac{\mu A}{mm^3}$, frequency 30 Hz, cycle on for 3 sec and off for 15 sec generated slow waves as in Figure 4.7 and 4.8. When the stimulus was injected into the ICC directly, pulse amplitude of 0.05 $\frac{\mu A}{mm^3}$ was sufficient to produce entrained slow wave activity.

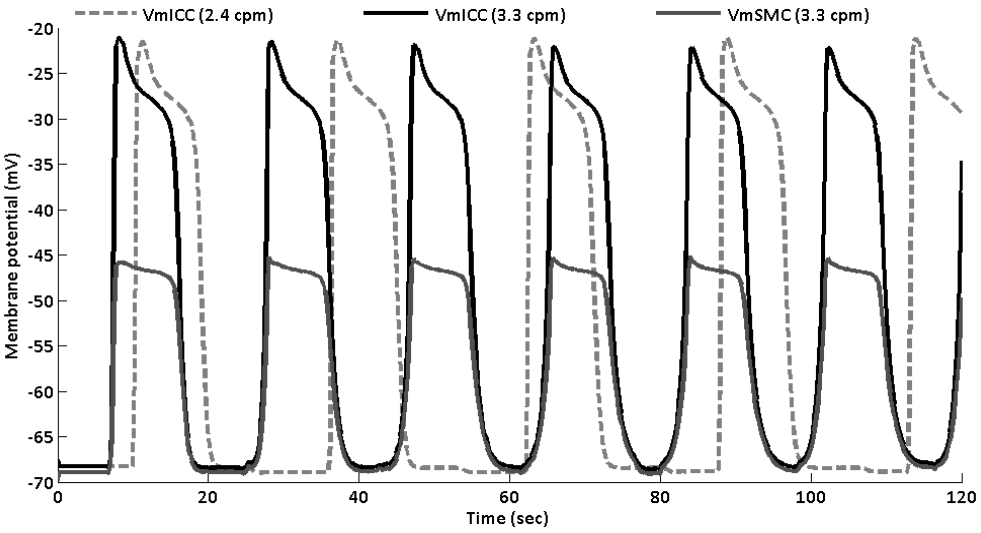

Figure 4.7: Gastric electric stimulation with pulse train stimulus at a frequency higher than the intrinsic one normalizes bradygastric slow wave activity. The graph shows slow wave activity at the distance of 20mm from the proximal corpus.

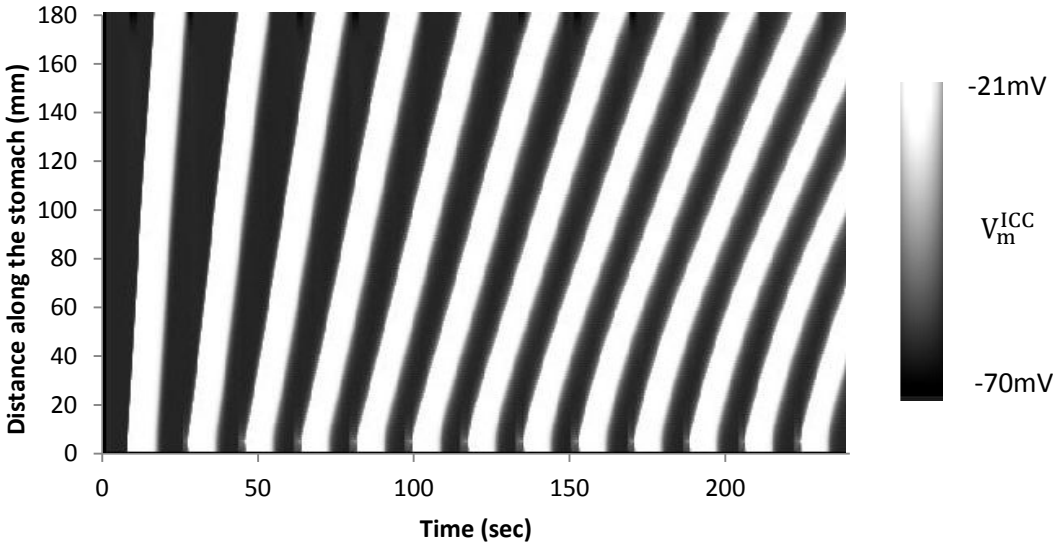

Figure 4.8: Spatiotemporal plot of V_m^{ICC} stimulated with pulse train stimulus (parameters: duration: 5.5 ms, amplitude: $5.5\frac{\mu A}{mm^3}$, frequency 30 Hz, cycle on for 3 sec and off for 15 sec, Energy utilized: 49413 $ms * \mu A^2$) demonstrating slow wave propagation along the greater curvature. The long term stability is equivalent to that shown on Figure 4.6.

4.3.5 Dual pulse stimulus

As the name indicates, a short pulse of the duration 300µs followed by a long pulse of duration 300ms was injected into the GES model hence comprising the dual pulse stimulus. Dual pulse stimulus was able to entrain slow waves with respect to time and space at an optimum frequency being 3.3 cpm (Figure 4.9 and 4.10). 100% entrainment was obtained for all frequency below the maximal driven frequency. An inverse variation of pulse width and amplitude was observed with dual pulse stimulus as well. From the observation of results in Sections 4.3.2 and 4.3.3 it has been concluded that the observed entrainment of slow waves with dual pulse stimulus was solely contributed by the long pulse stimulus of the dual pulse stimulus. However, in realistic GES scenario short pulse GES is expected to alleviate the chronic symptoms of gastroparesis.

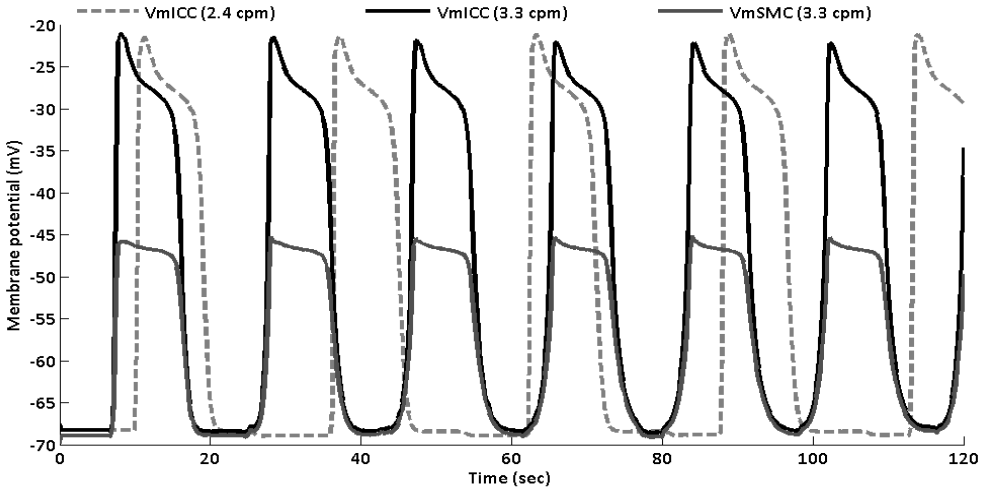

Figure 4.9: Gastric electric stimulation with dual pulse stimulus at a frequency higher than the intrinsic one normalizes bradygastric slow wave activity. The graph shows slow wave activity at the distance of 20mm from the proximal corpus.

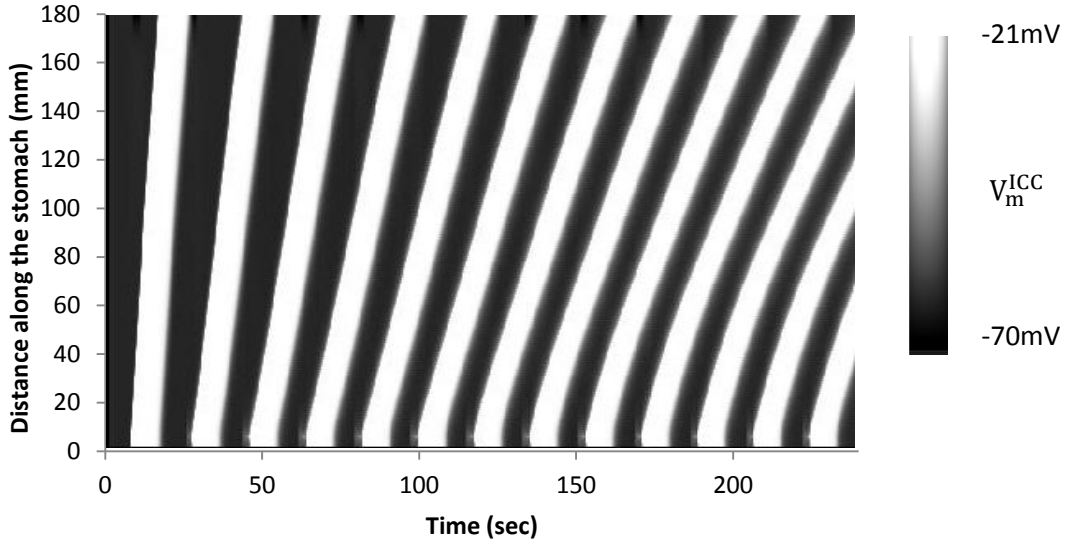

Figure 4.10: Spatiotemporal plot of V_m^{ICC} stimulated with dual pulse stimulus (pulse width 300ms for long pulse and 300μs for short pulse, amplitude: $5.0\frac{\mu A}{mm^3}$, frequency 3.3 cpm, Energy utilized: $24775ms * \mu A^2$) demonstrating slow wave propagation along the greater curvature. The long term stability is equivalent to that shown in Figure 4.6.

4.3.6 Synchronized stimulus

A Synchronized stimulus was delivered when maximum depolarization of ICC was detected. The stimulus frequency was same as the intrinsic frequency. The GES model responded to single channel synchronized stimulus by producing a higher depolarization at the point of stimulus injection. The increase in depolarization was found to be directly proportional to the pulse width and amplitude of the stimulus. A stimulus of amplitude $18\frac{\mu A}{mm^3}$ was injected on detection of peak ICC membrane potential for 300 ms (Figure 4.11). It was observed that the peak potential was increased form -21mV to -17mV. No other significant changes were noted.

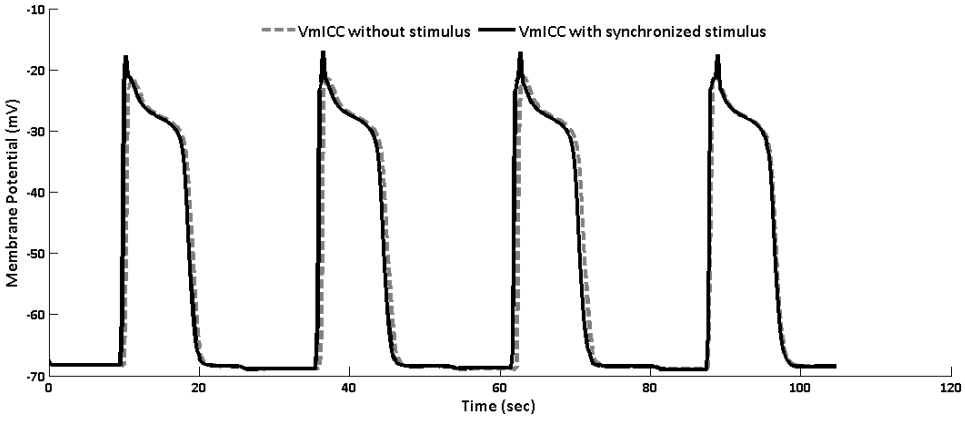

Figure 4.11: Synchronized stimulus producing an increase in the ICC peak potential. Energy utilized: $29.16 * 10^4$ ms $* \mu A^2$.

4.3.7 Enterra Therapy

Single channel Enterra Therapy as mentioned in the Chapter 1, was injected into the GES model with the parameters: frequency: 14Hz, 0.1seconds on and 5 seconds off, duration: 0.3ms, amplitude: 60μA. Enterra therapy is a type of pulse train stimulus with very short pulse duration of 0.3ms. As expected, the Enterra therapy parameters could neither evoke nor propagate slow wave activity as the duration and amplitude of the stimulus was very small (Figure 4.12). So, the slow wave profile and its spatiotemporal plot before and after stimulation with Enterra therapy parameters were the same. This is in line with the current understanding behind Enterra therapy that it works on the enteric nervous system rather than perturbing the gastric myoelectrical activity to alleviate the chronic symptoms of gastroparesis.

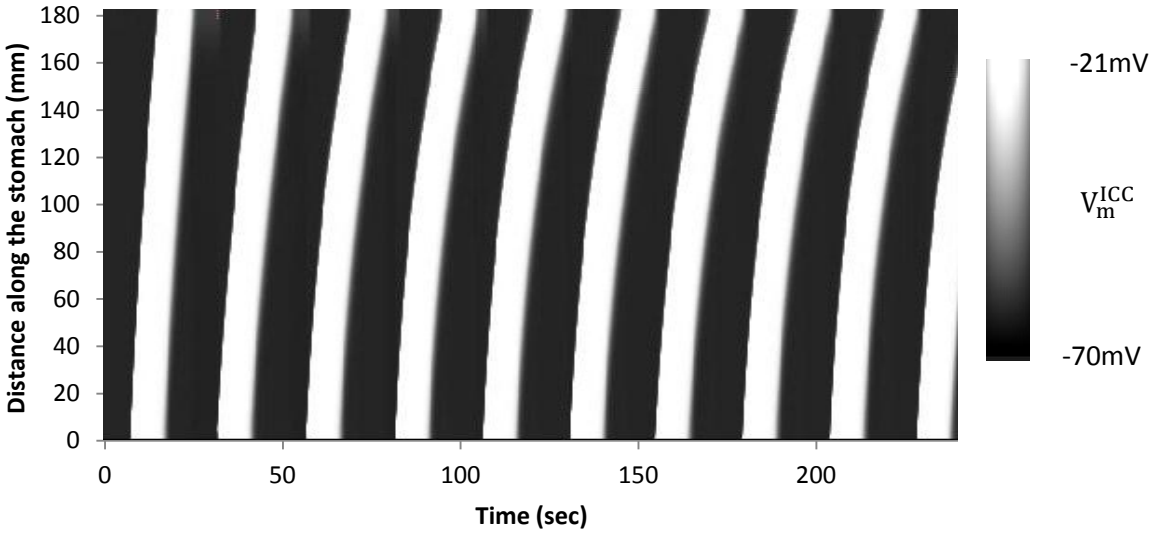

Figure 4.12: Spatiotemporal plot of V_m^{ICC} when stimulated with Enterra therapy parameters. Due to small pulse duration and amplitude these parameters did not alter intrinsic slow waves.

4.4 Discussion

Gastric electric stimulation has been shown to significantly alleviate gastrointestinal symptoms and considerably improve quality of life from as little as 6 weeks of therapy. Over the long term, it has been observed that GES maintains symptomatic relief and recovery of nutritional status. The efficiency of GES greatly depends on the chosen stimuli parameters. We have presented here a robust GES model which provides a platform by predicting if active entrainment of gastric electric activity is possible for the stimulation protocols employed. The developed GES model based on electrophysiological details of gastric ICC and SMC is an advancement over the previously constructed GES models, providing a platform to simulate the effects of single channel GES at different values of most pertinent stimulus parameters and hence make conclusions regarding their physiological significance.

Five different stimulus protocols, whose efficiency is currently being explored in experimental GES, were simulated. In order to reproduce impaired gastric slow waves and

normalize it by the application of GES, bradygastric conditions have been simulated. Single channel GES was modeled by injecting the stimulus in most proximal region of the cable (at a distance of 2mm along the 180mm long cable). On delivery of the stimulus at a more distal site (for example at a distance of 15mm along the 180 mm cable) the stimulated entrainment proceeded from the point of injection of the stimulus. As expected, retrograde entrainment of slow waves can be observed in region between start of the cable and the point of injection of the stimulus (Figure 4.13). It has been suggested that the resistance for retrograde slow wave propagation is higher than for antegrade propagation [59]. In addition, characteristics of retrograde slow wave propagation may be partly contributed by intrinsic activity and partly by stimulus entrained activity [66]. The occurrence of a bend observed in the spatiotemporal plot of V_m^{ICC} at the point of stimulus delivery can possibly be due to the intersection of antegrade and retrograde propagation and the difference in resistance offered by the gastric musculature for the two types of slow wave propagation. These results suggests that the point of injection of stimulus also plays a very important role in the determining the efficiency of GES. For single channel GES stimulus should always be injected in the proximal corpus to avoid retrograde propagation of slow waves.

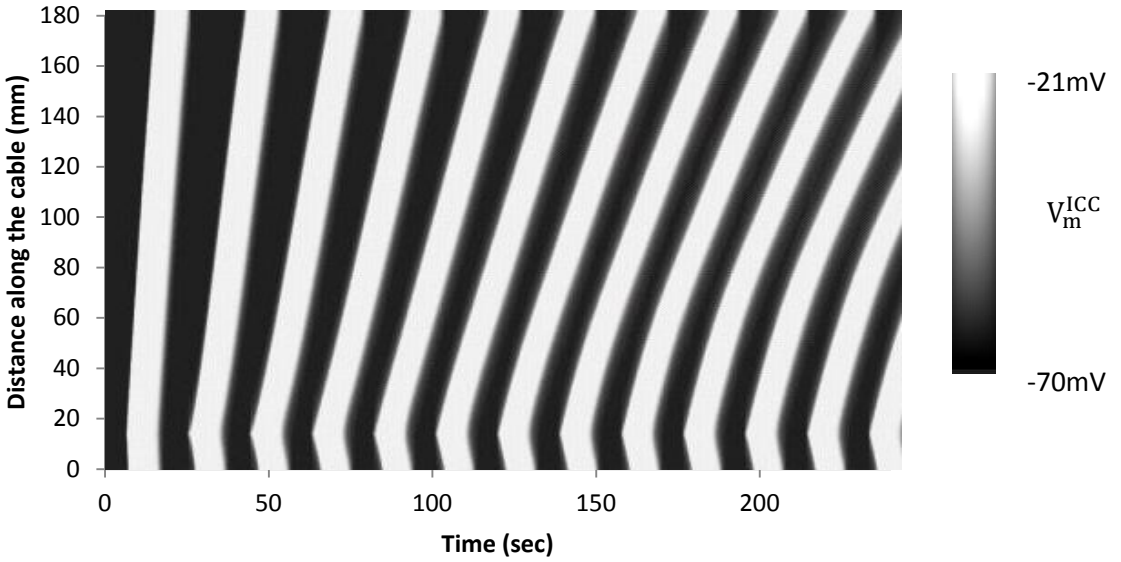

Figure 4.13: Stimulus injected at 15mm of 180mm cable give rise to a bend at the point of intersection of antegrade and retrograde propagation of slow waves.

The first stimulus was applied after 6.5 seconds of simulated time. The first stimulus time instant was chosen such that the stimulus appeared in close proximity to the onset of a slow wave and not in the refractory period of the pacemaker cells. However if the first stimulus instant was in the refractory period, the GES model would not respond to it and active entrainment would commence only from a subsequent stimulus that occurred close to the onset of a slow wave. For example the first stimulus (long pulse stimulus: same stimulus parameters as in Section 4.3.2) was given at the zeroth second of the simulated time with stimulus frequency set to 3.3cpm. From Figure 4.14 we see that the first two stimuli pulses (squared in blue) are only able to produce local depolarization. This can be explained due to the appearance of the stimulus during the refractory period of the pacemaker cells. The third stimulus is not shown in Figure 4.14 as it appears during descending phase of the second slow wave. Its effect is completely suppressed by the ongoing slow wave activity. Active slow wave generation and propagation is possible only when the stimulus appears close to the onset of a slow wave. Entrainment due to the

stimulus occurs only from the fourth stimulus pulse (Figure 4.14). As a consequence to the appearance of the first stimulus during the refractory period, the recorded frequency is 3.0 cpm yielding 66.66% entrainment in comparison to the same stimulus parameters, when delivered at a time instant approaching the commencement of a slow wave, producing a recorded frequency of 3.3 cpm giving 100% entrainment (Section 4.3.2).

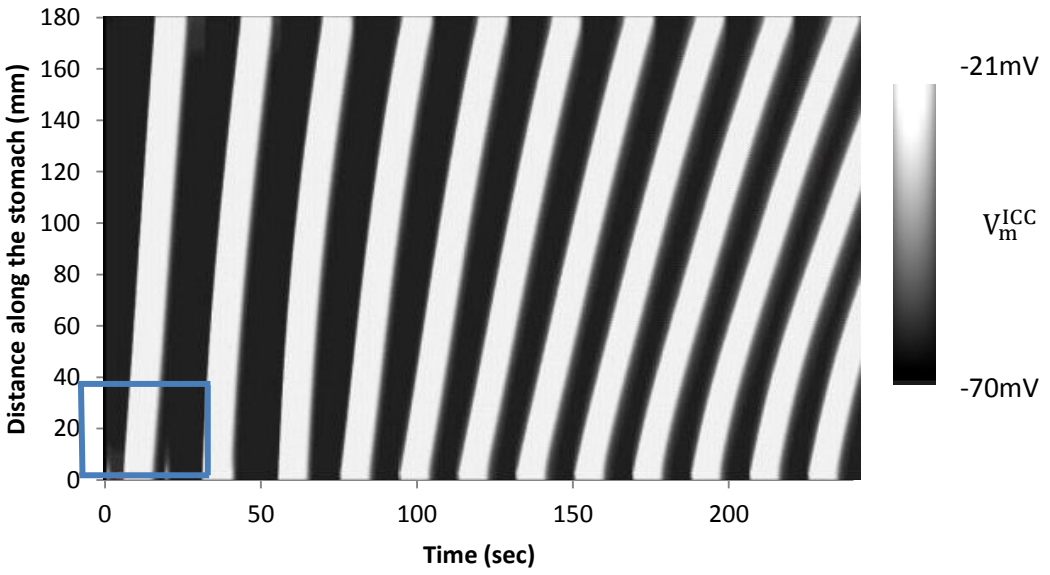

Figure 4.14: The region squared in blue highlights that the first two stimuli pulses generate local depolarization as their occurrence time is far from the onset of a slow wave. The third stimulus pulse appears during descending phase of the second slow wave and hence not portrayed in the graph. Entrainment starts from the fourth pulse.

For all the five stimulus protocols applied the most efficient frequency for stable entrainment of slow waves was 3.3cpm. However maximum driven frequency which can still sustain stable entrainment was 3.8 cpm. The maximum driven frequency can be decided based on the extent to which the refractory period can be reduced. As the frequency of the stimulus is increased the refractory period of the pacemaker cells may be considerably reduced. Figure 4.15 shows what happens when a stimulus was delivered at a frequency of 4.3 cpm. In this case the stimulus is able to invoke the generation of slow

waves, but the efficiency of slow wave propagation decreases with respect to both, time and space due to stimulus induced disturbed homeostatic condition prevailing in the ICC network. An ICC with considerably shorter refractory period will not be able to produce sustained long term entrainment of slow waves, explaining the instability that arises when the frequency is increased above 3.8 cpm.

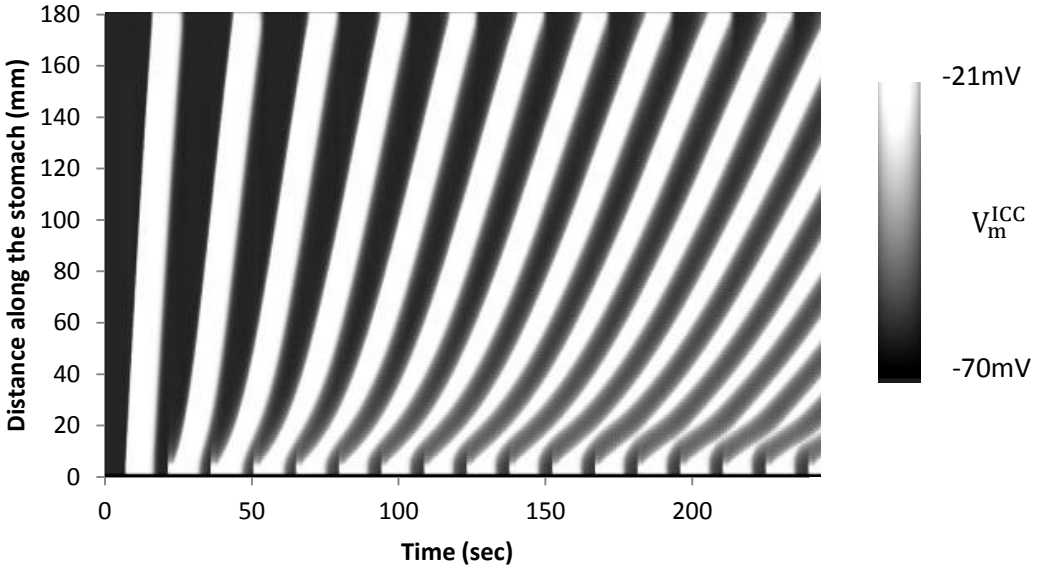

Figure 4.15: Spatiotemporal plot of ICC portraying unstable slow wave entrainment due to high frequency of the injected stimulus.

The results indicate that the pulse amplitude and pulse width are inversely related each other. Reciprocal variation in pulse duration and amplitude can be used to entrain gastric electric activity. Entrainment of slow waves can be still be achieved with a very short pulse duration (in the order of μA) but with a correspondingly high amplitude (greater than 75μA/mm^3). It should be noted that in realistic GES very high stimulus cannot be delivered at a single point in the proximal corpus to compensate a short pulse width. Injection of high amplitude stimulus even for a short period of time may damage the gastric musculature at that point aggravating gastroparetic symptoms rather than alleviating them. In addition to this, experimental GES employs stimulus amplitude for

long and short pulse stimulus almost in the same range. A balance should be maintained between the pulse amplitude and pulse width for any stimulus applied.

The developed GES model, which is a cable representation of the greater curvature of the stomach, has been discretized with a space step of 1mm. The extracellular space at each discrete point has been assumed to be a cube with each side measuring 1mm in length and hence a volume of $1mm^3$. The stimulus injected through I_{stim}^{EXT} represents the stimulus injected per unit volume of the extracellular space. Therefore, the stimuli applied were multiplied with the volume term and then utilized for energy calculation by Equations 4.2 and 4.3.

The conduction velocity of slow waves depends on the conductivities of ICC (σ_i^{ICC}), extracellular space (σ_e) and SMC (σ_i^{SMC}) [70]. These conductivities also influence the stimulus amplitude required for triggering the pacemaker cells. Depending on the domain into which the stimulus is injected, the corresponding conductivity will have a greater effect on the stimulus amplitude. As the presented GES model simulates the condition of injecting stimulus into the extracellular space, σ_e will have a greater impact on the stimulus amplitude compared to the other two conductivities. At a higher conductivity value the supplied stimulus decay quickly, requiring higher amplitude to trigger the pacemaker cells. So, it should be noted that the stimulus amplitude needed for activating the pacemaker cells mentioned in the Section 4.3 have been obtained with a σ_e value of $0.4\ \frac{mS}{mm}$.

As mentioned earlier, injection of stimulus into the ICC directly was also simulated. The pulse amplitude required to generate stable entrainment of slow waves when delivered into the ICCs was much less in comparison to that of a stimulus injected into the extracellular space. A direct pacemaker stimulus can be considered similar to an ionic current and hence its effect would be largely pronounced even with smaller amplitude, whereas stimulus for extracellular space will act like an impressed current and hence would require greater amplitude to trigger gastric electric activity.

In general, GES with long pulses is capable of entraining gastric slow waves. Short pulse GES has no effects on slow waves. In some circumstances, GES with short pulses was able to alter slow waves if the stimulation amplitude or pulse width is very high. GES with train of pulses was able to rectify gastric dysrhythmia. When the time interval between two subsequent pulses is small then the two short pulses may be assumed as a single pulse and hence a train of short pulses may be effectively considered as a single long pulse.

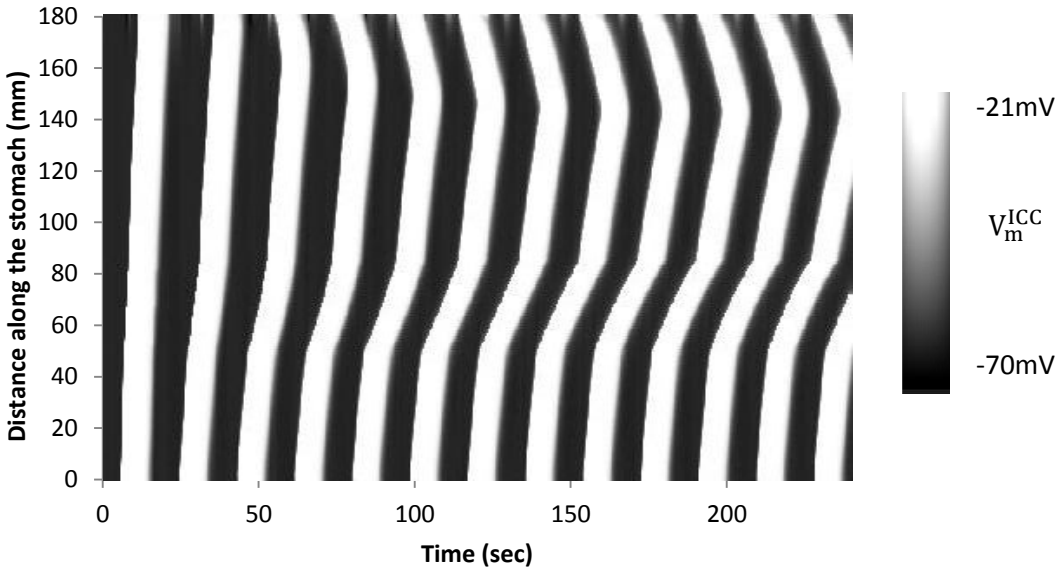

Figure 4.16: Single channel GES is not able to normalize slow waves impaired due to defective ICC coupling. Inspite of injecting a stimulus into the proximal corpus we see that retrograde entrainment has been triggered in the distal antrum.

From the results and discussion we can conclude that single channel GES is efficient in normalizing the impaired gastric electric activity arising due to decreased frequency (bradygastric) of gastric slow waves generated by defective pacemaker cells. Gastric dysrhythmia in diabetic gastroparesis, which in most cases arises due damaged or dysfunctioning vagus nerve, can also be efficiently normalized by single channel GES. On the other hand gastric dysrhythmia that arises due to defective coupling between the pacemaker cells may not be efficiently normalized using single channel GES. Retrograde

entrainment of slow waves may be activated due defective coupling between a patch of ICC in the cable network as shown in Figure 4.16. Defective coupling between the pacemaker cells would restrict the voltage dependant communication between the pacemaker cells, preventing the active entrainment of slow waves arising due to the delivered stimulus. Multi channel GES, placement of 2 to 4 electrodes so as to supply stimulus to entire region of corpus and antrum would be advantageous in such a situation. As a solution for the problem of weakened communication between the pacemaker cells, multi channel GES can be adopted to inject stimulus into different regions of corpus and antrum. Chapter 5 will throw light on modeling of multi channel GES for different stimulus protocols.

Chapter 5

Multi Channel GES

Introduction

Having presented a complete account of single channel GES with various stimulus protocols, a description of multi channel GES represents the next conceptual step towards the development of a fully integrated GES modeling framework. In this chapter, we will focus on gastric dysrhythmia arising due to defective coupling between the pacemaker cells and normalization of this gastric impairment through the application of multi channel GES with different stimulus protocols.

5.1 Background

Anatomically the stomach is divided into three functional segments: the fundus, corpus and antrum [9], with each segment participating in differing but complementary roles in the digestion process. General opinion is that the antrum is a greater contributor to the emptying of solids [87] [88]. During a meal, the fundus functions as a food reservoir and facilitates the chemical digestion of food by way of gastric acid and proteases. The antrum holds responsibility for grinding, mixing, and the process of reducing food into fine small particles [87]. The resulting chyme is cleared from the antrum into the proximal duodenum through peristaltic antral contractions [89]. In comparison to the proximal regions, the distal stomach plays a significant role in the process of gastric emptying. It is conceivable that direct stimulation of the distal stomach may be more efficient in alleviating the symptoms of gastroparesis rather that aiming at reduction of gastroparetic symptoms by giving a stimulus at the proximal corpus (conventional single channel GES). As mentioned in Section 4.4, when a single electrode delivers a stimulus at a distance further from the proximal corpus (start of the cable), there exists a greater

possibility for inducing retrograde slow wave propagation. Multi channel GES was suggested in order to directly stimulate the distal stomach without activating retrograde slow wave propagation.

Abnormal coupling between a patch of ICCs in the pacemaker network along the greater curvature may result in impairment of gastric slow waves. Damage or destruction of a patchy network of ICC may also induce gastric dysrhythmia. Each of these mechanisms may result in a drastic reduction of voltage dependant communication of the ICC network as a whole. For example, on considering a patch of ICC with defective coupling to be present between corpus and antrum (in the middle of ICC network) the entrainment mechanism across the network would be affected with a reduction in the conduction velocity especially in the region of ICC patch having defective coupling. This defective patch of ICC would act as a barrier for the slow wave propagation from the corpus to the antrum along the greater curvature. Further to this, intrinsic frequency gradient of the IP_3 concentration, as set by the intracellular IP_3 dynamics and self excitation property of pacemaking cells, should be taken into consideration. As a result the ICCs in distal antrum where normal coupling exists, would be activated ahead of the pacemaking cells with insufficient coupling. This would initiate antegrade slow wave propagation commencing from the proximal corpus followed by retrograde propagation commencing from the distal antrum resulting in gastric dysrhythmia. As mentioned in Section 4.4, in such a situation single channel GES may not be effective in normalizing the gastric dysrhythmia as the propagation of a stimulus delivered at the proximal corpus along the greater curvature would also be hindered. As an attempt to address the problem of retrograde slow wave propagation arising from reduction of communication between the ICCs in a network, multi channel GES has been suggested as an alternative strategy to single channel GES.

In multi channel GES, stimuli are injected at multiple locations from the corpus to the antrum along the greater curvature (Figure 5.1). In experimental GES, dual channel GES is practiced by delivering stimulus via two electrodes with the electrode being placed at the proximal corpus and the second electrode placed at a distance of 100mm from the first electrode. In case of multi channel GES stimulus is applied through four electrodes. The inter electrode distance is around 40mm and the last electrode is placed atleast 20mm from the pylorus.

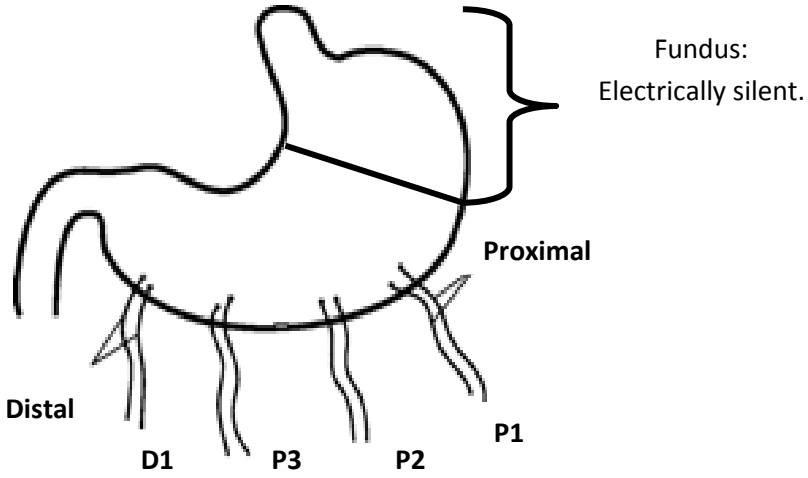

Figure 5.1: Placement of electrodes in multi channel GES. P1, P2, P3 represent the first three proximal electrodes and D1 represents the most distal electrode.

5.2 Modeling multi channel GES

A cable length of 180mm, representing corpus and antrum, was chosen for modeling of multi channel GES. A gastric dysrhythmia, induced by abnormal coupling between the patch of pacemaker cell in the cable network, was simulated by reducing the value of σ_i^{ICC} (of Equation 3.17) only for a selected region of ICCs in the cable. σ_i^{ICC} represents the ICC conductivity, in other words it can also be referred as the coupling factor between two neighboring ICCs. It controls the degree of communication between adjacent ICCs and was expressed in $\frac{mS}{mm}$. The value of σ_i^{ICC} in normal coupling condition was set to be $0.5\frac{mS}{mm}$ [69]. Abnormal coupling between the pacemaker cells was modeled by reducing

the value of σ_i^{ICC} by 99%; the value was decreased to 0.005 $\frac{mS}{mm}$. The defective region of ICC was set to approximately in the center of the 180mm cable. The reduced value of σ_i^{ICC} was assigned to all the ICCs from 50mm to 85mm of the cable. The original value of σ_i^{ICC} was ascribed to the rest of the cable. This strategy mimics the physiological situation of considering the greater curvature of a stomach having ICCs with defective coupling in the region of distal corpus extending for a length of 35mm (Figure 5.2). The rest of the region of cable can be assumed to have normal coupling. Reduction in the value of σ_i^{ICC} is synonymous with the decreasing the number of gap junctions between the ICC thereby weakening communication between the ICCs.

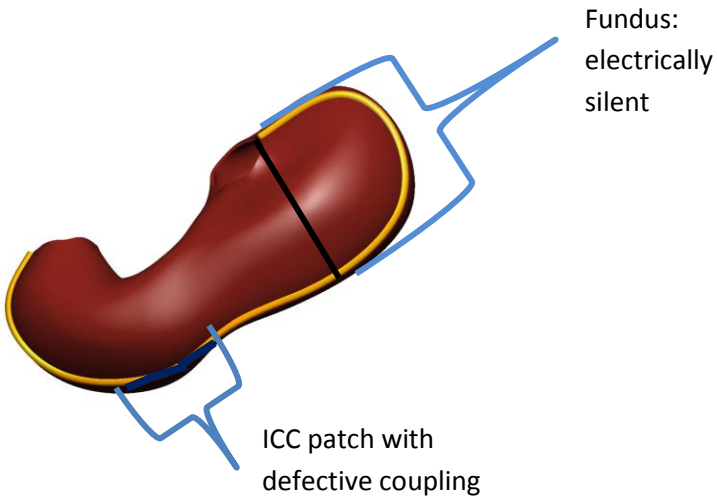

Figure 5.2: Greater curvature of the stomach with defective ICC-ICC coupling in a small region. Yellow cable indicates normal ICC-ICC coupling and blue cable indicates defective ICC-ICC coupling.

Stimuli were injected at two points along the cable. The first point of stimulus injection was at a distance of 4mm from the proximal corpus. The second point of stimulus injection was at a distance of 45mm from the proximal corpus. The second point was chosen considering the fact that the ICC patch with defective coupling would commence from 50mm of the cable. At the former stimulus injection site, the first stimulus instant was set to be after 6.5 seconds of simulated time. At the latter stimulus injection site, the first stimulus instant was set to be after 12.25 seconds of simulated time. Subsequent

stimuli were delivered thereafter as dictated by the stimulus frequency that was set. The first stimulus instant for both the locations was decided based on the appearance of rising phase of slow waves at its intrinsic frequency. The difference in the first stimulus instant time of the proximal and distal stimulus injection site corresponded to the phase shift that existed between these two points.

As in single channel GES, stimuli were delivered to the GES model through I_{stim}^{EXT} of Equation 3.19. On the basis of published experimental data (Chapter 2) starting values for the pertinent stimulus parameters i.e., pacing frequency, pulse width and amplitude, were determined. The stimulus frequency was chosen such that it was higher than the intrinsic slow wave frequency, with a value of 1.1 times the intrinsic frequency that was obtained as the optimum frequency for pacing (Section 4.3). It should be noted that gastric dysrhythmia has been induced by simulating the condition of defective coupling between the ICCs. So, the intrinsic frequency of the system was set to 3 cpm except in section 5.3.1 where bradygastria was simulated. Pulse width was decided depending upon the type of stimuli employed. The current amplitude of the stimuli was started with a low value and was gradually increased until stable entrainment was achieved. The parameters were optimized such that least amount of energy was consumed without compromising on the stability of slow wave entrainment. Percentage entrainment (Equation 4.1) was used to quantify the efficiency of pacing parameters and energy was calculated using Equations 4.2 and 4.3.

5.3 Simulation results

5.3.1 Multi channel GES for treating bradygastria

Gastric dysrhythmia (bradygastria) as mentioned in Section 4.2 was generated and the efficacy of multi channel GES in restoring gastric electric activity was analyzed. Long pulse stimuli with parameters pulse width 300ms, amplitude: $5.0\frac{\mu A}{mm^3}$, frequency 3.3 cpm were delivered at four points along the cable with a distance of 45mm between the points. The phase shift between the points was taken into consideration. The first point was at a distance of 2mm from the proximal corpus and the final point at a 137mm from the

proximal corpus. 100% entrainment was achieved at the stimulated frequency (Figure 5.3). Different combinations of the stimuli amplitude delivered at the second, third and fourth point were varied keeping the amplitude of the stimulus delivered at the first point constant. No significant changes were observed from Figure 5.3. The same phenomenon was observed with pulse train stimulus and dual pulse stimulus as well.

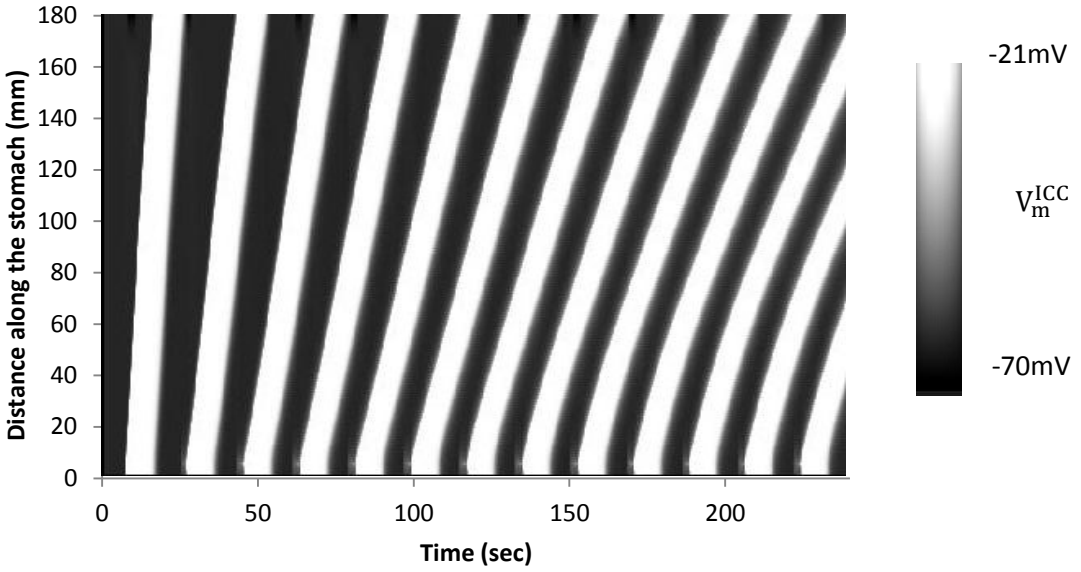

Figure 5.3: Normalizing bradygastric slow waves using multi channel GES. No significant change from Figure 4.6 was observed.

5.3.2 Generating dysrhythmia

Gastric dysrhythmias arising due to abnormal ICC-ICC coupling have been simulated. Retrograde entrainment of slow waves was observed at the intrinsic frequency of the system as per Section 5.2. Figure 5.4 displays the abnormal gastric electric activity induced by reduction in the value of σ_i^{ICC} for a patch of cells in the ICC cable network. The effectiveness of various stimuli types in normalizing the induced gastric dysrhythmia will be demonstrated in this chapter. Figure 4.16 shows that application of single channel GES is not sufficient to normalize this type of gastric dysrhythmia.

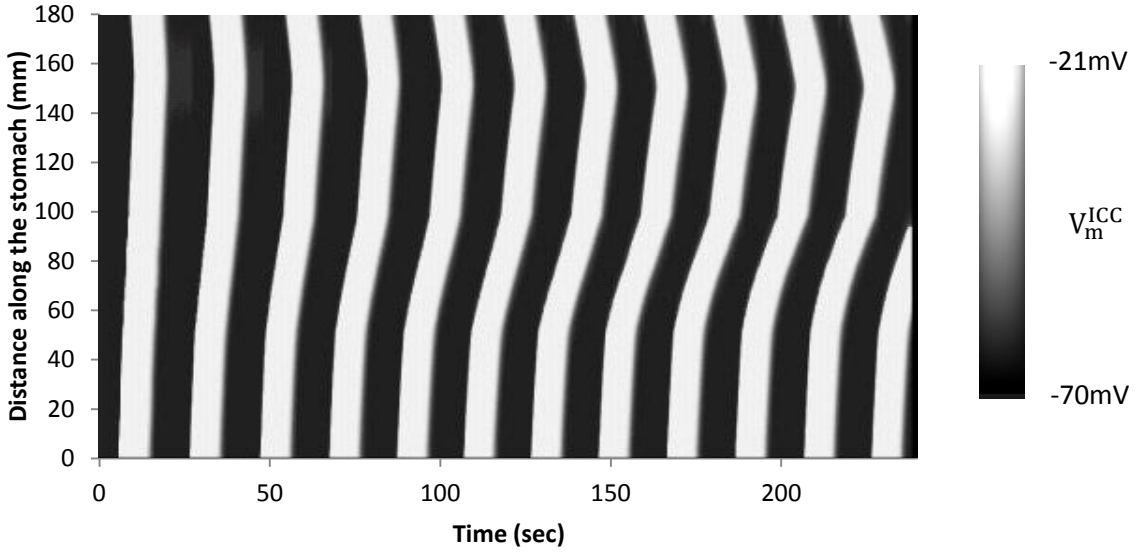

Figure 5.4: Gastric dysrhythmia due to defective ICC-ICC coupling.

5.3.3 Long pulse stimulus

For duration of 300ms stimulus amplitude of 2.0 $\frac{\mu A}{mm^3}$ at the proximal stimulus delivery site and 3.0 $\frac{\mu A}{mm^3}$ at the distal stimulus delivery site was required for triggering the pacemaker activity. Results have indicated that reciprocal variation in pulse duration and amplitude can be used to entrain gastric electric activity. The frequency of the stimulus was chosen to be slightly above the intrinsic frequency. The most optimal frequency for stimulation was found to be 1.1 times the intrinsic gastric slow wave frequency. So, a stimulated frequency of 3.3 cpm was used (Figure 5.5). The energy required for entrainment was 24750 ms $* \mu A^2$. When the stimulus was injected into the ICC a pulse amplitude of 0.04 $\frac{\mu A}{mm^3}$ was sufficient to stimulate pacemaker activity. 100% entrainment was achieved at the optimal frequency.

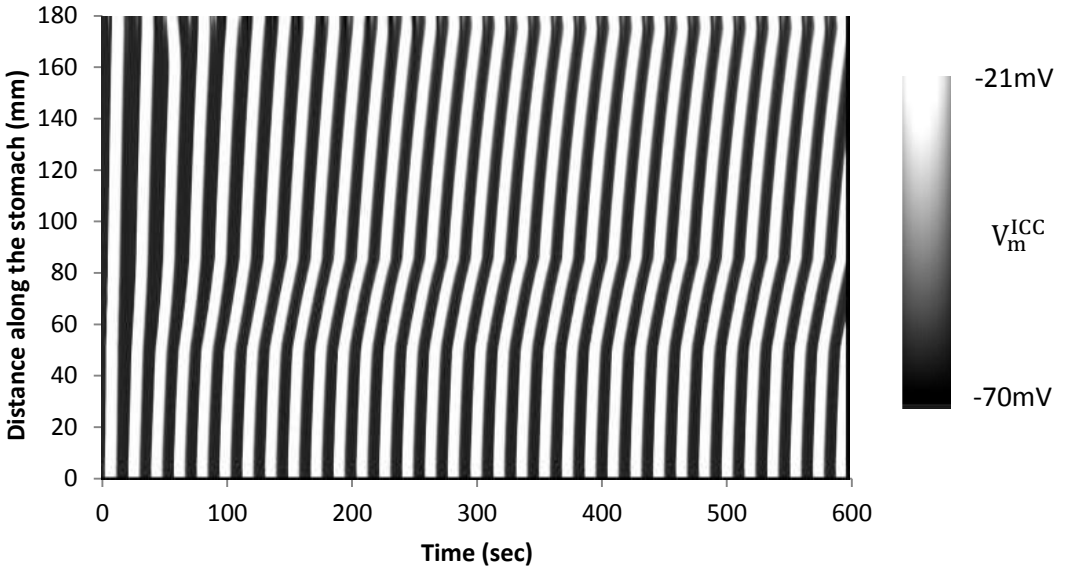

Figure 5.5: Spatiotemporal plot of V_m^{ICC} stimulated with long pulse stimulus (parameters: pulse width 300ms, amplitude: 2.0$\frac{\mu A}{mm^3}$ (at site 1) and 3.0 $\frac{\mu A}{mm^3}$ (at site 2), frequency 3.3 cpm demonstrating normalization of the slow wave activity.

5.3.4 Short pulse stimulus

The short pulse stimulus did not produce any effect on gastric slow wave activity i.e., it was not able to prevent retrograde entrainment of slow waves. As put forward by the experimental investigators short pulse GES, did not produce any effect on gastric slow wave activity. Even if the stimulus amplitude was very high, 75$\frac{\mu A}{mm^3}$ at both the stimuli injection sites, gastric dysrhythmia could not be normalized. From Section 4.3.4 and results observed on this section we can observe that electrical effects of short pulse stimulus may not be very prominent.

5.3.5 Pulse train stimulus

A train of pulses, when injected into the GES model, entrained gastric slow waves at the stimulated frequency and was also able to correct the retrograde entrainment of slow

waves. Reciprocal variation in current amplitude and pulse width was observed. Stimulus frequency was set to 3.3 cpm and 100% entrainment was achieved at this frequency. GES with pulse train stimulus of parameters: duration: 5.5, amplitude: 2.0 $\frac{\mu A}{mm^3}$ at site 1 and 3.0 $\frac{\mu A}{mm^3}$ at site 2, frequency 70 Hz, cycle on for 3 sec and off for 15 sec rectified the retrograde propagation of slow waves (Figure 5.6).

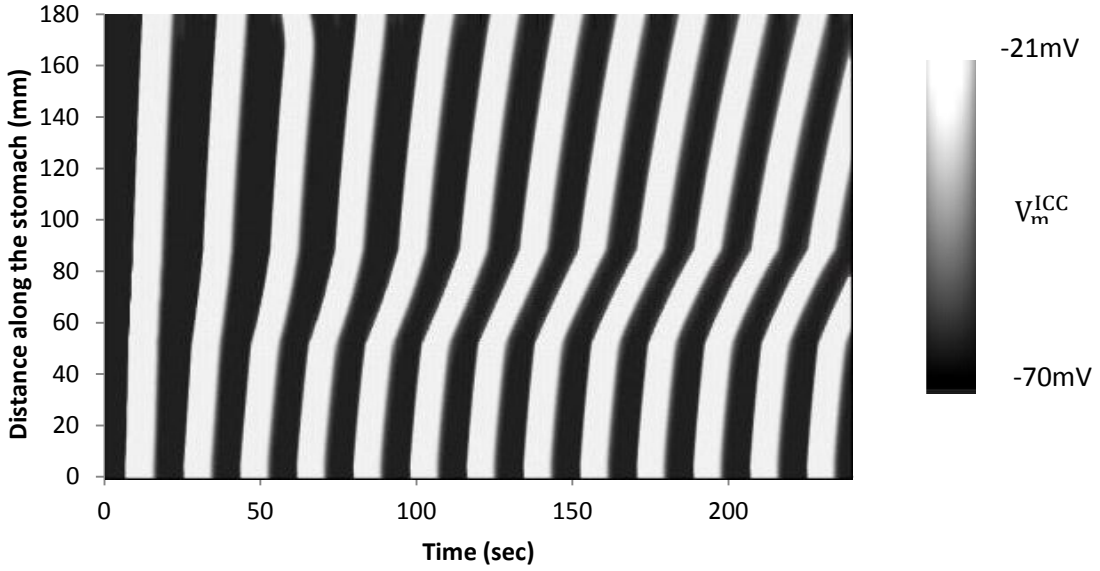

Figure 5.6: Spatiotemporal plot of V_m^{ICC} stimulated with pulse train stimulus (parameters: pulse width 5.5 ms, amplitude: 2.0$\frac{\mu A}{mm^3}$ (at site 1) and 3.0 $\frac{\mu A}{mm^3}$ (at site 2), frequency 70 Hz, cycle on for 3 sec and off for 15 sec, Energy utilized: $9.53 * 10^4$ $ms * \mu A^2$) demonstrating normalization of the slow wave activity. Long term stability is equivalent to that in Figure 5.5.

5.3.6 Dual pulse stimulus

A short pulse of the duration 300µs followed by a long pulse of duration 300ms was injected into the GES model. Dual pulse stimulus was able to entrain slow waves with respect to time and space at an optimum frequency being 3.3 cpm (Figure 5.7). 100%

entrainment was obtained at the optimal frequency. An inverse variation of pulse width and amplitude was observed with dual pulse stimulus as well.

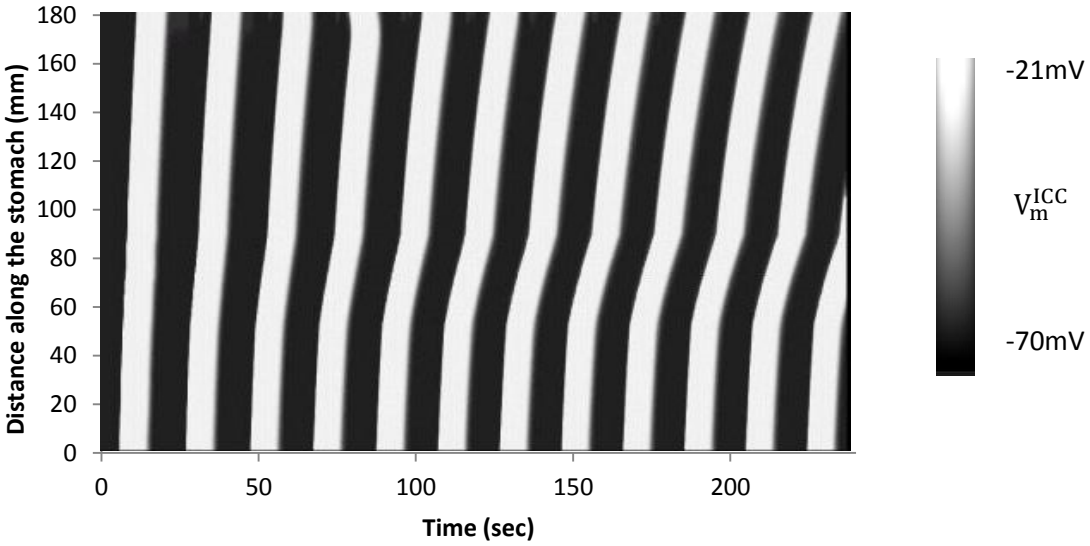

Figure 5.7: Spatiotemporal plot of V_m^{ICC} stimulated with dual pulse stimulus (pulse width 300ms for long pulse and 300µs for short pulse, amplitude: 2.0$\frac{\mu A}{mm^3}$ (at site 1) and 3.0 $\frac{\mu A}{mm^3}$ (at site 2), frequency 3.3 cpm, Energy utilized: 24775ms $*$ μA^2 demonstrating slow wave propagation along the greater curvature. Long term stability is equivalent to that in Figure 5.5

5.3.7 Synchronized stimulus

Synchronized stimulus was delivered when peak membrane potential of ICC was detected. The stimulus frequency was same as the intrinsic frequency. Synchronized stimulus was able to rectify retrograde entrainment of slow waves and thereby normalize gastric electric activity. Increase in depolarization at the point of stimulus injection was also observed at the point of stimulus injection. A stimulus of amplitude 2.0 $\frac{\mu A}{mm^3}$ and 3.0 $\frac{\mu A}{mm^3}$ was injected at the proximal and distal stimulus injection site on detection of peak ICC membrane potential for 300 ms.

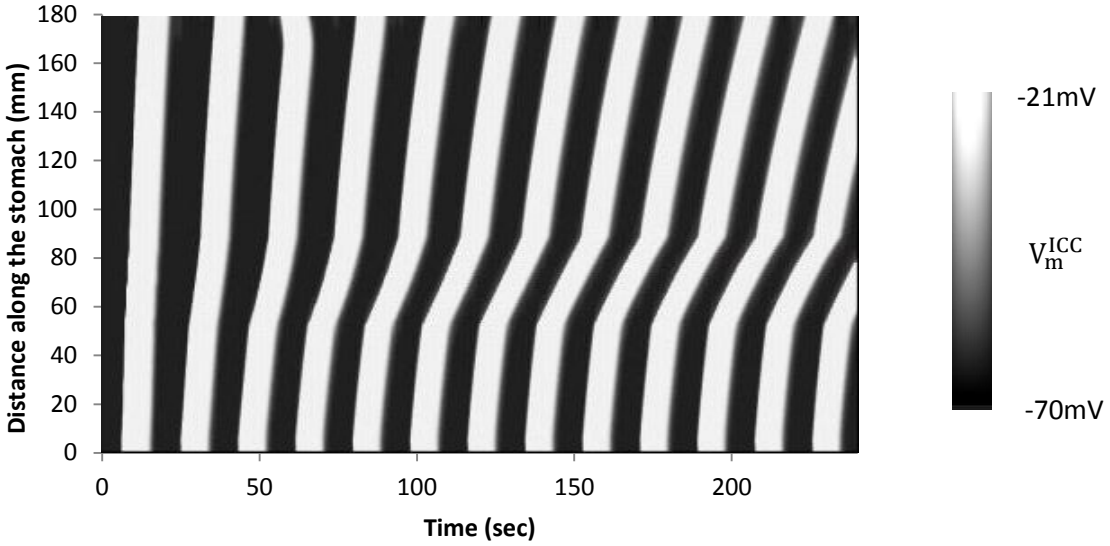

Figure 5.8: Spatiotemporal plot of V_m^{ICC} stimulated with synchronized stimulus (pulse width 300ms, amplitude: $2.0\frac{\mu A}{mm^3}$ (at site 1) and 3.0 $\frac{\mu A}{mm^3}$ (at site 2), frequency: 3 cpm Energy utilized: 22500 $ms * \mu A^2$) demonstrating normalization of retrograde slow wave propagation.

5.3.8 Enterra Therapy

Multi channel Enterra Therapy could not normalize gastric dysrhythmia Enterra due to very short pulse duration. As expected the Enterra therapy parameters could not rectify the retrograde entrainment of slow waves.

5.4 Discussion

Multi channel GES has been shown to significantly reduce gastroparetic symptoms by a number of experimental GES investigators [42], [55], [56], [57]. The efficacy of multi channel GES in normalizing bradygastric slow waves is similar to that of single channel GES (Figure 5.3). It can be observed that single channel GES posses an edge in terms of

consuming less energy and being less invasive over multi channel GES in a scenario where only bradygastric slow waves exist (without defective ICC patches).

Impaired gastric slow waves were generated by simulating the presence of an ICC patch with reduced coupling along the stomach's greater curvature. This chapter elucidates the efficiency of multi-channel GES with the available stimulus protocols in normalizing the simulated gastric dysrhythmia. Multi channel GES was modeled by injecting the stimulus at a proximal site (at a distance of 2mm from the corpus) and at a further distal site (at a distance of 45mm from the corpus). The site second stimulus injection was chosen such that it was in close proximity to the ICC patch with defective coupling. The first stimulus instant for both the stimulus injection sites was set such the pulses occurred close to the onset of a slow wave.

Injection of a stimulus at the beginning of a corpus would activate the pacemaker cells and invoke slow wave activity at the stimulus frequency. Due to the existence of a group of ICC with reduced coupling at the center of the cable the ICCs at the distal end of the cable will be activated resulting in retrograde entrainment of slow waves. Delivering a stimulus adjacent to the defective patch of ICC (along stimulus at the proximal corpus) would improve the entrainment characteristics of the defective ICC patch and hence reduce the hindrance to active slow wave propagation provided by the defective ICC patch. This would help in normalizing the existing gastric dysrhythmia. However, even if the entrainment characteristics of the defective ICC is ameliorated, the conduction velocity of this region still remains low compared to the rest of the cable with normal coupling (Figure 5.5). The aim of multi channel GES is to prevent the retrograde propagation of slow waves. So, the stimulus frequency was set to 3.3 cpm, which was found out to be the optimum frequency from Section 4.3. Four channel GES was also able to normalize the gastric dysrhythmia arising due to reduced inter ICC coupling. Stimuli parameters employed as in Section 5.3.3 were used, stimuli amplitude of 2.0 $\frac{\mu A}{mm^3}$ were used for the third and fourth stimulation sites. No significant changes from Figure 5.5 (dual channel GES) were observed with four channel GES. It should be noted that two channel GES in this scenario would be more efficient in terms of energy consumption.

In the physiological situation, the group of defective ICCs may not be restricted to single region along the greater curvature. They may be dispersed in small patches or spread as lengthy patches at more than a single location along the greater curvature. The stability of the developed GES model reduces as the presences of multiple defective ICC patches are simulated. It should be noted that the model uses stabilized bi conjugate gradient method (an iterative technique) to solve the matrix system. The convergence accuracy and hence the stability of this iterative method would be affected as the ICC's conductivities is varied randomly or as the presence of multiple defective ICC patches is simulated. Taking into consideration the stability of the GES model, we have chosen to simulate the presence of a single lengthy ICC patch with reduced number of gap junctions (reduced coupling) and normalize the arising gastric dysrhythmia by application of stimulus at two different sites along the greater curvature. As the ICC-ICC coupling is varied randomly, more than two electrodes may be needed to normalize the generated gastric dysrhythmia. However the concept behind the generation of gastric dysrhythmia due to reduced inter ICC coupling and the technique of introducing multiple stimulation sites to normalize it has been well elucidated by the strategy that we have adopted in multi channel modeling of GES.

The protocol for multi channel gastric pacing has been developed by considering and evaluating different combination of the stimulus parameters for each individual channel with a focus for normalizing the generated gastric dysrhythmia in the GES model. From results and discussion we see that multi channel GES with long pulse stimulus would be quite efficient for the treatment of gastric motility disorders arising due to defective coupling between the pacemaker cells.

Chapter 6

GES for obesity treatment

Introduction

Retrograde gastric pacing has been suggested as a potential therapy for the treatment of morbid obesity. In this chapter we have attempted to explore the capability of the developed GES model in the generation and propagation of slow waves in the retrograde direction in response to a stimulus delivered in the distal stomach.

6.1 Background

The principle behind retrograde gastric pacing is to simulate the presence of an artificial ectopic pacemaker in the distal stomach. Retrograde gastric pacing aims to decelerate the rate of propulsive contraction and thereby increase gastric emptying time without provoking intolerable symptoms. Consequently, this would result in early satiety and a reduced food intake. Slow waves propagating retrogradely, travelling against the antegrade slow waves that propagate from the proximal to the distal stomach induce gastric dysrhythmia. Many experimental investigators have demonstrated the efficiency of retrograde gastric pacing in disrupting normal gastric slow waves, generating dysrhythmia, inhibiting antral contractions, increasing gastric emptying time and reducing food intake hence resulting in weight loss.

6.2 Modeling retrograde gastric pacing

A cable length of 180mm representing the corpus and antrum was chosen for modeling retrograde gastric electric activity. The stimulus was injected at a distance of 60mm from the pylorus (Figure 6.1). The first stimulus instant was set to be after 10 seconds of

simulated time. Subsequent stimuli were delivered thereafter as dictated by the stimulus frequency that was set. Considering the existence of an intrinsic frequency gradient along the stomach the first stimulus instant was chosen such that it was close to the onset a slow wave at the point of stimulus injection. Retrograde gastric pacing with long pulse stimulus and pulse train stimulus has been modeled. The other stimuli types are not of significant importance in obesity treatment, as GES in this scenario is not expected to alleviate symptoms such as nausea, abdominal pain and vomiting. Stimulus is delivered to the GES model through I_{stim}^{EXT} of Equation 3.19. The intrinsic frequency of the system was set to 3 cpm. The stimulus frequency was always higher than the intrinsic slow wave frequency. Percentage entrainment (Equation 4.1) was used to quantify the efficiency of pacing parameters and energy was calculated using Equations 4.2 and 4.3.

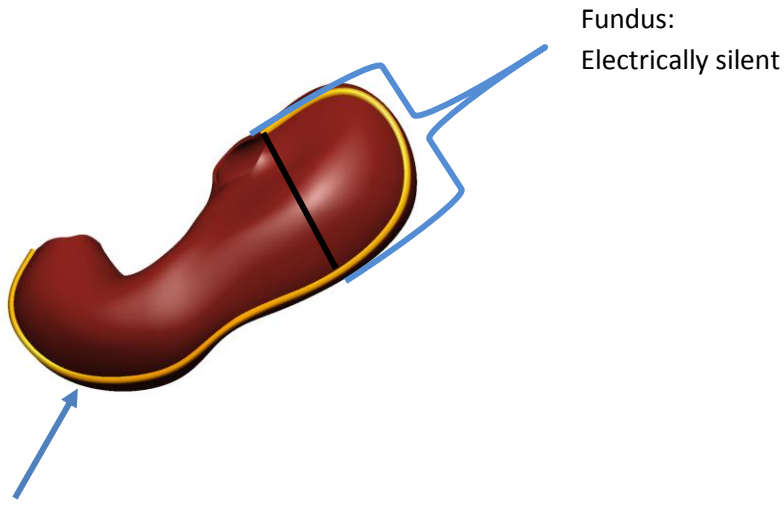

Figure 6.1: Placement of electrode at the distal stomach to trigger retrograde slow wave propagation. Blue arrow indicates the position of electrode.

6.3 Simulation results

6.3.1 Long pulse stimulus

For duration of 300ms stimulus amplitude of 7.0 $\frac{\mu A}{mm^3}$ was required for triggering retrograde propagation of slow waves (Figure 6.2). Inverse variation in pulse duration and amplitude was observed. The most optimal frequency for stimulation was found to be 1.1 times (3.3 cpm) the intrinsic gastric slow wave frequency. However upper limit of

frequency for stable entrainment was 1.25 times (3.75 cpm) the intrinsic frequency. The energy required for entrainment was 48510 ms $*$ μA^2. 100% entrainment was achieved at all frequencies below the upper limit.

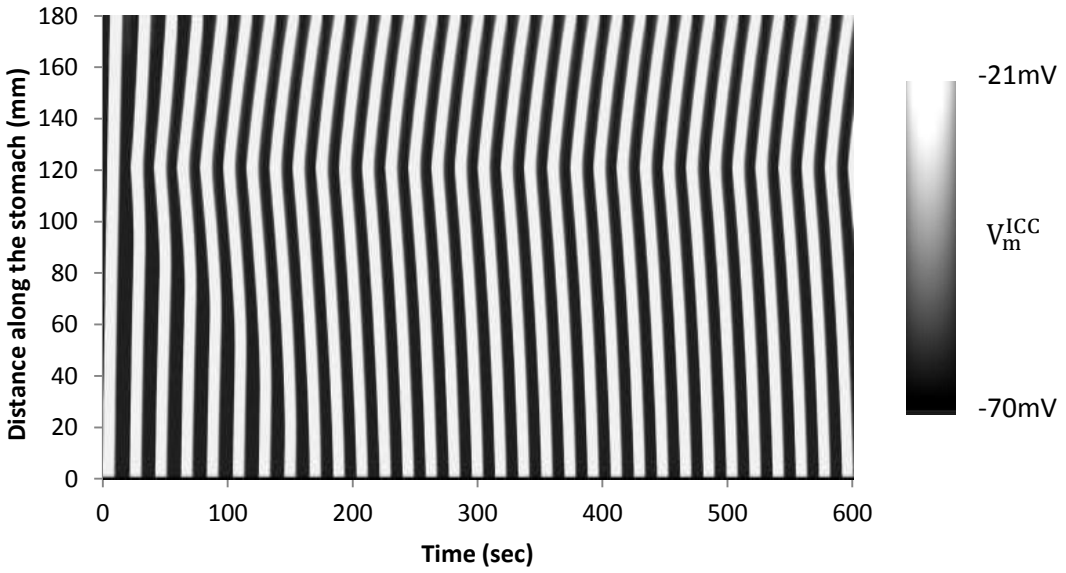

Figure 6.2: Spatiotemporal plot of V_m^{ICC} stimulated with long pulse stimulus at a distance of 60mm from the pylorus (parameters: pulse width 300ms, amplitude: 7.0$\frac{\mu A}{mm^3}$, frequency 3.3 cpm) for 10 minutes demonstrating the retrograde slow wave activity.

6.3.2 Pulse train stimulus

A train of pulses, when injected into the GES model, stimulated retrograde entrainment of gastric slow waves at the stimulated frequency. Reciprocal variation in current amplitude and pulse width was observed. Stimulus frequency was set to 3.3 cpm. However the upper limit for stable entrainment was 3.75 cpm and 100% entrainment was achieved at all frequency below the upper limit. Pulse train stimulus with parameters: duration: 5.5 ms, amplitude: 8.5 $\frac{\mu A}{mm^3}$, frequency 70 Hz, cycle on for 3 sec and off for 15 sec was employed to achieve retrograde propagation of slow waves (Figure 6.3).

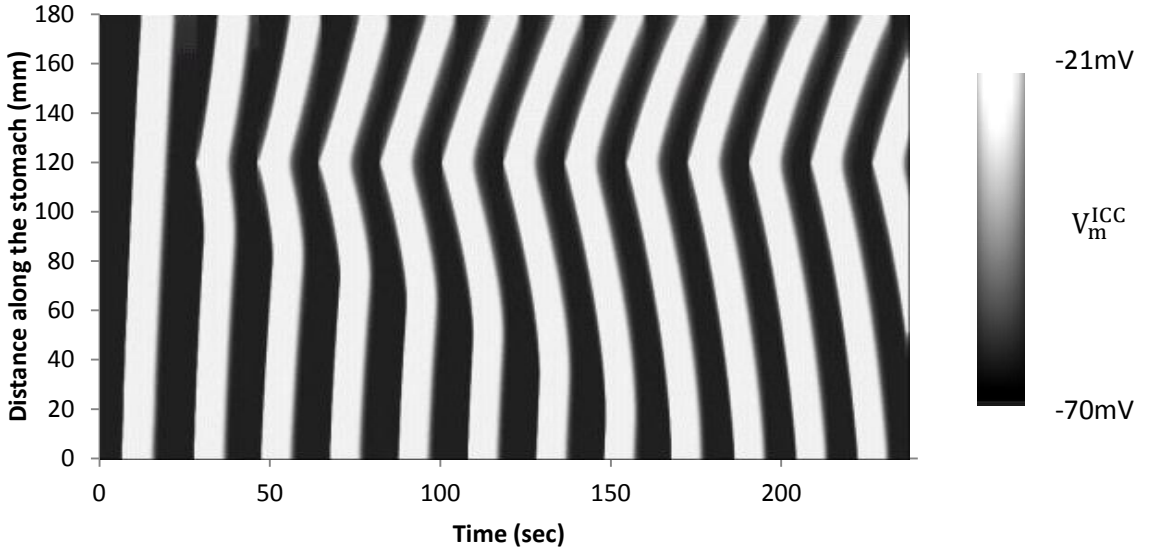

Figure 6.3: Spatiotemporal plot of V_m^{ICC} stimulated with pulse train stimulus (parameters: pulse width 5.5 ms, amplitude: 7.0$\frac{\mu A}{mm^3}$, frequency 70 Hz, cycle on for 3 sec and off for 15 sec, Energy utilized: $1.87 * 10^5$ ms $* \mu A^2$) demonstrating retrograde propagation of slow wave. Long term stability is equivalent to that in Figure 6.2.

6.3 Discussion

Even though many experimental investigators have suggested the placement of electrodes along the lesser curvature for obesity treatment [60], the efficiency of stimulus injection at a distal site along the greater curvature, inducing retrograde slow wave for obesity treatment has also been demonstrated experimentally [59]. Based on the latter hypothesis we have extended the GES model and explored its efficiency in the generation of retrograde slow wave propagation. A higher stimulus amplitude was required to stimulate retrograde propagation than to stimulate antegrade propagation of slow waves. For duration of 300ms minimum stimulus amplitude of 7.0 $\frac{\mu A}{mm^3}$ is required to trigger retrograde propagation in comparison to stimulus amplitude of 2.0 $\frac{\mu A}{mm^3}$ to stimulate antegrade propagation. One possible explanation for this phenomenon is that the resistance offered by gastric musculature for retrograde propagation is higher and

therefore requires higher stimulus amplitude for triggering retrograde propagation of slow waves.

The developed GES model is ideally suited to the research task of offering a platform to analyze the efficiency of pacing parameters in the generation and propagation of slow waves in the retrograde direction. Therefore, the developed GES model provides the flexibility to be employed for evaluating the efficiency of pacing parameters for the treatment of gastric motility disorders and obesity, while preserving the underlying electrophysiological principles that describes the interaction between the multiple active cell types present in the gastric musculature.

Chapter 7

Conclusions

The aim of this research project was to develop a realistic computational model for gastric electrical stimulation directed to study the efficiency of various stimulus protocols for the treatment of gastric motility disorders and obesity.

We have adapted the extended bidomain framework for gastric musculature as a foundation for the development of the GES model. An additional syncytium called the bath was integrated with the extended bidomain framework in order to simulate the presence of a closed circuit condition. Voltage coupling properties of the Corrias Buist ICC (2008) model had to be strengthened before incorporating it into the GES model. To achieve this the voltage coupling mechanism that was already present in the original Corrias and Buist ICC model was replaced by introducing intracellular IP_3 dynamics, as suggested by Imtiaz et al (2002) [71] followed by reduction in the value of h (fraction of IP_3 channel not inactivated by calcium). This updated Corrias Buist ICC model is more sensitive to voltage changes of adjacent ICC and can be effectively used to model the generation and propagation of gastric slow waves along the length of the stomach. It also possesses a robust mechanism of intracellular IP_3 dynamics. Hence voltage coupling mechanism of Corrias and Buist ICC model has been strengthened by the author.

The key advantage of this model is the flexibility that it offers to simulate normal gastric electric activity as well as different types of gastric dysrhythmia that may arise due to defective conditions in the gastric musculature. Two different types of gastric dysrhythmia have been simulated and the efficacy of different stimuli protocols (that are currently employed in experimental GES) in normalizing the generated gastric dysrhythmia are explored. The available stimuli protocols are modeled and their efficiency as single channel and multi channel GES has been demonstrated with an edge for analyzing their energy efficiency as well. Further, the developed GES model has also allowed us to investigate retrograde entrainment of slow waves which is considered to have therapeutic potential for obesity treatment.

7.1 Limitations and future work

We have presented in this research project a new computational model for gastric electrical stimulation which offers a significant advancement over the previously published GES models thereby providing a tool for optimizing different stimulus protocols and tailoring them specifically to the type of gastric dysrhythmia to be treated.

Construction of electrophysiological models usually follows a hierarchy of cell – tissue – and finally whole organ models. This model uses a cable representation of the greater curvature of the stomach and can be considered equivalent to a tissue level model of GES. Before construction of the presented tissue level GES model a cell level GES model was built using the single cell models of ICC and SMC to assess the feasibility and effectiveness of GES. Here a single ICC (updated version) was connected to a single SMC via gap junctions with an external stimulus been injected into the ICC. Once satisfying results were obtained we were able to move towards next higher level of modelling i.e. tissue model of GES (presented in the thesis). In the absence of a robust tissue level GES model it would not be appropriate to directly move on to whole stomach model. The most natural future development would be to construct a whole stomach model for GES. With the aid of a whole stomach model the possibility of stimulating the lesser curvature of the stomach, especially for evaluating the efficiency of pacing parameters for obesity treatment would be brighter.

In addition to it, a 3 D stomach model for GES would be effective only if both electrical and mechanical properties of the gastric musculature is presented i.e. the whole stomach model would be robust if it posses electro – mechanical coupling properties. This GES model can be used as a starting point for the development of a coupled electro-mechanical modelling framework for GES. An electro-mechanical model will facilitate our better understanding about the effects of different stimulus protocols on gastric tone, gastric compliance and gastric accommodation when applied for the treatment for gastroparesis and obesity. Stimulus protocols such as short pulse stimulus and Enterra Therapy whose electrical effects are not very prominent can be better evaluated with an electro-

mechanical GES model. The attempt to construct an electro – mechanical model for the gastric musculature is an ongoing project in the computational bioengineering laboratory. Once an electro mechanical model of the whole stomach is constructed, it can be further extended to build a 3 D model for GES.

The results obtained from the presented GES model has been compared with the experimental GES results. Good agreement with the experimental results has been observed. Most of the experimental work have achieved 100 % entrainment at the stimulated frequency (upto a maximal driven frequency). No significant electrophysiological changes were obtained with short pulse stimulus and enterra therapy. Similar results were also obtained with the GES model. This GES model can also be validated by testing the results on an animal model. In the near future there are plans to validate this model using an animal study. Experimental validation studies can be conducted in dogs, guinea pigs or in porcine models.

In conclusion, the modeling framework presented here is well suited to allow the simulation of an external stimuli leading to optimization of stimulus parameters which is at present an issue of controversy among the clinicians. We hope that this thesis paves the way for the establishment of computational electrophysiology as an efficient medium for the development of an effective gastric pacemaker in the near future to benefit the patients with gastric motility disorders and morbid obesity.

7.2 Publication and Seminar

The research project contained in this thesis has been presented in the following conference publications

- Kannan A, Buist ML "A Computational Investigation of Gastric Electrical Stimulation", Proceedings of 4th East asian pacific conference on nano biomedical engineering, Singapore, December 2010.

- Kannan A, Buist ML "A Computational Investigation of Gastric Electrical Stimulation", Poster presentation at 4th East asian pacific conference on nano biomedical engineering, Singapore, December 2010 and was **awarded best poster presentation award** for the same.

- Kannan A "A Computational Investigation of Gastric Electrical Stimulation". Oral presentation at the Graduate Students' seminars, Division of bioengineering, NUS, Singapore. March, 11th, 2011.

Bibliography

1. Szurszewski.J.H. (1987). Electrical basis for gastrointestinal motility. Physiology of Gastrointestinal Tract 2nd ed, 383-422.

2. Marvin Schuster center. (2008). URL: http://www.hopkinsbayview.org/motil/.

3. Medtronic fact sheet. (2003). URL: http://www.medtronic.com/downloadablefiles/Gastro-GastroparesisFactSheet.pdf.

4. Wang YR, Fisher RS, Parkman HP. (2008). Gastroparesis-related hospitalizations in the United States: trends, characteristics, and outcomes. Am J Gastroenterol. 103(2):313-322.

5. Bortolotti M. (2002). The Electrical way to cure gastroparesis. Am J Gastroenterol. 97(8):1874 - 1883.

6. Klein S. Clinical perspectives in gastroenterology. (2000). J Obes. 3: 232–236.

7. Silverthorn, D. (2004). Human Physiology: An Integrated Approach, 3rd ed. Benjamin Cummings.

8. Nelson RJ. (2005). Introduction to Behavioral Endocrinology. Sinauer Associates: Massachusetts. p: 57.

9. Marieb E. (2004). Human Anatomy and Physiology. Pearson.

10. Sanders K. M, Koh S. D & Ward S. M. (2006). Interstitial cells of cajal as pacemakers in the gastrointestinal tract. Annual Review of Physiology 68: 307–343.

11. Ward S. M & Sanders K. M. (2006). Involvement of intramuscular interstitial cells of Cajal in neuroeffector transmission in the gastrointestinal tract. J Physiol. 576(3), 675–82.

12. Lee H. T, Hennig G. W, Fleming N. W, Keef K. D, Spencer N. J, Ward S. M, Sanders K. M & Smith T. K . (2007). Septal interstitial cells of Cajal conduct pacemaker activity to excite muscle bundles in human jejunum. J Gastroenterol 133(3): 907–917.

13. Langton P, Ward S. M, Carl A, Norell M. A & Sanders K. M. (1989). Spontaneous electrical activity of interstitial cells of Cajal isolated from canine proximal colon. Proceedings of National Academy of Sciences; 86(18): 7280–4.

14. Daniel EE. (2004). Communication between interstitial cells of Cajal and gastrointestinal muscle. J Neurogastroenterol Motil, 16(Suppl1): 118–22.

15. Seki K, Zhou D. S & Komuro T. (1998). Immunohistochemical study of the c-kit expressing cells and connexin 43 in the guinea-pig digestive tract. J Auton Nerv Syst 68(3): 182–7.

16. Hirst G D S & Edwards F R (2006). Electrical events underlying organized myogenic contractions of the guinea pig stomach. J Physiol, 576.3: 659-665.

17. Ching-Liang L , Nancy Shidler & Chen J D Z. (2000). Enhanced Postprandial Gastric Myoelectrical Activity After Moderate-Intensity Exercise. Am J Gastroenterol 95(2): 425-431.

18. Lewis J H & Sarbin T H. (1943). The Influence of Hypnotic Stimulation on Gastric hunger Contractions. From the Otho S. A. Sprague Memorial Institute and the Department of Pathology, University of Chicago, Chicago, Illinois. 123-131.

19. Streutker C. J, Huizinga J. D, Driman D. K & Riddell R. H (2007). Interstitial cells of Cajal in health and disease. Part I: normal ICC structure and function with associated motility disorders. Histopathology 50(2): 176–89.

20. Parkman P.Henry. M.D. (2006). Motility and Functional Disorders of the Stomach: Diagnosis and Management of Functional Dyspepsia and Gastroparesis, Practical Gastroenterology.

21. Soykan I, Sivri B, Sarosiek I, Kiernan B, McCallum RW. (1998). Demography, clinical characteristics, psychological and abuse profiles, treatment, and long term follow-up of patients with gastroparesis. J Dig Dis Sc. 43(11):2398-2404.

22. Bityutskiy LP, Soykan I, McCallum RW. Viral gastroparesis: a subgroup of idiopathic gastroparesis—clinical characteristics and long-term outcomes. (1997). Am J Gastroenterol. 92(9):1501-1504.

23. Kashyap P, Farrugia G. (2010). Diabetic gastroparesis: what we have learned and had to unlearn in the past 5 years. J Gastroenterol Hepatol. 59(12):1716-26.

24. Karamanolis G, Caenepeel P, Arts J, Teck J. (2006). Association of the predominant symptom with clinical characteristics and pathophysiological mechanisms in functional dyspepsia. J Gastroenterol. 130(2):296-303.

25. Stanghellini V, Tosetti C, Paternicò A, De Giorgio R, Barbara G, Salvioli B, Corinaldesi R. (1999). Predominant symptoms identify different subgroups in functional dyspepsia. Am J Gastroenterol. 94(8):2080-2085.

26. Parkman H, M.D. (2006). Motility and Functional Disorders of the Stomach: Diagnosis and Management of Functional Dyspepsia and Gastroparesis, Practical Gastroenterology.

27. Friedenberg FK, Parkman HP. (2005). Management of delayed gastric emptying. Clin Gastroenterol Hepatol. 3(7):642-646.

28. Gentilcore D, Chaikomin R, Jones KL. (2006). Effects of fat on gastric emptying of and the glycemic, insulin, and incretin responses to a carbohydrate meal in type 2 diabetes. J Clin Endocrinol Metab. 91(6):2062-7.

29. Feldman M, Smith HJ. (1987). Effect of cisapride on gastric emptying of indigestible solids in patients with gastroparesis diabeticorum: A comparison with metoclopramide and placebo. J Gastroenterol. 92(1):171–174.

30. Eckhauser FE, Conrad M, Knol JA, Mulholland MW, Colletti LM. (1998). Safety and long term durability of completion gastrectomy in 81 patients with postsurgical gastroparesis syndrome. Am J Surg. 64(8):711-717.

31. Fontana RJ, Barnett JL. (1996). Jejunostomy tube placement in refractory diabetic gastroparesis: A retrospective review. Am J Gastroenterol. 91(10):2174–78.

32. Hasler WH. (2009). Methods of gastric electrical stimulation and pacing: A review of their benefits and mechanisms of action in gastroparesis and obesity, J Neurogastroenterol Motil. 21(3): 229–243.

33. Bellahsène BE, Lind CD, Schirmer BD, Updike OL, McCallum RW. (1992). Acceleration of gastric emptying with electrical stimulation in a canine model of gastroparesis. Am J physiol Gastrointest. Liver Physiol. 262(5): G826–G834.

34. Zhang J, Chen JDZ. (2006). Systematic review: applications and future of gastric electrical stimulation, J Aliment Pharmacol Ther. 24(7): 991–1002.

35. Xing JH, Chen JD. (2006). Effects and mechanisms of long-pulse gastric electrical stimulation on canine gastric tone and accommodation. J Neurogastroenterol Motil. 18(2):136–43.

36. Familoni BO, Abell TL, Nemoto D, Voeller G, Johnson B. (1997). Efficacy of electrical stimulation at frequencies higher than basal rate in canine stomach. J Dig Dis Sc. 42(5):892–7.

37. Song GQ and Chen JDZ. (2007). Synchronized gastric electrical stimulation improves delayed gastric emptying in non obese mice with diabetic gastroparesis. J Appl Physiol. 103(5): 1560-1564.

38. McCallum RW, Snape W, Brody F, Wo J, Parkman HP, Nowak T. (2010). Gastric electrical stimulation with enterra therapy improves symptoms from diabetic gastroparesis in a prospective study. Clin Gastroenterol Hepatol. 8(11):947-954.

39. Fact sheet Enterra therapy. (2003). URL: http://www.medtronic.com/downloadablefiles/Gastro-EnterraFactSheet.pdf.

40. Abrahamsson H. (2007). Treatment options for patients with severe gastroparesis. J Gastroenterol Hepatol. 56(6):877-883.

41. Song GQ, Hou XH, Yang B, Liu JS, Qian W, Chen JDZ. (2005). Two-channel gastric electrical stimulation accelerates delayed gastric emptying induced by vasopressin. J Dig Dis Sc. 50(4): 662-8.

42. Chen JD, Xu X, Zhang J, Abo M, Lin X, McCallum RW, Ross B. (2005). Efficiency and efficacy of multi-channel gastric electrical stimulation J Neurogastroenterol Motil. 17(6): 878–82.

43. Mintchev MP, Sanminguel CP, Bowes KL. (1998). Microprocessor controlled movement of liquid gastric content using sequential neural electrical stimulation. J Gastroenterol Hepatol. 43(5): 607–11.

44. Mintchev MP, Sanminguel CP, Amaris M, Bowes KL. (2000). Microprocessor-controlled movement of solid gastric content using sequential neural electrical stimulation. J Gastroenterol. 118(2): 258–63.

45. Shikora S. 2004. Implantable gastric stimulation – the surgical procedure: combining safety with simplicity. J Obes Surg; 14(Suppl 1): S9–13.

46. Xu XH, Brining DL, Wang LJ, Chen JD. (2002). Effects of retrograde gastric electrical stimulation (RGP) on food intake, gastric myoelectrical activity and gastric emptying in dogs. J Neurogastroenterol Motil. 50(9): 1569- 1575.

47. Ouyang H, Yin JY, Chen JDZ. (2004). Potent Inhibitory Potent inhibitory effect of tachygastria on antral motility in dogs. J Gastroenterol. 126: A–482.

48. Yin JY, Chen JD. (2005). Retrograde gastric electrical stimulation at a tachygastrial frequency reduces food intake and impairs gastric slow waves in obese rats. Obes Res. 13:1580 –1587.

49. McCallum RW, Chen JD, Lin Z, Schirmer BD, Williams RD, Ross RA. (1998). Gastric pacing improves emptying and symptoms in patients with gastroparesis. J Gastroenterol 1998. 114(3):456–461.

50. Lin ZY, McCallum RW, Schirmer BD, and Chen JDZ. (2010). Effects of pacing parameters on entrainment of gastric slow waves in patients with gastroparesis. 1998. Am J Physiol. (Gastrointestinal and Liver Physiol). 274(1): G186-G19.

51. Xing J, Brody F, Rosen M, Chen JDZ, and Soffer E. (2003) . The effect of gastric electrical stimulation on canine gastric slow waves. Am J Physiol. 284(6): G956-G962.

52. Abell TL, Van Cutsem E, Abrahamsson H, Huizinga JD, Konturek JW, Galmiche JP, VoelIer G, Filez L, Everts B, Waterfall WE, Domschke W, Bruley des Varannes S, Familoni BO, Bourgeois IM, Janssens J, Tougas G. (2002). Gastric Electrical Stimulation in Intractable Symptomatic Gastroparesis. J Gastroenterol. 66(4):204-212.

53. Song G, Hou X, Yang X, Sun Y, Liu Y, Qian W, Chen JDZ. (2006). Efficacy and efficiency of gastric electrical stimulation with short pulses in the treatment of vasopressin-induced emetic responses in dogs. J Neurogastroenterol Motil. 18(5): 385–391.

54. Mason RJ; Lipham J; Eckerling G; Schwartz A; DeMeester TR. (2005). Gastric Electrical Stimulation:An Alternative Surgical Therapy for Patients With Gastroparesis. Archives of Surgery. 140(9):841-6.

55. Yang B Hou XH Song GQ Liu JS Chen JD. (2009). Effect of two-channel gastric electrical stimulation with trains of pulses on gastric motility. World J Gastroenterol. 15(19): 2406–2411.

56. Lei Y and Chen JDZ. (2009). Effects of dual pulse gastric electrical stimulation on gastric tone and compliance in dogs. J Dig and Liver Disorder. 41(4): 277–282.

57. Song GQ, Hou X, Yang B, Sun Y, Qian W, Chen JD. (2007). A novel method of 2-channel dual-pulse gastric electrical stimulation improves solid gastric emptying in dogs. J Surg. 143(1):72-8.

58. Chen J, Koothan T and Chen JDZ. (2009). Synchronized gastric electrical stimulation improves vagotomy-induced impairment in gastric accommodation via the nitrergic pathway in dogs. Am J Physiol GI. 296(2): G310-G318.

59. Yao S, Ke M, Wang Z. (2005). Retrograde gastric pacing reduces food intake and delays gastric emptying in humans: A potential therapy for obesity? J Dig Dis Sci. 50(9):1569-1575.

60. Zhang J, Tang M, Chen JD. (2009). Gastric electrical stimulation for obesity: The need for a new device using wider pulses. J Obes. 17(3):474-80.

61. Sarna S.K, Daniel E.E, and Kingma Y.J. (1972). Premature control potentials in the dog stomach and in the gastric computer model, Am J Physiol. 222(6): 1518-1523.

62. Mintchev.M and Bowes.K. (1997). Computer model of gastric electrical stimulation. Ann Biomed Eng, 25(4), 726–730.

63. Wang, Z.S. Chen, J.D.Z. (2000). Mathematical modeling of nonlinear coupling mechanisms of gastric slow wave propagation and its SIMULINK simulation for

investigating gastric dysrhythmia and pacing. Computer-Based Medical Systems, CBMS 2000 Proceedings. 13th IEEE Symposium p: 89 – 94.

64. Rashev PZ, Bowes KL, and Mintchev MP. (2002). Three-Dimensional Object-Oriented Modeling of the Stomach for the Purpose of Microprocessor-Controlled Functional Stimulation, IEEE Transactions on biomedical engineering. 6(4):296-309.

65. Familoni BO, Abell TL, Gan Z, Voeller G. (2005). Driving gastric electrical activity with electrical stimulation. Ann Biomed Eng. 33(3):356-64.

66. Du P, Greg O'Grady, Windsor JA, Cheng LK and Pullan AJ. (2009). A Tissue Framework for Simulating the Effects of Gastric Electrical Stimulation and In Vivo Validation, IEEE Transactions on biomedical engineering. 56(12). 2755-2761.

67. Corrias A and Buist ML. (2008). A quantitative cellular description of gastric slow wave activity, Am J Gastrointestinal & Liver Physiol. 294(4), G989–G995.

68. Corrias A and Buist ML. (2007). A quantitative model of gastric smooth muscle cellular activation. Ann Biomed Eng. 35(9), 1595–1607.

69. Buist ML and Poh YC. (2010). An Extended Bidomain Framework Incorporating Multiple Cell Types. Biophys J. 99(1):13-18.

70. Buist ML, Corrias A, and Poh YC. (2010). A model of slow wave propagation and entrainment along the stomach. Ann Biomed Eng. 38(9):3022–3030.

71. Imtiaz, M. S., D. W. Smith, and D. F. van Helden. (2002). A theoretical model of slow wave regulation using voltage-dependent synthesis of inositol 1,4,5-trisphosphate. Biophys. J. 83:1877–1890.

72. van Helden D F, Imtiaz MS, Nurgaliyeva K, von der Weid P, and Dosen PJ. (2000). Role of calcium stores and membrane voltage in the generation of slow wave action potentials in guinea-pig gastric pylorus. J. Physiol. 524:245–265.

73. Fall C P and Keizer J E. (2001). Mitochondrial modulation of intracellular Ca^{2+}signaling. J Theor Biol. 210(2): 151–65.

74. Wagner J, Li YX,Pearson J, and Keizer J. (1998). Simulation of the Fertilization Ca21 Wave in *Xenopus laevis* Eggs**.** Biophys. J. 75:2088–2097.

75. Lee H. T, Hennig G. W, Fleming N. W, Keef K. D, Spencer N. J, Ward S. M, Sanders K. M & Smith T. K (2007). The mechanism and spread of pacemaker activity through myenteric interstitial cells of Cajal in human small intestine. Gastroenterology. 132(5): 1852–65.

76. Stratton C. J, Ward S. M, Horiguchi K & Sanders K. M (2007). Immunocytochemical identification of interstitial cells of Cajal in the murine fundus using a live-labelling technique. Neurogastroenterol Motil 19(2), 152–9.

77. Komuro T (2006). Structure and organization of interstitial cells of Cajal in the gastrointestinal tract. J Physiol 576(3), 653–8.

78. Lammers W. J, Stephen B, Adeghate E, Ponery S & Pozzan O (1998). The slow wave does not propagate across the gastroduodenal junction in the isolated feline preparation. Neurogastroenterol Motil 10(4), 339–49.

79. Wang XY, Lammers WJ, Bercik P, Huizinga JD. (2005). Lack of pyloric interstitial cells of Cajal explains distinct peristaltic motor patterns in stomach and small intestine. Am. J. Physiol. Gastrointest.Liver. Physiol. 289:G539–549.

80. Diamant NE, Bortoff A. (1969). Effects of transection on the intestinal slowwave frequency gradient. Am. J. Physiol. 216:734–743.

81. Bedard C & Destexhe A (2008). A modified cable formalism for modeling neuronal membranes at high frequencies. Biophys J. 94(4), 1133–1143.

82. Huang C. L & Peachey L. D (1992). A reconstruction of charge movement during the action potential in frog skeletal muscle. Biophys J. 61(5):1133–1146.

83. Bondarenko V. E & Rasmusson R. L (2007). Simulations of propagated mouse ventricular action potentials: effects of molecular heterogeneity. Am J Physiol Heart Circ Physiol. 293(3): H1816–1832.

84. Spitzer V, Ackerman M. J, Scherzinger A. L & Whitlock D (1996). The visible human male: a technical report. J Am Med Inform Assoc 3(2): 118–30.

85. Sun Y, Qin C, Foreman RD, Chen JDZ. (2005). Intestinal electric stimulation modulates neuronal activity in the nucleus of the solitary tract in rats Neuroscience Letters 385: 64–69.

86. Enterra Gastric Neurostimulator: Features and Specifications
URL: http://professional.medtronic.com/pt/gastro/ges/prod/enterra-gastric-neurostimulator/features-specifications/index.htm

87. Kelly KA. (1980). Gastric emptying of liquids and solids: roles of proximal and distal stomach. Am J Physiol. 239(2):G71-6.

88. Collins PJ, Houghton LA, Read NW. (1991). Role of the proximal and distal stomach in mixed solid and liquid meal emptying. Gut. 32(6):615-9.

89. Friedenberg FK, Parkman HP. Advances in the management of gastroparesis. (2007). Curr Treat Options Gastroenterol. 10(4):283-93.